Title

DYNAMICAL EVOLUTION OF ANGULAR MOMENTUM IN DAMPED NUCLEAR REACTIONS. I. ACCUMULATION OF ANGULAR MOMENTUM BY NUCLEON TRANSFER

Authors

Dossing, T.
Randrup, J.

Publication Date

1983-12-01

LBL-16825
Preprint

Lawrence Berkeley Laboratory
UNIVERSITY OF CALIFORNIA

Submitted to Nuclear Physics A

DYNAMICAL EVOLUTION OF ANGULAR MOMENTUM IN DAMPED NUCLEAR REACTIONS. I. ACCUMULATION OF ANGULAR MOMENTUM BY NUCLEON TRANSFER

T. Døssing and J. Randrup

December 1983

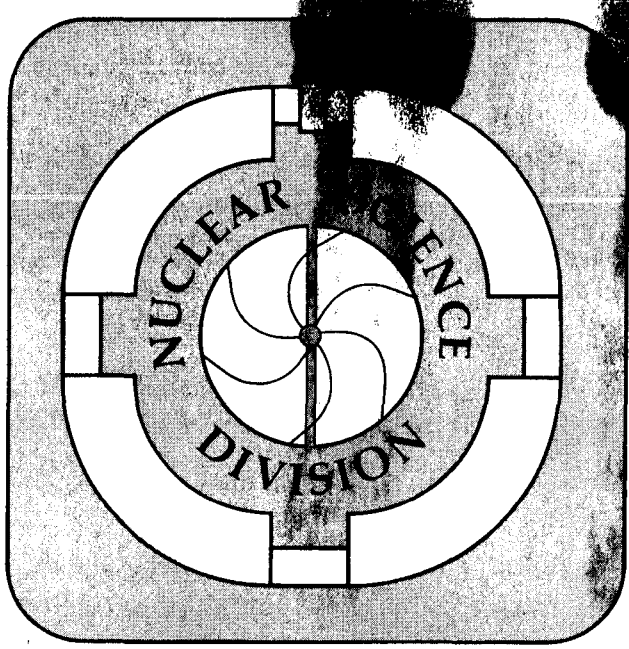

Prepared for the U.S. Department of Energy under Contract DE-AC03-76SF00098

DISCLAIMER

LBL-16825

Dynamical Evolution of Angular Momentum in Damped Nuclear Reactions

I. Accumulation of Angular Momentum by Nucleon Transfer

Thomas Døssing and Jørgen Randrup

Nuclear Science Division
Lawrence Berkeley Laboratory
University of California
Berkeley, California 94720

December 1983

This work is supported by the Director, Office of Energy Research Division, of Nuclear Physics of the Office of High Energy and Nuclear Physics of the U.S. Department of Energy under Contract No. DE-AC03-76SF00098.

Abstract

The dynamical accumulation of angular momentum in the course of a damped nuclear reaction is studied within the framework of the nucleon exchange transport model. The dinuclear spin distribution is described by the mean values and the covariances of the two prefragment spins and their orbital angular momentum $\vec{L}$. Using an intrinsic coordinate system aligned with the fluctuating direction of $\vec{L}$, the equations of motion for the spin distribution are derived and discussed. The ultimate transformation to an externally defined reference frame is also discussed. The evolution of other observables and their coupling to the spin variables are included and, by integrating conditional distributions over all impact parameters, results are obtained for differential cross sections corresponding to a specified loss of relative kinetic energy. The characteristic features of the evolution of the spin distribution is discussed in detail. First the stationary solution of the equations of motion is considered and its different appearance in the various relevant coordinate systems is exhibited. The dynamical evolution is discussed in terms of the time-dependent relaxation times associated with the six different intrinsic modes of rotation in the disphere. Due to the relative smallness of the window size the positive modes will dominate (for not too long times), resulting in a predominantly positive correlation between the fragment spin fluctuations. Illustrative applications to cases of experimental interest are made and a critical discussion is given of other models addressing angular momentum in damped nuclear reactions.

Introduction

The exploration of damped reactions between atomic nuclei has been a central theme in nuclear physics during the last decade. Through this period, steady improvements in instrumentation have permitted the taking of increasingly detailed data and have paved the way for an ever better understanding of those processes.

A damped nuclear reaction typically proceeds as follows. A heavy projectile nucleus A with a kinetic energy of several MeV per nucleon is bombarded onto a heavy target nucleus B. The two nuclei engage in a rather intimate reaction during which a substantial part of the available energy is lost from the relative motion and two fragments emerge with severely reduced relative kinetic energy. The two fragments are highly excited and subsequently dispose of their excitation by various decay processes, typically neutron evaporation followed by gamma emission.

In addition to the large energy loss, typically hundreds of MeV, a characteristic feature of a damped reaction is its binary character. Not only is the exit channel binary (prior to the sequential decay processes, of course), but the emerging nuclei exhibit a great resemblance with the original ones with respect to their mass and charge numbers. This dynamical preservation of the entrance asymmetry implies that the system must have maintained its binary character throughout the reaction phase. Thus, on the one side, damped nuclear reactions are distinguished from the gentler quasi-elastic reactions by their large energy loss, while on the other side, their binary character

distinguishes them from reactions in which a mononucleus is formed, such as fast fission or compound nucleus reactions.

The most important observables characterizing the binary system shortly after the reaction phase are:

1) the relative motion of the two nuclei, as specified by their relative kinetic energy E and the direction of relative motion,

2) the partition of the total mass and charge among the two fragments, as specified by the mass number A and the charge number Z of the projectile-like fragment, and

3) the state of rotation of the two fragments, as specified by their angular momenta $\vec{S}^A$ and $\vec{S}^B$.

In addition, the partition of the residual excitation energy between the two fragments is of some interest and in principle susceptible to experimental determination.

The experimental data can be briefly, and roughly, characterized by stating that the multivariate distribution of the above observables resembles that of a transport process, with the kinetic energy loss TKEL playing the role of the generalized time parameter. That is to say, when the data is organized with respect to TKEL the distribution of any of the other observables, for example the mass partition, the angular momentum, or the scattering angle, develops steadily from being rather narrow for small TKEL to having an appreciable width for the largest values of TKEL. Well known illustrations of this general feature are the so-called Wilczyinski plots, which display the yields

in the θ_{CM}-TKEL plane, and the plots of the element distribution for fixed TKEL. A review of damped nuclear reactions can be found in ref[1].

The discussion of the dynamics of damped nuclear reactions naturally organizes itself into a conceptual hierarchy, with the first level concerning the evolution of the mean values (the first moments of the multivariate distribution of the observables) and the second level concerning the accumulation of the associated fluctuations, as described by the corresponding covariance matrix.

Early on in the development of the field efforts concentrated on understanding the mean evolution. It was demonstrated, within many different models, that the reactions can be described by classical equations of motion for two (possibly deformable) spheres interacting via conservative nuclear and Coulomb forces and subject to a mutual friction force which is responsible for the dissipation of relative energy and the associated accumulation of fragment spins and excitation. Of special relevance to the discussion in the present paper is the early recognition[2] that the friction acting between the two nucleides has three distinct components: 1) a radial friction acting on the relative separation of the two nucleides, 2) a sliding friction acting on the tangential component of the relative nuclear velocity, and 3) a rolling friction acting to achieve a sticking configuration in which the entire system rotates rigidly as a single body.

Nörenberg was the first to address the second conceptual level when demonstrating the linear growth of the charge variance with scattering angle for the Ar+Th reaction and arguing for the introduction of transport theoretical concepts in the discussion of damped nuclear reactions[3]. He then proceeded

to develop a transport theory for damped reactions, first considering only the mass partition degree of freedom, but later on including an increasing number of observables.

It is important to realize that in a dissipative system the mean evolution and the growth of the fluctuations are intimately related since both are caused by the same fundamental processes. The friction constants and the diffusion coefficients should therefore not be treated as independent quantities. Furthermore, since again the same fundamental processes effect changes in several macroscopic variables at the same time, the transport coefficients pertaining to different observables are also mutually related and can not be treated as independent.

On the basis of linear response theory, Hofmann and Siemens have developed a quantum-mechanical framework for treating the macroscopic dynamics in moderately excited nuclear systems[4]. In this theory, the transport coefficients are given in terms of the response functions of the system and the drift coefficients are related to the diffusion coefficients via the fluctuation-dissipation theorem. It is also demonstrated that the general equation of motion for the macroscopic density matrix reduces to a transport equation of the Fokker-Planck type in the classical limit, thus lending additional theoretical support for the discussion of nuclear dynamics in terms of transport theory.

An important goal in the theory of nuclear dynamics is to understand the observed transport phenomena in terms of the basic microscopic processes in the system. For this purpose a model was developed[5] in which the dissipative mechanism is the transfer of nucleons between the two reacting

nucleides. From the observed mass and charge widths, it is evident that many nucleons are tranferred in the course of a damped reaction. Each nucleon transfer affects the partition of charge and mass as well as the radial and angular momentum in the dinucleus and elementary kinematical considerations indicate that the transfer of a single nucleon typically generates a substantial amount of excitation. Therefore nucleon transfer is expected to be an important dissipative mechanism in nuclear reactions. The developed model[5] expresses the transport coefficients pertaining to mass, charge, radial and angular momentum in terms of one common form factor describing the rate of individual nucleon transfers between the binary partners. A detailed account of the numerical implementation of the model has been given in ref.[6].

Until now most efforts to confront that theory with data have concentrated on the evolution of the charge and mass distributions, as functions of the energy loss. By considering the dependence of the charge or mass width on the energy loss it was shown[7] that the energy dissipated per nucleon transfer agrees well with the general model predictions which are substantially above what would be expected in a classical picture, due to the effect of the Pauli blocking. In a subsequent study[8] the projected two-dimensional distribution function in the NZ-plane was considered and good agreement with the data was found for the isotopic distribution for a given element as well as the element distribution for a given mass partition, both considered as functions of the energy loss. More recently, a somewhat similar study[9] was made for lighter reaction systems. After due account was taken of the sequential evaporation process, good agreement with the data was obtained for the NZ-distribution as a function of TKEL. In all of these confrontations no

parameter adjustments were made in the theory and the overall good agreement for a variety of features lends strong support to the theory and suggests that nucleon exchange is the dominant dissipation mechanism in these reactions.

In view of this success it is important to put the theory to further tests, particularly regarding other aspects of the data. Therefore, it is important to also consider the angular momenta of the reaction products. This brings in six new observables (three for each fragment spin) in addition to A and Z considered so far, and thus the angular-momentum variables provide a rich testing ground for the theory.

The treatment of the angular-momentum observables within the theory was especially considered in ref.[8]. Furthermore, a preliminary study of the spin-spin correlations as probed in a double-fission experiment was made in ref.[10]. In the present paper we reconsider the treatment of the angular momentum in the theory making several important improvements over ref.[6]. In Section 2 the equations of motion for the spin mean values and covariances are derived and the importance of adopting an intrinsic fluctuating coordinate system is brought out. Section 3 describes the treatment of other observables, such as the mass and charge partition, the relative position and momentum, and the relative energy. In Section 4 it is shown how to obtain actual differential cross sections, conditioned by a specified energy loss. Then, in Section 5, an instructive discussion is made of the characteristic features of the spin evoution. Section 6 contains illustrative applications to cases of experimental interest. Finally, in light of the insight gained in the present study, Section 7 gives a critical discussion of other contributions to the description of angular momentum in damped nuclear reactions.

The present paper focusses on the accumulation of angular momenta during the reaction and is the first in a series of two. The second paper (which shall be referred to as II) deals with the subsequent decay process and the confrontation with data.

2. Derivation of the equations of motion

This section is devoted to the derivation of the equations of motion for the moments of the angular-momentum distribution in the dinucleus. This problem was already considered in ref.[6]. Relative to that work, the present treatment differs in that the angular momenta are referred to a "body-fixed" coordinate system aligned with the fluctuating direction of the orbital angular momentum. This refinement ensures that the tilting mode is fully included in the treatment, contrary to the approximate treatment of ref.[6] based on a non-fluctuating coordinate system. This important difference will become evident during the derivation.

2.1. Setting the stage

We idealize the reacting system as two spherical nucleides A and B. Their relative position is $\vec{R} = \vec{R}^A - \vec{R}^B$ and their relative velocity is $\vec{U} = \vec{U}^A - \vec{U}^B$. (When vectors or tensors are involved we shall reserve subscripts for their spatial indices so we indicate the labels A and B as superscripts.) Their relative orbital angular momentum is then $\vec{L} = \mu\vec{R} \times \vec{P}$ where $\vec{P} = \mu\vec{U}$ is the relative momentum, $\mu \approx mAB/(A+B)$ being the reduced mass. (We shall also use the symbols A and B to denote the nucleon numbers of the nucleides A and B.)

The associated moment of inertia is $\mathcal{I}_R = \mu R^2$. The angular momenta, or spins, of the individual nucleides are $\vec{S}^A$ and $\vec{S}^B$, and $\mathcal{I}_A$ and $\mathcal{I}_B$ are the associated moments of inertia. Specific details about this model can be found in Appendix A of ref.[6]. The total angular momentum $\vec{J} = \vec{S}^A + \vec{S}^B + \vec{L}$ is a constant of motion since no external torques are acting on the system.

Let us first recall the form of the transport coefficients for the angular momentum bearing modes in the disphere. The mobility tensors ralating to the two fragment spins $\vec{S}^A$ and $\vec{S}^B$ are given by[6)]

$$\begin{aligned} \overleftrightarrow{M}^{AA} &= mN\,(a^2\overleftrightarrow{T} + c_{ave}^2\overleftrightarrow{I}) \\ \overleftrightarrow{M}^{AB} &= mN\,(ab\overleftrightarrow{T} - c_{ave}^2\overleftrightarrow{I}) = \overleftrightarrow{M}^{BA} \\ \overleftrightarrow{M}^{BB} &= mN\,(b^2\overleftrightarrow{T} + c_{ave}^2\overleftrightarrow{I}) \end{aligned} \qquad (2.1)$$

Here $\overleftrightarrow{I}$ is the identity tensor (which has the representation $\overleftrightarrow{I} = \hat{x}\hat{x} + \hat{y}\hat{y} + \hat{z}\hat{z}$ in any orthonormal coordinate system xyz) and $\overleftrightarrow{T} = \overleftrightarrow{I} - \hat{R}\hat{R}$ projects onto the plane perpendicular to the dinuclear axis $\hat{R}$. The distances to the "window" plane from the two nuclear centers are denoted by a and b, with a + b = R, while c_{ave} is the average off-axis displacement of the transferred nucleons. The nucleon mass is denoted m, and N is the overall form factor governing the rate of nucleon transfer between the two nucleides A and B.

In addition to the fragment spins $\vec{S}^A$ and $\vec{S}^B$, it is also necessary to consider the evolution of the orbital angular momentum $\vec{L} = \vec{J} - \vec{S}^A - \vec{S}^B$. This is because we wish to use a coordinate system whose direction fluctuates with respect to an external inertial system (and hence the components of the total angular momentum J will fluctuate).

As in ref.[6)], it is notationally convenient to denote any of the angular-momentum labels A, B, L by the letters F, G, ...so that $\vec{S}^F = \vec{S}^A$, $\vec{S}^B$, $\vec{L}$ for F = A, B, L, respectively. The mobility tensor relating to the orbital angular momentum can then be obtained by using the general relation,

$$\overleftrightarrow{M}^{FL} = -\overleftrightarrow{M}^{FA} - \overleftrightarrow{M}^{FB} = \overleftrightarrow{M}^{LF} \tag{2.2}$$

(which follows from angular-momentum conservation) for F = A, B, L:

$$\begin{aligned}
\overleftrightarrow{M}^{AL} &= -\overleftrightarrow{M}^{AA} - \overleftrightarrow{M}^{AB} = \overleftrightarrow{M}^{LA} = -mN\,aR\,\overleftrightarrow{T} \\
\overleftrightarrow{M}^{BL} &= -\overleftrightarrow{M}^{BA} - \overleftrightarrow{M}^{BB} = \overleftrightarrow{M}^{LB} = -mN\,bR\,\overleftrightarrow{T} \\
\overleftrightarrow{M}^{LL} &= -\overleftrightarrow{M}^{LA} - \overleftrightarrow{M}^{BA} = mNR^2\,\overleftrightarrow{T}
\end{aligned} \tag{2.3}$$

In terms of the mobility coefficients the spin transport coefficients are given as follows. The diffusion coefficients are simply the corresponding mobility coefficients multiplied by the "effective temperature" τ^*,

$$\overleftrightarrow{D}^{FG} = \overleftrightarrow{M}^{FG}\,\tau^* \tag{2.4}$$

The drift coefficients are obtained by multiplying the mobility tensor with the corresponding generalized forces, i.e., minus the rotational frequencies $\vec{\omega}^F = \vec{S}^F/\mathcal{J}_F$,

$$\vec{V}^F = -\sum_G \overleftrightarrow{M}^{FG} \cdot \vec{\omega}^G = -\sum_G \overleftrightarrow{M}^{FG} \cdot \vec{S}^G/\mathcal{J}_G \tag{2.5}$$

Here and in the following the sum over the labels G extends over G = A, B, L.

As mentioned in the beginning of this chapter we employ a "body-aligned" orthonormal reference system defined by

$$\hat{z} = \hat{R} \ , \quad \hat{y} = \hat{L} \ , \quad \hat{x} = \hat{y} \times \hat{z} \tag{2.6}$$

The choice of $\hat{z} = \hat{R}$ ensures that the mobility tensors $\overleftrightarrow{M}^{FG}$ are diagonal in the spatial indices. Since $\hat{y} = \hat{L}$, the orbital angular momentum $\vec{L}$ has only components in the y-direction. We need then consider the temporal evolution of S_x^A, S_y^A, S_z^A, S_x^B, S_y^B, S_z^B, L_y and their covariances. In a standard collision experiment, all are initially zero except for L_y which equals the total angular moentum J. It follows from the symmetry of the problem that the mean values $\langle S_x^F \rangle$ and $\langle S_z^F \rangle$ and also the covariances σ_{xy}^{FG} and σ_{yz}^{FG} will remain zero throughout the collision. Therefore our attention can be restricted to the following 19 quantities

$$\begin{aligned}
&\langle S_y^A \rangle \ , \quad \langle S_y^B \rangle \ , \quad \langle L_y \rangle \\
&\sigma_{xx}^{AA} \ , \quad \sigma_{xx}^{AB} \ , \quad \sigma_{xx}^{BB} \\
&\sigma_{yy}^{FG} \ , \quad F,G = A,B,L \\
&\sigma_{zz}^{AA} \ , \quad \sigma_{zz}^{AB} \ , \quad \sigma_{zz}^{BB} \\
&\sigma_{xz}^{AA} \ , \quad \sigma_{xz}^{AB} \ , \quad \sigma_{zx}^{AB} \ , \quad \sigma_{xz}^{BB}
\end{aligned} \tag{2.7}$$

Any distribution with vanishing $\langle S_x^F \rangle$, $\langle S_z^F \rangle$, σ_{xy}^{FG} and σ_{yz}^{FG} will be referred to as a standard distribution.

2.2. Dynamical equations

In order to derive the equations of motion for the above quantities (2.7) we proceed as follows. First we imagine that the system has been prepared in a dynamical state with definite values of the angular momenta $\vec{S}^A$, $\vec{S}^B$, and $\vec{L}$. We then consider the system after a small (infinitesimal) time increment δt during which interval the spins have received the increments $\delta\vec{S}^F$ due to the nucleon transfer process; these random increments are characterized by the following moments,

$$\langle \delta\vec{S}^F \rangle_{transf} = \vec{V}^F \delta t$$
$$\langle \delta\vec{S}^F \delta\vec{S}^G \rangle_{transf} = 2\overleftrightarrow{D}^{FG} \delta t \qquad (2.8)$$

where the brackets denote the mean value over the transfer during the small time interval δt. During that time interval the dinucleus has rotated an angle $\delta\mathcal{O} = \omega_R \delta t$ around the y-axis. Furthermore, the direction of $\vec{L}$ may have changed, due to the increment $\delta\vec{L}$. When the orbital angular momentum is large in comparison with the increments caused by a nucleon transfer the corresponding change in $\vec{L}$ is small. The directional changes of $\hat{R}$ and $\hat{L}$ can then be considered separately and the necessary reorientation of the coordinate system can be made by two infinitesimal rotations. Subsequently the time averages (2.8) can be carried out. Finally, the fact that the dynamical state of the system is usually characterized by an entire distribution of angular momenta at the outset of the time interval is taken into account by performing the

corresponding ensemble average. In this way, the time derivatives of the moments (2.7) are obtained.

At the outset of the small time interval we have $\vec{L} = (0, L, 0)$ and at the end we have $\vec{L}' = \vec{L} + \delta\vec{L} = (\delta L_x, L + \delta L_y, 0)$ since L remains perpendicular to $\hat{R}$. Thus, ignoring for the time being the effect of the orbital rotation, the new aligned coordinate system is obtained from the old one by rotating an angle λ around the z-axis. The angle λ is determined by

$$\tan \lambda = - \frac{\delta L_x}{L + \delta L_y} \tag{2.9}$$

which, with the assumed relative smallness of the increments $\delta\vec{L}$, yields

$$\begin{aligned} \sin \lambda &\approx - \frac{\delta L_x}{L} + \frac{\delta L_x \, \delta L_y}{L^2} \\ \cos \lambda &\approx 1 - \tfrac{1}{2} \left(\frac{\delta L_x}{L} \right)^2 \end{aligned} \tag{2.10}$$

The corresponding rotation operator is

$$\overleftrightarrow{\mathcal{R}}_z(\lambda) = e^{i \overleftrightarrow{S}_z \lambda} = \begin{pmatrix} \cos\lambda & \sin\lambda & 0 \\ -\sin\lambda & \cos\lambda & 0 \\ 0 & 0 & 1 \end{pmatrix} \tag{2.11}$$

where

$$\overleftrightarrow{S}_z = \begin{pmatrix} 0 & -i & 0 \\ i & 0 & 0 \\ 0 & 0 & 0 \end{pmatrix} \tag{2.12}$$

is the standard spin matrix.

2.2a. Mean values

Therefore, we find at the end of the time interval

$$\begin{aligned} (S_y^F)^{new} &= -(S_x^F + \delta S_x^F)\sin\lambda + (S_y^F + \delta S_y^F)\cos\lambda \\ &\approx S_x^F \frac{\delta L_x}{L} - S_x^F \frac{\delta L_x \delta L_y}{L^2} + \frac{\delta S_x^F \delta L_x}{L} + S_y^F - \frac{1}{2} S_y^F \left(\frac{\delta L_x}{L}\right)^2 + \delta S_y^F \end{aligned} \tag{2.13}$$

through second order in the increments $\delta\vec{S}^F$. Thus, averaging with respect to the random nucleon transfers with the use of (2.8), we have

$$\begin{aligned} &\langle (S_y^F)^{new} \rangle_{transf} \\ &= S_y^F + (V_y^F + \frac{1}{L} S_x^F V_x^L + \frac{2}{L} D_{xx}^{FL} - \frac{1}{L^2} S_y^F D_{xx}^{LL}) \delta t \end{aligned} \tag{2.14}$$

We have here used that $D_{xy}^{LL} = 0$. Finally, performing the ensemble average over the distribution of values S_y^F, we obtain

$$\begin{aligned} &\frac{d}{dt} \langle S_y^F \rangle \\ &= \langle V_y^F + \frac{1}{L} S_x^F V_x^L + \frac{2}{L} D_{xx}^{FL} - \frac{1}{L^2} S_y^F D_{xx}^{LL} \rangle \end{aligned} \tag{2.15}$$

2.2b. Covariances

The equations for the spin covariances can be obtained in a similar manner. We consider first the xx-component:

$$
\begin{aligned}
(S_x^F S_x^G)^{new} &= [(S_x^F + \delta S_x^F)\cos\lambda + (S_y^F + \delta S_y^F)\sin\lambda] \\
&\quad [(S_x^G + \delta S_x^G)\cos\lambda + (S_y^G + \delta S_y^G)\sin\lambda] \qquad (2.16)\\
&\approx S_x^F S_x^G + \delta S_x^F \delta S_x^G + S_x^F \delta S_x^G + \delta S_x^F S_x^G \\
&\quad -(\delta L_x S_x^F + \delta L_x \delta S_x^F)\frac{S_y^G}{L} - \frac{S_y^F}{L}(S_x^G \delta L_x + \delta S_x^G \delta L_x) \\
&\quad -(S_x^F S_x^G - S_y^F S_y^G)\left(\frac{\delta L_x}{L}\right)^2 \\
&\quad -(\delta L_x \delta S_y^F - \delta L_x \delta L_y \frac{\delta S_y^F}{L})\frac{S_x^G}{L} - \frac{S_x^F}{L}(\delta S_y^G \delta L_x - \frac{S_y^G}{L}\delta L_x \delta L_y)
\end{aligned}
$$

After averaging over the transfers the last line disappears and we obtain

$$
\begin{aligned}
&\langle (S_x^F S_x^G)^{new} \rangle_{transf} \\
&= S_x^F S_x^G + [2D_{xx}^{FG} + S_x^F V_x^G + V_x^F S_x^G \qquad (2.17)\\
&\quad -(2D_{xx}^{LF} + V_x^L S_x^F)\frac{S_y^G}{L} - \frac{S_y^F}{L}(2D_{xx}^{GL} + S_x^G V_x^L) \\
&\quad -\frac{2}{L^2} D_{xx}^{LL}(S_x^F S_x^G - S_y^F S_y^G)]\,\delta t
\end{aligned}
$$

Subsequent ensemble averaging over a standard spin distribution then yields

$$\dot{\sigma}^{FG}_{xx}$$

$$= \langle 2D^{FG}_{xx} + S^F_x V^G_x + V^F_x S^G_x$$

$$- \frac{1}{L}\left[(2D^{LF}_{xx} + V^L_x S^F_x) S^G_y + S^F_y (2D^{GL}_{xx} + S^G_x V^L_x)\right]$$

$$- \frac{2}{L^2} D^{LL}_{xx} (S^F_x S^G_x - S^F_y S^G_y) \rangle \qquad (2.18)$$

Next we consider the yy-components:

$$(S^F_y S^G_y)^{new} = [-(S^F_x + \delta S^F_x)\sin\lambda + (S^F_y + \delta S^F_y)\cos\lambda]$$

$$[-(S^G_x + \delta S^G_x)\sin\lambda + (S^G_y + \delta S^G_y)\cos\lambda] \qquad (2.19)$$

$$\approx S^F_y S^G_y + \delta S^F_y \delta S^G_y + S^F_y \delta S^G_y + \delta S^F_y S^G_y$$

$$+ (\delta L_x S^F_x + \delta L_x \delta S^F_x)\frac{S^G_y}{L} + \frac{S^F_y}{L}(S^G_x \delta L_x + \delta S^G_x \delta L_x)$$

$$+ (S^F_x S^G_x - S^F_y S^G_y)\left(\frac{\delta L_x}{L}\right)^2$$

$$+ (\delta L_x \delta S^F_y - \delta L_x \delta L_y \frac{S^F_y}{L})\frac{S^G_x}{L} + \frac{S^F_x}{L}(\delta S^G_y \delta L_x - \frac{S^G_y}{L}\delta L_x \delta L_y)$$

Again transfer averaging eliminates the last line so we obtain

$$\langle (S^F_y S^G_y)^{new} \rangle_{transf}$$

$$= S^F_y S^G_y + [2D^{FG}_{yy} + S^F_y V^G_y + V^F_y S^G_y$$

$$+ (2D^{LF}_{xx} + V^L_x S^F_x)\frac{S^G_y}{L} + \frac{S^F_y}{L}(2D^{GL}_{xx} + S^G_x V^L_x)$$

$$+ \frac{2}{L^2} D^{LL}_{xx} (S^F_x S^G_x - S^F_y S^G_y)]\,\delta t \qquad (2.20)$$

Therefore, after averaging over a standard spin distribution we arrive at

$$\dot{\sigma}^{FG}_{yy} = \frac{d}{dt}\langle S^F_y S^G_y\rangle - \frac{d}{dt}\langle S^F_y\rangle\langle S^G_y\rangle - \langle S^F_y\rangle\frac{d}{dt}\langle S^G_y\rangle$$

$$= \Big\langle 2D^{FG}_{yy} + S^F_y V^G_y + V^F_y S^G_y + \frac{2}{L^2} D^{LL}_{xx}\left(S^F_x S^G_x - S^F_y S^G_y\right)\Big\rangle + \Big\langle \frac{1}{L^2} S^F_y D^{LL}_{xx}\Big\rangle\langle S^G_y\rangle + \langle S^F_y\rangle\Big\langle \frac{1}{L^2} S^G_y D^{LL}_{xx}\Big\rangle \tag{2.21}$$

The zz-components are the simplest ones:

$$(S^F_z S^G_z)^{new} = (S^F_z + \delta S^F_z)(S^G_z + \delta S^G_z)$$

$$= S^F_z S^G_z + \delta S^F_z \delta S^G_z + S^F_z \delta S^G_z + \delta S^F_z S^G_z \tag{2.22}$$

so that

$$\langle (S^F_z S^G_z)^{new}\rangle_{transf}$$

$$= S^F_z S^G_z + \left[2D^{FG}_{zz} + S^F_z V^G_z + V^F_z S^G_z\right]\delta t \tag{2.23}$$

and, consequently,

$$\dot{\sigma}^{FG}_{zz}$$

$$= \langle 2D^{FG}_{zz} + S^F_z V^G_z + V^F_z S^G_z\rangle \tag{2.24}$$

Finally, we consider the off-diagonal elements:

$$(S^F_x S^G_z)^{new} = \left[(S^F_x + \delta S^F_x)\cos\lambda + (S^F_y + \delta S^F_y)\sin\lambda\right](S^G_z + \delta S^G_z)$$

$$\approx S^F_x S^G_z + \delta S^F_x \delta S^G_z + S^F_x \delta S^G_z + \delta S^F_x S^G_z$$

$$- \left(\frac{(\delta L_x)^2}{2L} S^F_x + \delta L_x S^F_y\right)\frac{S^G_z}{L}$$

$$- S^F_y \frac{\delta L_x \delta S^G_z}{L} - \frac{\delta S^F_y \delta L_x}{L} S^G_z + S^F_y \frac{\delta L_x \delta L_y}{L^2} S^G_z \tag{2.25}$$

so that

$$\langle (S_x^F S_z^G)^{new} \rangle_{transf}$$

$$= S_x^F S_z^G + [S_x^F V_z^G + V_x^F S_z^G - (D_{xx}^{LL} \frac{S_x^F}{L} + V_x^L S_y^F) \frac{S_z^G}{L}] \delta t \qquad (2.26)$$

and, in turn,

$$\dot{\sigma}_{xz}^{FG}$$

$$= \langle S_x^F V_z^G + V_x^F S_z^G - (D_{xx}^{LL} \frac{S_x^F}{L} + V_x^L S_y^F) \frac{S_z^G}{L} \rangle \qquad (2.27)$$

Analogously, we find

$$\dot{\sigma}_{zx}^{FG}$$

$$= \langle S_z^F V_x^G + V_z^F S_x^G - \frac{S_z^F}{L} (\frac{S_x^G}{L} D_{xx}^{LL} + S_y^G V_x^L) \rangle \qquad (2.28)$$

2.2c. Effect of orbital motion

During the small time interval δt the dinuclear axis $\hat{R}$ turns a small angle $\delta\Theta = \omega_R \delta_t$ around the $\hat{L}$-direction. In order to refer the dynamical quantities to an inertial system aligned with the new direction of $\hat{R}$ it is thus necessary to perform a small rotation around that y-axis. The corresponding rotation operator is

$$\overleftrightarrow{\mathcal{R}}_y(\phi) = e^{i \overleftrightarrow{S}_y \phi} = \begin{pmatrix} \cos\phi & 0 & -\sin\phi \\ 0 & 1 & 0 \\ \sin\phi & 0 & \cos\phi \end{pmatrix} \qquad (2.29)$$

where the spin matrix is

$$\overleftrightarrow{S}_y = \begin{pmatrix} 0 & 0 & i \\ 0 & 0 & 0 \\ -i & 0 & 0 \end{pmatrix} \tag{2.30}$$

Thus, any vector transforms as

$$\begin{aligned} (\overleftarrow{S}^F)^{new} &= \overleftrightarrow{R}_y(\phi) \cdot \overleftarrow{S}^F \\ &\approx (\overleftrightarrow{I} + i\,\omega_R\,\overleftrightarrow{S}_y\,\delta t) \cdot \overleftarrow{S}^F \end{aligned} \tag{2.31}$$

Therefore, in the limit $\delta t \to 0$, we have

$$(\dot{\overleftarrow{S}}^F)^{rot} = i\,\omega_R\,\overleftrightarrow{S}_y \cdot \overleftarrow{S}^F \tag{2.32}$$

That is

$$\begin{aligned} (\dot{S}_x^F)^{rot} &= -\omega_R\,S_z^F \\ (\dot{S}_y^F)^{rot} &= 0 \\ (\dot{S}_z^F)^{rot} &= \omega_R\,S_x^F \end{aligned} \tag{2.33}$$

It follows that for a standard spin distribution, which has $\langle S_x^F \rangle = \langle S_z^F \rangle = 0$, there is no effect on the mean values.

The spin covariances are seen to be affected as follows:

$$(\dot{\overleftrightarrow{\sigma}}^{FG})^{rot} = i\omega_R [\overleftrightarrow{\epsilon}_y, \overleftrightarrow{\sigma}^{FG}] \tag{2.34}$$

That is

$$\begin{aligned}
(\dot{\sigma}^{FG}_{xx})^{rot} &= -\omega_R (\sigma^{FG}_{xz} + \sigma^{FG}_{zx}) \\
(\dot{\sigma}^{FG}_{zz})^{rot} &= \omega_R (\sigma^{FG}_{xz} + \sigma^{FG}_{zx}) \\
(\dot{\sigma}^{FG}_{xz})^{rot} &= \omega_R (\sigma^{FG}_{xx} - \sigma^{FG}_{zz}) = (\dot{\sigma}^{FG}_{zx})^{rot}
\end{aligned} \tag{2.35}$$

with all the other components remaining unaffected for a standard distribution.

The above differential increments are to be added to the increments determined in the preceeding, in order to obtain the total rate of change in the moments of the spin distribution.

2.2d. Harmonic expansion around the mean trajectory

In the derived equations of motion the RHS contains averages over the spin distribution. The general evaluation of these averages would be very cumbersome and render the equations impractical. However, as is most often the case, when the spin distribution is reasonably narrow one may evaluate the averages to a good approximation by expanding the mobility coefficients to first order around the mean spin values, ignoring the variation of other

quantities such as τ^* and N. This method is referred to as the mean trajectory method since it requires only information along the mean dynamical trajectory. It consists in the following approximations:

$$\begin{aligned} \langle \vec{V}^F \rangle &\approx \vec{V}^F \\ \langle \overleftrightarrow{D}^{FG} \rangle &\approx \overleftrightarrow{D}^{FG} \\ \langle \overleftarrow{S}^F \vec{V}^H \rangle &\approx \langle \overleftarrow{S}^F \sum_G (\vec{S}^G - \langle \vec{S}^G \rangle) \rangle \frac{\partial \vec{V}^H}{\partial \overleftarrow{S}^G} \\ &= -\sum_G \overleftrightarrow{\sigma}^{FG} \cdot \overleftrightarrow{M}^{GH} / \mathcal{J}_G \end{aligned} \tag{2.36}$$

where the RHS is understood to be evaluated for the mean spin values.

2.2e. Final dynamical equations

By combining the effect of the orbital rotation with the preceding equations and making the mean-trajectory approximation we can derive the final form of the dynamical equations for the spin moments.

In deriving this final form, the occurrence of L in the denominator poses a special problem. Under the general assumption that the fluctuations are small relative to the size of L_y:

$$|\sigma^{FG}_{ij}| \ll \langle L_y \rangle^2 \qquad \forall F,G \quad \forall i,j \tag{2.37}$$

1/L can be expanded around its mean value, and we may neglect all terms containing variances in the numerator, for example:

$$\left\langle \frac{1}{L_y} \right\rangle = \frac{1}{\langle L_y \rangle} + \frac{\sigma_{yy}^{LL}}{\langle L_y \rangle^3} + \cdots$$

$$= \frac{1}{\langle L_y \rangle} \left(1 + \sigma\left(\frac{\sigma_{yy}^{LL}}{\langle L_y \rangle^2} \right) \right) \tag{2.38}$$

$$\left\langle \frac{S_y^F S_y^G}{L_y^2} \right\rangle = \frac{\langle S_y^F \rangle \langle S_y^G \rangle}{\langle L_y \rangle^2} + \frac{\sigma_{yy}^{FG}}{\langle L_y \rangle^2} - 2 \frac{\langle S_y^F \rangle \sigma_{yy}^{LG} + \sigma_{yy}^{FL} \langle S_y^G \rangle}{\langle L_y \rangle^3}$$

$$= \frac{\langle S_y^F \rangle \langle S_y^G \rangle}{\langle L_y \rangle^2} + \sigma\left(\frac{\sigma_{yy}}{\langle L_y \rangle^2} \right)$$

When inserted into the equations, the neglected terms will always be of the order of $\sigma_{ij}^{FG}/\langle L_y \rangle^2$ relative to the main terms. Some of the retained terms, for example $\langle S_y^F \rangle \langle S_y^H \rangle / \langle L_y \rangle^2$, may generally be of the same size as the main terms although, in certain cases, they are actually smaller than the neglected terms.

Proceeding as just described, we arrive at the following final equations for the spin moments:

$$\dot{S}_y^F = -\sum_G \left(M_t^{FG} S_y^G + \frac{1}{L_y} \sigma_{xx}^{FG} M_t^{GL} \right) / \mathcal{I}_G + \frac{\tau^*}{L_y} \left(2 M_t^{FL} - \frac{S_y^F}{L_y} M_t^{LL} \right)$$

$$\dot{\sigma}_{xx}^{FH} = 2\tau^* M_t^{FH} - \sum_G \left(\sigma_{xx}^{FG} M_t^{GH} + M_t^{FG} \sigma_{xx}^{GH} \right) / \mathcal{I}_G - \omega_R \left(\sigma_{xz}^{FH} + \sigma_{zx}^{FH} \right)$$

$$- \frac{S_y^F}{L_y} \left(2\tau^* M_t^{LH} - \sum_G M_t^{LG} \sigma_{xx}^{GH} / \mathcal{I}_G \right) - \left(2\tau^* M_t^{FL} - \sum_G \sigma_{xx}^{FG} M_t^{GL} / \mathcal{I}_G \right) \frac{S_y^H}{L_y} \tag{2.39}$$

$$+ 2\tau^* \frac{S_y^F}{L_y} M_t^{LL} \frac{S_y^H}{L_y}$$

$$\dot{\sigma}_{yy}^{FH} = 2\tau^* M_t^{FH} - \sum_G \left(\sigma_{yy}^{FG} M_t^{GH} + M_t^{FG} \sigma_{yy}^{GH} \right) / \mathcal{I}_G$$

$$\dot{\sigma}^{FH}_{zz} = 2\tau^* M^{FH}_n - \sum_G (\sigma^{FG}_{zz} M^{GH}_n + M^{FG}_n \sigma^{GH}_{zz})/\mathcal{J}_G + \omega_R(\sigma^{FH}_{xz} + \sigma^{FH}_{zx})$$

$$\dot{\sigma}^{FH}_{xz} = -\sum_G (\sigma^{FG}_{xz} M^{GH}_n + M^{FG}_t \sigma^{GH}_{xz})/\mathcal{J}_G + \omega_R(\sigma^{FH}_{xx} - \sigma^{FH}_{zz}) + \frac{S^F_y}{L_y} \sum_G M^{LG}_t \sigma^{GH}_{xz}/\mathcal{J}_G$$

$$\dot{\sigma}^{FH}_{zx} = -\sum_G (\sigma^{FG}_{zx} M^{GH}_t + M^{FG}_n \sigma^{GH}_{zx})/\mathcal{J}_G + \omega_R(\sigma^{FH}_{xx} - \sigma^{FH}_{zz}) + \sum_G \sigma^{FG}_{zx} M^{GL}_t/\mathcal{J}_G \frac{S^H_y}{L_y}$$

Here we have omitted the bracket around the mean values of S^F_y for notational simplicity, since confusion can hardly arise.

It can readily be verified that the equations satisfy the following necessary conditions implied by our specific treatment:

i) the y-axis remains directed along $\vec{L}$:

$$\sigma^{LF}_{ij} = 0 \quad \Rightarrow \quad \dot{\sigma}^{LF}_{ij} = 0 \qquad (i,j \neq y) \tag{2.40}$$

ii) The size of the angular momentum is conserved to the order of terms kept in the equations:

$$\frac{d}{dt}\langle|\vec{J}|\rangle = \dot{J}_y + \frac{1}{2}\frac{1}{J_y}[J_y(\dot{\sigma}^{JJ}_{xx} + \dot{\sigma}^{JJ}_{yy} + \dot{\sigma}^{JJ}_{zz}) - \dot{J}_y(\sigma^{JJ}_{xx} + \sigma^{JJ}_{yy} + \sigma^{JJ}_{zz})]$$

$$= \frac{1}{2}\frac{1}{J_y}(\sigma^{JJ}_{xx} + \sigma^{JJ}_{yy} + \sigma^{JJ}_{zz})\frac{1}{L_y}\left(\sum_G \sigma^{JG}_{xx} M^{GL}_t/\mathcal{J}_G - \tau^* \frac{J_y}{L_y} M^{LL}_t\right) \tag{2.41}$$

Since J_y is of the order of L_y, the last expression for $d\langle|J|\rangle/dt$ is of the order of the terms neglected in the expansion of $1/L$, cf. equations (2.37)-(2.38). Furthermore, it can be shown that the equations (2.39) ensure that $d\langle J^2\rangle/dt = 0$. Hence the variance of $J = |\vec{J}|$, $\sigma_J^2 \equiv \langle J^2\rangle - \langle|\vec{J}|\rangle^2$, which is initially zero, remains so in time, and consequently the magnitude of $\vec{J}$ remains sharply defined and equal to its initial value.

2.3 Transformation to external coordinate system

In the preceeding we have derived the equations of motion for the spin moments with reference to a coordinate system defined in terms of the instantaneous values of $\hat{R}$ and $\hat{L}$. However, the direction $\hat{L}$ can not be determined in a collision experiment, so it is necessary to reexpress the results with reference to a coordinate system which can be externally defined.

In a collision experiment two directions are readily determined: the beam direction $\hat{t}$ and the asymptotic dinuclear direction $\hat{R}(\infty)$. In terms of these two directions we define the following external coordinate system XYZ:

$$\hat{Z} = \hat{R}\,, \quad \hat{Y} = \hat{R} \times \hat{t}\,, \quad \hat{X} = \hat{Y} \times \hat{Z} \tag{2.42}$$

Although $\hat{R}$ is only experimentally accessible at very large times we may generalize the above defintion to yield an "external" coordinate system at an arbitrary time (by using the dinuclear direction $\hat{R}(t)$ at that particular time t).

Since the internal and the external coordinate systems have the same z-axis, the two are related by a rotation around the z-axis, $\mathcal{R}_z(\zeta)$. The angle ζ between the directions $\hat{L}$ and $\hat{Y}$ can be determined by exploiting the fact that $\hat{L}$ is perpendicular to the dinuclear axis $\hat{R}$ and $\hat{J}$ is perpendicular to

the beam direction $\hat{t}$. We shall make the assumption that the directional dispersions in $\hat{L}$ and $\hat{J}$ are relatively small, as is consistent with the derived equations of motion. In that case also ζ is small and elementary trigonometric considerations, described in Fig. 1, yield

$$\zeta \approx \hat{J}_x + \hat{J}_z \cot\Theta \tag{2.43}$$

where Θ is the angle between $\hat{z}$ and $\hat{t}$, i.e., the CM scattering angle for large times.

With the above relation between ζ and $\hat{J}$ it is straightforward to derive the relevant transformations. For the mean values we find

$$\begin{aligned} \langle S_Y^F \rangle &= \langle S_x^F \sin\zeta + S_y^F \cos\zeta \rangle \\ &\approx \langle S_x^F \zeta + S_y^F \rangle \\ &= \langle S_x^F (\hat{J}_x + \hat{J}_z \cot\Theta) + S_y^F \rangle \end{aligned} \tag{2.44}$$

i.e.,

$$S_Y^F \approx S_y^F + \frac{1}{J}(\sigma_{xx}^{FJ} + \sigma_{xz}^{FJ} \cot\Theta) \tag{2.45}$$

where we again omit the brackets for convenience. Similarly it follows that $S_X^F, S_Z^F = 0$ for a standard distribution.

Furthermore, for the spin covariance we find,

$$\langle S_X^F S_X^G \rangle = \langle (S_x^F \cos\zeta - S_y^F \sin\zeta)(S_x^G \cos\zeta - S_y^G \sin\zeta) \rangle$$
$$\approx \langle S_x^F S_x^G \rangle - S_y^F \langle S_x^G \zeta \rangle - \langle \zeta S_x^F \rangle S_y^G + \langle S_y^F S_y^G \zeta^2 \rangle \qquad (2.46)$$

so that

$$\sigma_{XX}^{FG} \approx \sigma_{xx}^{FG} - \frac{S_y^F}{J}(\sigma_{xx}^{GJ} + \sigma_{x2}^{GJ}\cot\Theta) - (\sigma_{xx}^{JF} + \sigma_{2x}^{JF}\cot\Theta)\frac{S_y^G}{J}$$
$$+ \frac{S_y^F S_y^G}{J^2}(\sigma_{xx}^{JJ} + 2\sigma_{x2}^{JJ}\cot\Theta + \sigma_{22}^{JJ}\cot^2\Theta) , \qquad (2.47)$$

$$\langle S_Y^F S_Y^G \rangle = \langle (S_x^F \sin\zeta + S_y^F \cos\zeta)(S_x^G \sin\zeta + S_y^G \cos\zeta) \rangle$$
$$\approx \langle S_y^F S_y^G \rangle + S_y^F \langle S_x^G \zeta \rangle + \langle \zeta S_x^F \rangle S_y^G \qquad (2.48)$$

so that

$$\sigma_{YY}^{FG} \equiv \langle S_Y^F S_Y^G \rangle - S_Y^F S_Y^G \approx \sigma_{yy}^{FG} , \qquad (2.49)$$

$$\sigma_{ZZ}^{FG} = \sigma_{zz}^{FG} , \qquad (2.50)$$

$$\langle S_X^F S_Z^G \rangle = \langle (S_x^F \cos\zeta - S_y^F \sin\zeta) S_z^G \rangle$$
$$\approx \langle S_x^F S_z^G \rangle - S_y^F \langle S_z^G \zeta \rangle \qquad (2.51)$$

so that

$$\sigma_{xz}^{FG} \approx \sigma_{xz}^{FG} - \frac{S_y^F}{J}\left(\sigma_{zx}^{GJ} + \sigma_{zz}^{GJ}\cot\Theta\right), \tag{2.52}$$

$$\begin{aligned}\langle S_z^F S_x^G\rangle &= \langle S_z^F\,(S_x^G\cos\zeta - S_y^G\sin\zeta)\rangle \\ &\approx \langle S_z^F S_z^G\rangle - \langle\zeta S_z^F\rangle S_y^G\end{aligned} \tag{2.53}$$

so that

$$\sigma_{zx}^{FG} \approx \sigma_{zx}^{FG} - \left(\sigma_{xz}^{JF} + \sigma_{zz}^{JF}\cot\Theta\right)\frac{S_y^G}{J} \tag{2.54}$$

and the rest of the elements remaining zero, for a standard spin distribution.

3. Other observables

In the preceding section we have concentrated on the description of the angular momentum observables in the dinucleus. It is usually of interest to consider other observables as well. In particular, it is necessary to consider the relative energy since the data is usually given as function of energy loss.

3.1. Mass and charge partition

The partition of mass and charge in the dinucleus is conveniently described by specifying the neutron number N and the proton number Z associated with the projectile-like nucleide (those associated with the partner then follow by conservation of the total baryon number and charge). The final values of N and Z are readily determined experimentally by measuring the charge and mass number of either fragment, with due correction for sequential decay processes, of course (see the subsequent paper II).

The general expressions for the transport coefficients relating to N and Z were derived in ref.[5]. The key quantities are the mobility coefficients

$$M_{NN} = N'_N \,, \quad M_{ZZ} = N'_Z \,, \quad M_{NZ} = M_{ZN} = 0 \tag{3.1}$$

for which explicit expressions are given in ref.[6] in our standard model. In terms of these, the drift and diffusion coefficients are

$$\begin{aligned} V_N &= M_{NN} F_N \,, & D_{NN} &= M_{NN} \tau^* \\ V_Z &= M_{ZZ} F_Z \,, & D_{ZZ} &= M_{ZZ} \tau^* \end{aligned} \tag{3.2}$$

with $D_{NZ} = M_{NZ}\tau^* = 0$. Furthermore, within the approximations made in developing the model[7], the diffusion coefficients mixing N or Z with any of the other basic observables vanish. Here $F_N = -\partial\mathcal{H}/\partial N$ and $F_Z = -\partial\mathcal{H}/\partial Z$ are the driving forces acting on N and Z; explicit expressions for these are given in ref.[8].

The mean values of N and Z then evolve according to

$$\begin{aligned} \frac{d}{dt}\langle N\rangle &= \langle V_N\rangle \approx M_{NN} F_N \\ \frac{d}{dt}\langle Z\rangle &= \langle V_Z\rangle \approx M_{ZZ} F_Z \end{aligned} \tag{3.3}$$

where the RHS is understood to be evaluated at the average position of the ensemble. Furthermore, the covariences are governed by the following three coupled equations.

$$\begin{aligned} \dot{\sigma}_{NN} &= 2\left(M_{NN}\tau^* + \sigma_{NN}\frac{\partial V_N}{\partial N} + \sigma_{NZ}\frac{\partial V_N}{\partial Z}\right) \\ \dot{\sigma}_{NZ} &= \sigma_{NN}\frac{\partial V_Z}{\partial N} + \sigma_{ZZ}\frac{\partial V_N}{\partial Z} + \sigma_{NZ}\left(\frac{\partial V_N}{\partial N} + \frac{\partial V_Z}{\partial Z}\right) \\ \dot{\sigma}_{ZZ} &= 2\left(M_{ZZ}\tau^* + \sigma_{ZZ}\frac{\partial V_Z}{\partial Z} + \sigma_{NZ}\frac{\partial V_Z}{\partial N}\right) \end{aligned} \tag{3.4}$$

where again the quantities on the RHS are to be evaluated at the mean position. Explicit expressions for the derivatives are given in ref.[6] The above dynamical equations were already given in ref.[8] They can be solved by integration along the mean trajectory.

3.2. Radial motion

The dinuclear separation degree of freedom is described by the center separation R and the conjugate radial momentum P. They are important to study in order to obtain information on the loss of relative energy (see section 3.3) or the fluctuations in scattering angle (which we are not concerned with in the present paper).

In the present theory, where recoil terms are consistently neglected, the transport coefficients relating to the radial motion are given by

$$V_R = 0 \quad , \quad D_{RR} = 0$$

$$V_P = -2 \frac{m}{\mu} N P \quad , \quad D_{PP} = 2 m N \tau^* \tag{3.5}$$

with D_{RP} as well as the mixed diffusion coefficients coupling R or P to any other basic observable vanishing. (In (3.5) $N = N_N + N_Z$ is the total nucleon current [6].)

The evolution of the observables R and P is complicated by the fact that they are not constants of motion in the absence of the dissipative coupling. Thus the equations of motion for the associated mean values and covariances have addditional terms arising from the conservative propagation of the system. These terms were included in the general equations given in ref.[6]) for the mean values (eq. (2.4) and covariances (eq. (2.6)). The results below follow from straightforward insertion into those formulas.

Thus, the mean values of R and P evolve as

$$\frac{d}{dt}\langle R\rangle = \langle \{R, \mathcal{H}\} + V_R \rangle = \langle \frac{\partial \mathcal{H}}{\partial P} \rangle$$

$$= \langle \frac{P}{\mu} \rangle \approx \frac{1}{\mu} \langle P \rangle$$

$$\frac{d}{dt}\langle P\rangle = \langle \{P, \mathcal{H}\} + V_P \rangle = \langle -\frac{\partial \mathcal{H}}{\partial R} - 2\frac{m}{\mu} N P \rangle \tag{3.6}$$

$$\approx F_R - 2\frac{m}{\mu} N \langle P \rangle$$

where, as usual, the quantitities in the last expressions are to be evaluated at the mean position. In the above equations $F_R = -\partial\mathcal{H}/\partial R$ is the radial driving force. The evolution of the associated covariances is governed by the three coupled equations

$$\dot{\sigma}_{RR} = \langle \{\Delta R \Delta R, \mathcal{H}\} + 2D_{RR} + 2\Delta R V_R \rangle$$

$$= \langle \frac{2}{\mu} \Delta R P \rangle \approx \frac{2}{\mu} \sigma_{RP}$$

$$\dot{\sigma}_{RP} = \langle \{\Delta R \Delta P, \mathcal{H}\} + 2D_{RP} + \Delta R V_P + \Delta P V_R \rangle \tag{3.7}$$

$$= \langle \Delta R F_R + \frac{P}{\mu} \Delta P + \Delta R \Delta P \frac{\partial V_P}{\partial P} \rangle$$

$$\approx \frac{\partial F_R}{\partial R} \sigma_{RR} + \frac{1}{\mu} \sigma_{PP} - 2\frac{m}{\mu} N \sigma_{RP}$$

$$\dot{\sigma}_{PP} = \langle \{\Delta P \Delta P, \mathcal{H}\} + 2D_{PP} + 2\Delta P V_P \rangle$$

$$= 2\langle \Delta P F_R + 2m N \tau^* + \Delta P \Delta P \frac{\partial V_P}{\partial P} \rangle$$

$$\approx 2\frac{\partial F_R}{\partial R} \sigma_{RP} + 4mN\tau^* - 4\frac{m}{\mu} N \sigma_{PP}$$

In the above equations the terms containing the Poisson bracket are those arising from the conservative propagation of R and P. It is noteworthy that the equations (3.7) do not couple to other observables than R and P.

3.3. Dependent observables

In the present transport theory the macroscopic variables $\mathcal{C} = (\zeta_1, \zeta_2, \ldots)$ represent one-particle observables, specifically the quantities $\vec{R}$, $\vec{P}$, $\vec{L}$, $\vec{S}^A$, $\vec{S}^B$, N, Z. Often it is of interest to also study observables which are non-linear functions of these basic observables. The most frequent example is the relative energy of the two nucleides. Being expressible in terms of the basic observables $\mathcal{C}$, such dependent quantities are of course redundant and need not be included in the dynamical equations. Below we first discuss the general evaluation of mean values and covariances for dependent observables and subsequently we consider specifically the relative energy.

3.3.a. General treatment of dependent observables

We consider a dependent observable $F(\mathcal{C})$ which is locally harmonic. In the region of interest it then has the form

$$F(\mathcal{C}) = \underline{F} + \sum_i \underline{F}'_i \, \Delta\zeta_i + \tfrac{1}{2} \sum_{ij} \underline{F}''_{ij} \, \Delta\zeta_i \, \Delta\zeta_j \qquad (3.8)$$

where $\Delta\zeta_i = \zeta_i - \langle\zeta_i\rangle$ is the deviation of ζ_i from the ensemble average value, as usual, and the derivatives are $F'_i = \partial F/\partial\zeta_i$ and $F''_{ij} = \partial^2 F/\partial\zeta_i\partial\zeta_j$. A bar under a quantity indicates that it should be evaluated at the mean value $\mathcal{C} = \langle\mathcal{C}\rangle$.

The ensemble average of F is then given by

$$\langle F \rangle = \underline{F} + \frac{1}{2} \sum_{ij} \underline{F}''_{ij} \sigma_{ij} \tag{3.9}$$

Moreover, the covariance between two dependent observables $F(\mathcal{C})$ and $G(\mathcal{C})$ is

$$\begin{aligned}
\sigma_{FG} &= \langle FG \rangle - \langle F \rangle \langle G \rangle \\
&= \underline{F}\,\underline{G} + \sum_{ij} \underline{F}'_i \underline{G}'_j \sigma_{ij} + \frac{1}{2} \sum_{ij} (\underline{F}\,\underline{G}''_{ij} + \underline{F}''_{ij}\,\underline{G}) \sigma_{ij} \\
&+ \frac{1}{4} \sum_{ij} \sum_{kl} \underline{F}''_{ij}\,\underline{G}''_{kl} \langle \Delta\zeta_i \Delta\zeta_j \Delta\zeta_k \Delta\zeta_l \rangle \\
&- (\underline{F}\,\underline{G} + \frac{1}{2} \sum_{ij} (\underline{F}\,\underline{G}''_{ij} + \underline{F}''_{ij}\,\underline{G}) \sigma_{ij} + \frac{1}{4} \sum_{ij} \sum_{kl} \underline{F}''_{ij}\,\underline{G}''_{kl}\, \sigma_{ij}\, \sigma_{kl}) \\
&= \sum_{ij} \underline{F}'_i \underline{G}'_j \sigma_{ij} + \frac{1}{2} \sum_{ijkl} \underline{F}''_{ij}\,\underline{G}''_{kl}\, \sigma_{ik}\, \sigma_{jl}
\end{aligned} \tag{3.10}$$

where we have invoked that

$$\langle \Delta\zeta_i \Delta\zeta_j \Delta\zeta_k \Delta\zeta_l \rangle = \sigma_{ij}\sigma_{kl} + \sigma_{ik}\sigma_{jl} + \sigma_{il}\sigma_{jk} \tag{3.11}$$

for a gaussian ensemble. A special case of the above formula is when G is taken as one of the basic observables ζ. Then

$$\sigma_{F\zeta} = \sum_i \underline{F}'_i \sigma_{i\zeta} \tag{3.12}$$

since then $G'_j = \delta_{j\zeta}$ and $G''_{ij} = 0$.

The above expressions can be used to calculate mean values and covariances for any (locally harmonic) dependent observable of interest. While thus strictly unneeded, it is instructive to consider the form of the time derivative of the mean value of a dependent observable:

$$\frac{d}{dt}\langle F\rangle = \sum_i \underline{F}'_i \langle V_i\rangle + \sum_{ij} \underline{F}''_{ij} \langle V_i \Delta\zeta_j + D_{ij}\rangle$$
$$= \sum_i \underline{F}'_i V_i + \sum_{ijk} \underline{F}''_{ij} \frac{\partial V_i}{\partial \zeta_k} \sigma_{kj} + \sum_{ij} \underline{F}''_{ij} D_{ij} \qquad (3.13)$$

This expression can be obtained either by using the Fokker-Planck equation for the evolution of the distribution function $f(\boldsymbol{\zeta})$ or by simply taking the time derivative of (3.9). [For simplicity, the possible occurrence of conservative terms has been ignored.] The first term is the rate of change in $\langle F\rangle$, induced by the motion of the system along the mean trajectory; this is usually the dominant term away from equilibrium. The second term is the (second-order) correction due to the finite width of the distribution $f(\boldsymbol{\zeta})$ as given through the covariances σ_{kj}. The third term is the contribution arising from the diffusive growth of the distribution; it would be the dominant term if the ensemble was prepared as a narrow distribution close to the equilibrium point. It is readily verified that (3.13) vanishes for the equilibrium distribution, as it should be.

3.3b. Relative energy

The loss of relative energy, usually denoted TKEL (for Total Kinetic Energy Loss), is an important observable in the study of damped nuclear reactions. Loosely speaking, it can be thought of as a generalized time

parameter which expresses the degree of intimacy achieved in a given reaction and it is instructive to consider the other observables as functions of TKEL.

After the two reacting nucleides have lost contact, i.e., after their mutual nuclear interaction has ceased, their relative energy is a constant of motion given by

$$E = \frac{P^2}{2\mu} + \frac{L^2}{2\mu R^2} + e^2 \frac{Z_A Z_B}{R} \tag{3.14}$$

Of course, any sequential decays of the primary reaction products will modify this quantity but this need not concern us here; this aspect is discussed in the subsequent paper II. The formulas derived above can be used to calculate the ensemble average of E and its covariances.

Since E only depends on the basic observables R, P, L (neglecting the usually very small effect from the dependence on mass asymmetry through the reduced mass μ), the summations in (3.9-10) only extend over these variables. For the first derivatives of E we then have

$$\begin{aligned} E'_R &\equiv \frac{\partial E}{\partial R} = -\frac{2}{R}\,\frac{L^2}{2\mu R^2} - \frac{1}{R}\,V_c \\ E'_P &\equiv \frac{\partial E}{\partial P} = \frac{P}{\mu} \\ E'_L &\equiv \frac{\partial E}{\partial L} = \frac{L}{\mu R^2} \end{aligned} \tag{3.15}$$

The second derivatives are

$$E''_{RR} = \frac{6}{R^2}\,\frac{L^2}{2\mu R^2} + \frac{2}{R^2}\,V_c$$

$$E''_{PP} = \frac{1}{\mu}\,, \quad E''_{LL} = \frac{1}{\mu R^2} \tag{3.16}$$

$$E''_{RL} = -\frac{2}{R}\,\frac{L}{\mu R^2}$$

with the remaining ones vanishing. Therefore, we find the mean value

$$\langle E\rangle = \underline{E} + \tfrac{1}{2}\left(\underline{E}''_{RR}\,\sigma_{RR} + \underline{E}''_{PP}\,\sigma_{PP} + \underline{E}''_{LL}\,\sigma_{LL}\right), \tag{3.17}$$

the variance

$$\begin{aligned}\sigma_{EE} = {} & (\underline{E}'_R)^2\sigma_{RR} + (\underline{E}'_P)^2\sigma_{PP} + (\underline{E}'_L)^2\sigma_{LL} + 2\underline{E}'_R\,\underline{E}'_P\,\sigma_{RP} \\ & + \tfrac{1}{2}\left((\underline{E}''_{RR}\,\sigma_{RR})^2 + (\underline{E}''_{PP}\,\sigma_{PP})^2 + (\underline{E}''_{LL}\,\sigma_{LL})^2\right) \\ & + \underline{E}''_{RR}\,\underline{E}''_{PP}\,\sigma_{RP}^2 + (\underline{E}''_{RL})^2\,\sigma_{RR}\,\sigma_{LL}\end{aligned} \tag{3.18}$$

and the covariances with the spin observables

$$\sigma_{EF} = \underline{E}'_L\,\sigma_{LF}\,, \quad F = S^A_y\,,\ S^B_y\,,\ L_y \tag{3.19}$$

The above results can be used to calculate the mean value and covariances of TKEL = E(0) - E(∞) (by simply performing the proper sign change in (3.17) and (3.19)) resulting from a reaction with a specified impact parameter. These quantities, in turn, make it possible to express the results as functions of TKEL, after integration over the impact parameter, as the experimental conditions dictate. This is described in the next section.

In the original development[5] of the theory of transfer-induced transport in damped nuclear reactions the dissipated energy was treated in a simple approximate manner: the heat Q was represented as an effective one-body operator, using for the matrix elements the exciton energies ω associated with individual nucleon transfers. This approach is strictly valid when the macroscopic hamiltonian $\mathcal{H}$ is a linear function of the basic one-body observables $\mathcal{C}$. Hence, when $\mathcal{H}$ can be idealized as locally linear, the dependent observable Q can be treated on an equal footing with the basic observables $\mathcal{C}$. The resulting mean dissipated energy <Q> then corresponds to the energy dissipated along the mean trajectory in $\mathcal{C}$-space. This is usually a reasonably good approximation since the second-order corrections appearing in (3.17) tend to be at the percentage level. However, the idealized treatment is unsatisfactory for the covariances associated with Q and when they are needed recourse must be taken to the above formulas (3.18) and (3.19).

3.3c. Scattering angle

It is of some interest to estimate the variance in the scattering angle Θ for a given value of the total angular momentum J. There are two contributions to this quantity: One is the variance accumulated in the orientation angle Φ during the reaction phase; this contribution is quite analogous to the variance accumulated in the separation R. The other contribution arises from the fact that there are fluctuations in N, Z, R, P, L at the time of neck rupture when contact is lost between the two nucleides; these fluctuations are propagated along the respective Coulomb trajectories, thus resulting in different increments of Φ during the exit phase. The two contributions are of comparable magnitude and therefore need both be considered.

The variance in the angle ϑ, which orients the dinuclear axis in the (instantaneous) reaction plane, can be calculated by employing the same method as in section 3.2. We thus obtain the following dynamical equations for the relevant covariances,

$$\dot{\sigma}_{\vartheta\vartheta} = 2\,\frac{\sigma_{\vartheta L}}{\mathcal{I}_R} \tag{3.20}$$

$$\dot{\sigma}_{\vartheta F} = \frac{\sigma^{LF}_{yy}}{\mathcal{I}_R} - \sum_G M_t^{FG}\,\frac{\sigma_{\vartheta G}}{\mathcal{I}_G} \quad , \quad F,G = A,B,L$$

where $\sigma_{\vartheta F} \equiv \langle \vartheta S_y^F \rangle - \langle \vartheta \rangle \langle S_y^F \rangle$ is the covariance between ϑ and the spin component S_y^F. These equations can be solved along with the other moment equations of motion to yield the value of $\sigma_{\vartheta\vartheta}$ the exit time t_{exit} when the neck vanishes.

In order to calculate the variance in the scattering angle arising from the fluctuations in the starting conditions for the exit orbit we make use of the fact that the scattering angle is given by $\Theta = \pi - \vartheta(t_{exit}) - \Delta\vartheta_{out}$ where $\Delta\vartheta_{out}$ is the increment in ϑ accumulated along the outgoing Coulomb orbit. This quantity is

$$\Delta\vartheta_{out} = \arccos\frac{1}{\epsilon}\left(1 + \frac{L^2}{\mu e^2 Z_A Z_B R}\right) - \arccos\frac{1}{\epsilon} \tag{3.21}$$

where the eccentricity of the orbit is

$$\epsilon = \left[1 + \frac{2EL^2}{\mu (e^2 Z_A Z_B)^2}\right]^{1/2} \tag{3.22}$$

with the relative energy E given by (3.14). The scattering angle Θ can thus be considered as a function of the exit values of the basic variables N, Z, R, P, L and the general formula (3.10) for the variance of a dependent observable can be employed. Since Θ(N, Z, R, P,L) is fairly well-behavied, only the first-order terms in (3.10) need be included. So we arrive at the result

$$\sigma_{\theta\theta} = \sigma_{\theta\theta}(t_{exit}) + (\underline{\theta}'_N)^2\sigma_{NN} + (\underline{\theta}'_Z)^2\sigma_{ZZ} + 2\,\underline{\theta}'_N\,\underline{\theta}'_Z\,\sigma_{NZ} \qquad (3.23)$$

$$+ (\underline{\theta}'_L)^2\sigma_{LL} + (\underline{\theta}'_R)^2\sigma_{RR} + (\underline{\theta}'_P)^2\sigma_{PP} + 2\,\underline{\theta}'_R\,\underline{\theta}'_P\,\sigma_{RP}$$

where the partial derivatives $\underline{\theta}'_N$, θ'_Z, $\underline{\theta}'_L$, $\underline{\theta}'_R$, $\underline{\theta}'_P$ are readily calculated on the basis of (3.21). Usually the largest term in the exit-phase contribution to $\sigma_{\Theta\Theta}$ is that arising from the fluctuations in the orbital angular momentum L, but the other terms are typically of the same order of magnitude and should therefore be retained.

4. Differential cross sections

In the present study, the calculated results are obtained by solving the coupled moment equations of motion, starting from an initial condition specified by a definite impact parameter s. This procedure yields the normalized probability distribution $f(\vec{\vec{c}})$, as characterized by the mean values $\langle \vec{\vec{c}} \rangle$ and associated covariances $\overleftrightarrow{\sigma}$. In this section, $\vec{\vec{c}}$ denotes a set of observables in which some of the basic one-body observables may have been replaced by dependent observables. These dependent observables are assumed to be sufficiently smooth functions of the independent ones so that the distribution in $\vec{\vec{c}}$ can be considered as gaussian. Especially, the observables R and P may have been replaced by the relative energy E whose mean value and covariances are given by (3.9) and (3.12).

Since experimental conditions preclude measurement of the impact parameter s, this variable must be eliminated by integration. This yields the multi-differential cross section

$$\frac{d\sigma}{d\vec{\vec{c}}} = \int f_s(\vec{\vec{c}})\, d\vec{s} \tag{4.1}$$

which is practically amenable to experimental observation. The above expression is of course singular since the s-integration is unbounded. However, this standard problem is purely formal, since in practice one is only interested in cross sections for non-trivial reactions leading to a finite energy loss TKEL. Therefore, this quantity, or, equivalently but notationally more conveniently, the final relative energy E, takes the place of s as a parameter for the distribution function.

4.1 Analytical approximation

When the interest is focussed on a reaction leading to a specified final relative energy E, the integrand in (4.1) is peaked around that impact parameter s_0 which leads to the specified energy E on the average. Therefore it is natural to attempt an analytical approximation by expansion around that value. Thus one may assume

$$\langle \vec{\vec{C}} \rangle_s \approx \vec{\vec{C}}_0 + (s - s_0)\, \vec{\vec{C}}_0' \qquad \vec{\vec{\sigma}}_s \approx \vec{\vec{\sigma}}_0 \tag{4.2}$$

where $\vec{\vec{C}}_0 \equiv \langle \vec{\vec{C}} \rangle_{s_0}$, $\vec{\vec{\sigma}}_0 \equiv \vec{\vec{\sigma}}_{s_0}$ and $\vec{\vec{C}}_0' \equiv (d\langle \vec{\vec{C}} \rangle_s / ds)_{s=s_0}$.

Insertion of this approximation into the gaussian integrand in (4.1) yields an exponent which is a second-order polynomial in s. Assuming furthermore that $d\vec{s} \approx 2\pi s_0 ds$, the s-integration can be carried out by "completing the square". This leaves the exponent

$$(\vec{\vec{C}} - \vec{\vec{C}}_0) \cdot \vec{\vec{\sigma}}_0^{-1} \cdot \left(\vec{\vec{I}} - \frac{\vec{\vec{C}}_0' \vec{\vec{C}}_0' \cdot \vec{\vec{\sigma}}_0^{-1}}{\vec{\vec{C}}_0' \cdot \vec{\vec{\sigma}}_0^{-1} \cdot \vec{\vec{C}}_0'} \right) \cdot (\vec{\vec{C}} - \vec{\vec{C}}_0) \tag{4.3}$$

In order to proceed it is useful to write the N macroscopic variables as $\vec{\vec{\mathcal{C}}} = (\vec{C},E)$ where E is the final relative energy and $\vec{C}$ denotes the remaining N-1 macroscopic variables.

When the expansion (4.2) is made around that impact parameter which leads to the specified final relative energy on the average, the E-conditioned differential cross section $d\sigma/d\vec{C}dE$ is characterized by the N-1 mean values

$$\langle \vec{C} \rangle|_E = \vec{C}_o \tag{4.4}$$

and the (N-1)x(N-1) covariance matrix

$$\overleftrightarrow{\sigma}|_E = \left[\left(\overleftrightarrow{I} - \frac{\vec{\vec{\mathcal{C}}}_o' \vec{\vec{\mathcal{C}}}_o' \cdot \overleftrightarrow{\sigma}_o^{-1}}{\vec{\vec{\mathcal{C}}}_o' \cdot \overleftrightarrow{\sigma}_o^{-1} \cdot \vec{\vec{\mathcal{C}}}_o'} \right)^{-1} \cdot \overleftrightarrow{\sigma}_o \right]_{(N-1)\times(N-1)} \tag{4.5}$$

where the row and column associated with E is to be eliminated from the matrix in the brackets.

In order to illustrate the above result (4.5) we consider the simplest non-trivial case, when there is only one macroscopic variable in addition to the energy E, for example the total fragment spin S. We then have $\vec{\vec{\mathcal{C}}} = (S,E)$ and expand around that impact parameter for which $\langle E \rangle_S = E$. The relevant derivatives are $S_o' = (d\langle S \rangle_s / ds)_{s=s_o}$ and $E_o' = (d\langle E \rangle_s / ds)_{s=s_o}$. Insertion into (4.5) then yields, after some elementary manipulation,

$$\sigma_{ss}|_E = \sigma_{ss} - 2\frac{S_o'}{E_o'}\sigma_{sE} + \left(\frac{S_o'}{E_o'}\right)^2 \sigma_{EE} \tag{4.6}$$

This result illustrates how the variance of the E-conditional differential cross section is modified relative to the unconditional variance associated with the corresponding mean-trajectory calculation.

The method outlined above provides a general analytical approximation to the E-conditioned differential cross sections. However, the result is mostly of instructive value since the linear expansion (4.2) is not generally sufficiently accurate. Therefore, in our actual calculations we resort to the essentially exact numerical method described in the following.

4.2 Exact method

4.2a Conditional distributions

It is often of interest to study the distribution of some of the macroscopic variables under the condition that the remaining ones be equal to definite specified values. For example, one may study the isotopic distribution of a specified element or one may study the spin distribution for a specified energy loss. When the unconditional distribution is of gaussian form, the same is true for such conditional distributions and these can therefore be characterized by their zeroth, first and second moments.

Let now $\vec{\vec{C}}$ denote all the N macroscopic variables considered and assume that we wish to specify the last N-n of them and consider the corresponding conditional distribution at the first n variables. We shall then write $\vec{\vec{C}} = (\vec{C},\vec{C})$ where $\vec{C} = (C_1,\ldots,C_n)$ are the n unspecified variables and $\vec{C} = (C_{n+1},\ldots,C_N)$ are the N-n specified ones. If we let $\overleftrightarrow{\sigma}$ denote the N x N covariance matrix for the unconditional distribution, the conditional distribution can be written

$$f(\vec{C};\underset{\rightarrow}{C}) = f(\vec{\mathcal{C}}) = [(2\pi)^N |\overleftrightarrow{\sigma}|]^{-1/2} \; e^{-\frac{1}{2}\Delta\vec{\mathcal{C}}\cdot\overleftrightarrow{M}\cdot\Delta\vec{\mathcal{C}}} \tag{4.7}$$

where $\Delta\vec{\mathcal{C}} = \vec{\mathcal{C}} - \langle\vec{\mathcal{C}}\rangle$, as usual, and $\overleftrightarrow{M} = \overleftrightarrow{\sigma}^{-1}$. This distribution is to be considered as a function of the n variables $\vec{C}$, depending parametrically on the specified N-n variables $\underset{\rightarrow}{C}$. We therefore rewrite the scalar product in the exponent as follows, with a self-explanatory notation for the various submatrices of $\overleftrightarrow{M}$,

$$\begin{aligned}
&\Delta\vec{\mathcal{C}}\cdot\overleftrightarrow{M}\cdot\Delta\vec{\mathcal{C}} \\
&= \Delta\vec{C}\cdot\overleftarrow{M}\cdot\Delta\overleftarrow{C} + \Delta\vec{C}\cdot\underset{\rightarrow}{\overleftarrow{M}}\cdot\Delta\underset{\leftarrow}{C} + \Delta\underset{\rightarrow}{C}\cdot\underset{\leftarrow}{\vec{M}}\cdot\Delta\overleftarrow{C} + \Delta\underset{\rightarrow}{C}\cdot\underset{\leftrightarrow}{M}\cdot\Delta\underset{\leftarrow}{C} \qquad (4.8)\\
&= (\Delta\vec{C}-\vec{\delta})\cdot\overleftarrow{M}\cdot(\Delta\overleftarrow{C}-\overleftarrow{\delta}) + \Delta\underset{\rightarrow}{C}\cdot\underset{\leftrightarrow}{M}\cdot\Delta\underset{\leftarrow}{C} - \vec{\delta}\cdot\overleftarrow{M}\cdot\overleftarrow{\delta}
\end{aligned}$$

The last relation holds provided the shift $\vec{\delta}$ is given by

$$\vec{\delta} = -\overleftarrow{M}^{-1}\cdot\underset{\rightarrow}{\overleftarrow{M}}\cdot\Delta\underset{\leftarrow}{C} \tag{4.9}$$

Therefore, the conditional distribution has the n x n covariance matrix

$$\overleftrightarrow{\sigma}\Big|_{\underset{\rightarrow}{C}} = \overleftarrow{M}^{-1} \tag{4.10}$$

and the mean values

$$\langle\vec{C}\rangle\Big|_{\underset{\rightarrow}{C}} = \langle\vec{C}\rangle - \overleftarrow{\sigma}\cdot\underset{\rightarrow}{\overleftarrow{M}}\cdot\Delta\underset{\leftarrow}{C} \tag{4.11}$$

Thus, as is intuitively clear from the simple two-dimensional case, the conditional covariance matrix is independent of the specific value of the conditioning variables $\underset{\rightarrow}{C}$ while the conditional mean values are shifted by amounts proportional to the deviation of $\underset{\rightarrow}{C}$ from the mean value $\langle \underset{\rightarrow}{C} \rangle$.

Furthermore, we note that the nomalization of the conditional distribution is given by the projected, or inclusive, distribution of the N-n variables $\underset{\rightarrow}{C}$,

$$
\begin{aligned}
f(\underset{\rightarrow}{C}) &= \int f(\vec{C}; \underset{\rightarrow}{C})\, d\vec{C} \\
&= \left[(2\pi)^N |\overleftrightarrow{\sigma}|\right]^{-1/2} \left[(2\pi)^n |\overleftrightarrow{\sigma}|\right]^{1/2} e^{-\frac{1}{2}(\Delta\underset{\rightarrow}{C} \cdot \overleftrightarrow{M} \cdot \Delta\underset{\leftarrow}{C} - \vec{\delta} \cdot \overleftrightarrow{M} \cdot \vec{\delta})} \\
&= \left[(2\pi)^{N-n} |\overleftrightarrow{\sigma}| / |\overleftrightarrow{\sigma}|\right]^{-1/2} e^{-\frac{1}{2}\Delta\underset{\rightarrow}{C} \cdot (\overleftrightarrow{M} - \vec{M} \cdot \overleftrightarrow{\sigma} \cdot \overleftarrow{M}) \cdot \Delta\underset{\leftarrow}{C}}
\end{aligned}
\tag{4.12}
$$

In order to illustrate the above results, we consider a two-dimensional case, for example $\vec{C} = S$ and $\underset{\rightarrow}{C} = E$, as in Section 4.1. We then have

$$
\overleftrightarrow{M} = \begin{pmatrix} \sigma_{SS} & \sigma_{SE} \\ \sigma_{ES} & \sigma_{EE} \end{pmatrix}^{-1} = \frac{1}{d} \begin{pmatrix} \sigma_{EE} & -\sigma_{SE} \\ -\sigma_{ES} & \sigma_{SS} \end{pmatrix} \tag{4.13}
$$

where $d = \sigma_{SS}\sigma_{EE} - \sigma_{SE}\sigma_{ES}$. Consequently we find the conditional variance

$$\sigma_{ss}|_E = \left(\frac{\sigma_{EE}}{d}\right)^{-1} = \sigma_{ss} - \frac{\sigma_{sE}\,\sigma_{Es}}{\sigma_{EE}} \tag{4.14}$$

and the conditional mean value

$$\langle s\rangle|_E = \langle s\rangle - \frac{d}{\sigma_{EE}}\,\frac{-\sigma_{Es}}{d}\,\Delta E = \langle s\rangle + \frac{\sigma_{Es}}{\sigma_{EE}}(E - \langle E\rangle) \tag{4.15}$$

Finally, the conditional norm is

$$\begin{aligned} &f(E) \\ &= \left[2\pi d/\left(\frac{d}{\sigma_{EE}}\right)\right]^{-1/2} e^{-\frac{1}{2}\Delta E\left(\frac{\sigma_{ss}}{d} - \frac{-\sigma_{sE}}{d}\,\frac{d}{\sigma_{EE}}\,\frac{-\sigma_{Es}}{d}\right)\Delta E} \\ &= \left[2\pi\sigma_{EE}\right]^{-1/2} e^{-\frac{\Delta E^2}{2\sigma_{EE}}} \end{aligned} \tag{4.16}$$

as it should be.

4.2b Energy-conditioned cross sections

We are now in a position to describe the calculation of the E-conditioned differential cross section. The solution of the moment equations yields the unconditional distribution $f_s(\vec{\vec{C}})$ for any specified impact parameter s, as characterized by the mean values $\langle\vec{\vec{C}}\rangle_s$ and covariances $\overleftrightarrow{\sigma}_s$. By use of the results in 4.2a it is possible to calculate the associated conditional norms, mean values and covariances corresponding to specifying a definite final relative energy E: $f_s(E)$, $\langle\vec{C}\rangle_s|_E$ and $\overleftrightarrow{\sigma}_s|_E$. These, in turn, can be used to express the zeroth, first and second moments of the conditional distribution $f_s(\vec{C};E)$:

$$
\begin{aligned}
m_s(E) &\equiv \int f_s(\vec{C};E)\, d\vec{C} = f_s(E) \\
\vec{m}_s(E) &\equiv \int \vec{C}\, f_s(\vec{C};E)\, d\vec{C} = \langle \vec{C} \rangle_s |_E\, f_s(E) \\
\overleftrightarrow{m}_s(E) &\equiv \int \vec{C}\vec{C}\, f_s(\vec{C};E)\, d\vec{C} \\
&= \left(\langle \vec{C} \rangle_s |_E \langle \vec{C} \rangle_s |_E + \overleftrightarrow{\sigma}_s |_E \right) f_s(E)
\end{aligned}
\tag{4.17}
$$

The E-conditioned differential cross section is obtained by integrating the conditional distribution $f_s(\vec{C};E)$ over the impact parameter s:

$$
\frac{d\sigma}{d\vec{C}} = \frac{d\sigma}{d\vec{C}\, dE} = \int f_s(\vec{C};E)\, d\vec{s} \tag{4.18}
$$

Therefore, the corresponding moments of $d\sigma/d\vec{C}$ are given by a similar impact-parameter integration of the moments in (4.17),

$$
\begin{aligned}
M(E) &\equiv \int \frac{d\sigma}{d\vec{C}\, dE}\, d\vec{C} = \int m_s(E)\, d\vec{s} \\
\vec{M}(E) &\equiv \int \vec{C}\, \frac{d\sigma}{d\vec{C}\, dE}\, d\vec{C} = \int \vec{m}_s(E)\, d\vec{s} \\
\overleftrightarrow{M}(E) &\equiv \int \vec{C}\vec{C}\, \frac{d\sigma}{d\vec{C}\, dE}\, d\vec{C} = \int \overleftrightarrow{m}_s(E)\, d\vec{s}
\end{aligned}
\tag{4.19}
$$

This integration is readily performed numerically by addition of the moments associated with a specified impact parameter. The E-conditioned differential cross section is thus characterized by the mean values

$$
\langle \vec{C} \rangle |_E = \vec{M}(E) / M(E) \tag{4.20}
$$

and the covariance

$$\overleftrightarrow{\sigma}\Big|_E = \overleftrightarrow{M}(E) / M(E) - \langle \overleftarrow{C} \rangle\Big|_E \langle \vec{C} \rangle\Big|_E \qquad (4.21)$$

while the total cross section leading to the final energy E is given by $d\sigma/dE = M(E)$.

The above method is essentially exact for calculating the moments of the differential cross section up to second order, relying as it does only on the gaussian approximation to the individual distributions $f_s(\vec{\vec{C}})$. The method can readily be used to calculate higher moments of $d\sigma/d\vec{\vec{C}}$, should that appear of interest.

5. Characteristic features of the spin evolution

In the preceding sections we have outlined how the dynamical evolution of the dinuclear spins can be calculated. The results of such calculations can best be understood in terms of the appropriate equilibrium solutions and the associated relaxation times. Therefore, before presenting the numerical results (Section 6), we discuss some instructive situations amenable to analytical treatment.

5.1 Stationary solution

In analogy with the treatment of the two-particle problem, we introduce the following spins and associated moments of inertia,

$$\vec{S}^{+} = \vec{S}^{A} + \vec{S}^{B} , \qquad \mathcal{J}_{+} = \mathcal{J}_{A} + \mathcal{J}_{B}$$
$$\vec{S}^{-} = \mathcal{J}_{-} \left(\frac{\vec{S}^{A}}{\mathcal{J}_{A}} - \frac{\vec{S}^{B}}{\mathcal{J}_{B}} \right) , \qquad \mathcal{J}_{-} = \frac{\mathcal{J}_{A}\,\mathcal{J}_{B}}{\mathcal{J}_{A} + \mathcal{J}_{B}} \tag{5.1}$$

They are analogous to the total and relative motion, respectively. The transformation from the individual fragment spins $\vec{S}^{A}$ and $\vec{S}^{B}$ to $\vec{S}^{+}$ and $\vec{S}^{-}$ has a jacobian equal to minus one; this choice of sign is made in order that $\vec{S}^{-}$ be positive, under normal circumstances.

The mobility tensors involving $\vec{S}^{+}$ and $\vec{S}^{-}$ are

$$\overleftrightarrow{M}^{++} = \overleftrightarrow{M}^{LL} = m N R^{2} \overleftrightarrow{T} = - \overleftrightarrow{M}^{+L}$$
$$\overleftrightarrow{M}^{--} = m N \frac{\mathcal{J}_{A} b - \mathcal{J}_{B} a}{\mathcal{J}_{A} + \mathcal{J}_{B}} \overleftrightarrow{T} + m N c_{ave}^{2} \overleftrightarrow{I} \tag{5.2}$$
$$\overleftrightarrow{M}^{+-} = m N R \left(\frac{\mathcal{J}_{A} b - \mathcal{J}_{B} a}{\mathcal{J}_{A} + \mathcal{J}_{B}} \right)^{2} \overleftrightarrow{T} = - \overleftrightarrow{M}^{-L}$$

where $\overleftrightarrow{T} = \hat{x}\hat{x} + \hat{y}\hat{y}$ projects onto the plane perpendicular to the dinuclear axis. Furthermore, in the equations of motion the sums over $G = S^A, S^B, L$ can be replaced by sums over $G = S^+, S^-, L$.

$$\sum_{G=A,B,L} \frac{M_{ij}^{FG}}{\mathcal{J}_G} \sigma_{jk}^{GH} = \sum_{G=+,-,L} \frac{M_{ij}^{FG}}{\mathcal{J}_G} \sigma_{jk}^{GH} \tag{5.3}$$

For a given total angular momentum J, and under the standard assumption that the variances are small compared to $\langle L_y \rangle^2$, it is straightforward (albeit tedious) to demonstrate that the dynamical spin equations (2.39) have a unique stationary solution given by

$$\begin{aligned}
\langle L_y \rangle &= \frac{\mathcal{J}_R}{\mathcal{J}_0} J \\
\langle S_y^+ \rangle &= \frac{\mathcal{J}_+}{\mathcal{J}_0} J - \tau^* \mathcal{J}_+ \frac{\mathcal{J}_0}{\mathcal{J}_R} \frac{1}{J} \\
\langle S_y^- \rangle &= 0 \\
\overleftrightarrow{\sigma}^{LL} &= \tau^* \mathcal{J}_+ \frac{\mathcal{J}_R}{\mathcal{J}_0} \hat{y}\hat{y} \\
\overleftrightarrow{\sigma}^{++} &= \tau^* \mathcal{J}_+ \frac{\mathcal{J}_0}{\mathcal{J}_R} (\hat{x}\hat{x} + \hat{z}\hat{z}) + \tau^* \mathcal{J}_+ \frac{\mathcal{J}_R}{\mathcal{J}_0} \hat{y}\hat{y} \\
\overleftrightarrow{\sigma}^{--} &= \tau^* \mathcal{J}_- \overleftrightarrow{I}
\end{aligned} \tag{5.4}$$

where we have included terms to the first order in the effective temperature τ^*.

During the reaction, the moments of the spin distribution will at each instant evolve towards these equilibrium values, which in turn vary in time

due to the time dependence of the relative moment of inertia $\mathcal{I}_R$ and the effective temperature τ^*. Below we shall first discuss the stationary solution in terms of a statistical model, and next we shall discuss the time scales for the approach towards equilibrium.

5.2 Statistical equilibrium

The part of the macroscopic hamiltonican $\mathcal{H}$ containing the angular-momentum variables in the disphere is

$$\mathcal{H}_{rot} = \frac{\vec{S}^{A\,2}}{2\mathcal{I}_A} + \frac{\vec{S}^{B\,2}}{2\mathcal{I}_B} + \frac{\vec{L}^{\,2}}{2\mathcal{I}_R} \tag{5.5}$$

For a given value of the total angular momentum $\vec{J} = \vec{S}^A + \vec{S}^B + \vec{L}$, the lowest-energy mode of rotational motion in the disphere is a rigid rotation with each of the three angular momenta given by $\vec{S}^F = \mathcal{I}_F \vec{J}/\mathcal{I}_0$ where $\mathcal{I}_0 = \mathcal{I}_A + \mathcal{I}_B + \mathcal{I}_R$. Relative to this yrast mode of motion, intrinsic rotational excitations are possible. These excitations carry no net angular momentum and can be classified in two groups according to whether the two spheres turn in the same or in the opposite sense, i.e., a purely positive mode has $\vec{S}^- = \vec{0}$ and a purely negative mode has $\vec{S}^+ = \vec{0}$, where $\vec{S}^+$ and $\vec{S}^-$ are given in Equation (5.1).

5.2a I-aligned coordinate system

We first consider the problem using the coordinate system x'y'z' defined by $\hat{z}' = \hat{R}$, $\hat{y}' = \hat{I}$, $\hat{x}' = \hat{y}' \times \hat{z}'$, where $\vec{I} = \vec{J} - \vec{J}\cdot\hat{R}\,\hat{R}$ is the projection of the total angular momentum $\vec{J}$ on the plane perpendicular to $\hat{R}$. In order to bring the rotational hamiltonian (5.5) on normal form we introduce the following auxillary spin variable

$$\vec{\varepsilon} = \vec{S}^{+} - \frac{\mathcal{I}_{+}}{\mathcal{I}_{0}} J_{y'} \hat{y}' \tag{5.6}$$

This transformation has unit jacobian since $\hat{y}'$ is independent of $\vec{S}^{+}$. By inverting the transformation (5.2) and inserting into (5.1) we then obtain

$$\mathcal{H}_{rot} = \frac{1}{2\mathcal{I}_A}\left(\frac{\mathcal{I}_A}{\mathcal{I}_{+}}\vec{S}^{+} + \vec{S}^{-}\right)^2 + \frac{1}{2\mathcal{I}_B}\left(\frac{\mathcal{I}_B}{\mathcal{I}_{+}}\vec{S}^{+} - \vec{S}^{-}\right)^2 + \frac{1}{2\mathcal{I}_R}\left(\vec{J} - \vec{S}^{+}\right)^2$$

$$= \frac{J^2}{2\mathcal{I}_0} + \frac{1}{2\mathcal{I}_{+}}\frac{\mathcal{I}_0}{\mathcal{I}_R}\left(S_{x'}^2 + S_{y'}^2\right) + \frac{1}{2\mathcal{I}_{+}}\frac{\mathcal{I}_R}{\mathcal{I}_0}S_{z'}^2 + \frac{\vec{S}^{-2}}{2\mathcal{I}_{-}} \tag{5.7}$$

Here the first term represents the yrast energy associated with a rigid rotation while the additional terms arise from the six normal modes of intrinsic rotational excitation of the disphere. The first of these terms is the energy of the two degenerate "wriggling" modes, where the two spheres rotate in the same sense around an axis perpendicular to $\hat{R}$. The next term is associated with the "tilting" mode arising when $\vec{J}$ has a component along the dinuclear axis $\hat{R}$; the two spheres thus turn in the same sense around $\hat{R}$. These three are the positive modes. The last term arises from the three degenerate negative modes: the "twisting" mode, where the two spheres rotate oppisitely around $\hat{R}$, and the two "bending" modes, where the spheres turn oppositely around an axis perpendicular to $\hat{R}$.

Assume that the rotational modes are weakly coupled to the remainder of the system, which is considered as a heat reservoir with the temperature τ.

When $\tau \ll J^2/2\mathcal{I}_o$ the six normal rotational modes are approximately harmonic. Therefore, the ensuing thermal equilibrium distribution is characterized by

$$\begin{aligned}
&\langle \vec{s} \rangle = \langle \vec{S}^- \rangle = \vec{0} \\
&\langle (\vec{s}\cdot\hat{z}')^2 \rangle = \frac{\mathcal{I}_+ \mathcal{I}_o}{\mathcal{I}_R}\,\tau \\
&\langle (\vec{s}\cdot\hat{x}')^2 \rangle = \langle (\vec{s}\cdot\hat{y}')^2 \rangle = \frac{\mathcal{I}_+ \mathcal{I}_R}{\mathcal{I}_o}\,\tau \\
&\langle (\vec{S}^-\cdot\hat{x}')^2 \rangle = \langle (\vec{S}^-\cdot\hat{y}')^2 \rangle = \langle (\vec{S}^-\cdot\hat{z}')^2 \rangle = \frac{\mathcal{I}_A \mathcal{I}_B}{\mathcal{I}_+}\,\tau
\end{aligned} \tag{5.8}$$

with all covariances vanishing. This implies the following results, to first order in τ. We first consider the y'-components, which are the most complicated ones:

$$\begin{aligned}
&\langle J_{y'} \rangle = \langle I \rangle = \langle (J^2 - J_{z'}^2)^{1/2} \rangle \approx J - \frac{\langle s_{z'}^2 \rangle}{2J} = J - \frac{\mathcal{I}_+ \mathcal{I}_o}{\mathcal{I}_R}\,\frac{\tau}{2J} \\
&\langle J_{y'}^2 \rangle = \langle I^2 \rangle = \langle J^2 - J_{z'}^2 \rangle = J^2 - \frac{\mathcal{I}_+ \mathcal{I}_o}{\mathcal{I}_R}\,\tau \\
&\sigma_{y'y'}^{JJ} = \sigma_{II} = \langle I^2 \rangle - \langle I \rangle^2 = \sigma(\tau^2)
\end{aligned} \tag{5.9}$$

$$\begin{aligned}
&\langle L_{y'} \rangle = \langle I - S_{y'}^+ \rangle = \langle I - (\tfrac{\mathcal{I}_+}{\mathcal{I}_o} I + s_{y'}) \rangle = \frac{\mathcal{I}_R}{\mathcal{I}_o} \langle I \rangle = \frac{\mathcal{I}_R}{\mathcal{I}_o} J - \mathcal{I}_+ \frac{\tau}{2J} \\
&\langle L_{y'}^2 \rangle = \langle (I - S_{y'}^+)^2 \rangle = \langle (\tfrac{\mathcal{I}_R}{\mathcal{I}_o} I - s_{y'})^2 \rangle = (\tfrac{\mathcal{I}_R}{\mathcal{I}_o})^2 \langle I^2 \rangle + \langle s_{y'}^2 \rangle \\
&\qquad = (\tfrac{\mathcal{I}_R}{\mathcal{I}_o})^2 J^2 - \frac{\mathcal{I}_R \mathcal{I}_+}{\mathcal{I}_o}\,\tau + \frac{\mathcal{I}_+ \mathcal{I}_R}{\mathcal{I}_o}\,\tau = (\tfrac{\mathcal{I}_R}{\mathcal{I}_o} J)^2 + \sigma(\tau^2) \\
&\sigma_{y'y'}^{LL} = \langle L_{y'}^2 \rangle - \langle L_{y'} \rangle^2 = \frac{\mathcal{I}_+ \mathcal{I}_R}{\mathcal{I}_o}\,\tau
\end{aligned} \tag{5.10}$$

$$\langle S^+_{y'} \rangle = \langle \frac{\mathcal{J}_+}{\mathcal{J}_o} I + s_{y'} \rangle = \frac{\mathcal{J}_+}{\mathcal{J}_o} J - \frac{\mathcal{J}_+^2}{\mathcal{J}_R} \frac{\tau}{2J}$$

$$\langle S^{+2}_{y'} \rangle = \langle (\frac{\mathcal{J}_+}{\mathcal{J}_o} I + s_{y'})^2 \rangle = (\frac{\mathcal{J}_+}{\mathcal{J}_o} J)^2 - \frac{\mathcal{J}_+^3}{\mathcal{J}_R \mathcal{J}_o} \tau + \frac{\mathcal{J}_+ \mathcal{J}_R}{\mathcal{J}_o} \tau \qquad (5.11)$$

$$\sigma^{++}_{y'y'} = \langle S^{+2}_{y'} \rangle - \langle S^+_{y'} \rangle^2 = \frac{\mathcal{J}_+ \mathcal{J}_R}{\mathcal{J}_o} \tau$$

$$\sigma^{+L}_{y'y'} = \langle S^+_{y'} L_{y'} \rangle - \langle S^+_{y'} \rangle \langle L_{y'} \rangle$$

$$= \langle (\frac{\mathcal{J}_+}{\mathcal{J}_o} I + s_{y'})(\frac{\mathcal{J}_R}{\mathcal{J}_o} I - s_{y'}) \rangle - \langle \frac{\mathcal{J}_+}{\mathcal{J}_o} I + s_{y'} \rangle \langle \frac{\mathcal{J}_R}{\mathcal{J}_o} I - s_{y'} \rangle \qquad (5.12)$$

$$= \frac{\mathcal{J}_+ \mathcal{J}_R}{\mathcal{J}_o^2} \sigma^{II}_{y'y'} - \langle s_{y'}^2 \rangle = - \frac{\mathcal{J}_+ \mathcal{J}_R}{\mathcal{J}_o} \tau$$

The components along the other axes are simpler to treat:

$$\langle L_{x'} \rangle = \langle S_{x'} \rangle = 0$$

$$\sigma^{LL}_{x'x'} = \sigma^{++}_{x'x'} = - \sigma^{+L}_{x'x'} = \langle S^2_{x'} \rangle = \frac{\mathcal{J}_+ \mathcal{J}_R}{\mathcal{J}_o} \tau \qquad (5.13)$$

$$\sigma^{++}_{z'z'} = \sigma^{JJ}_{z'z'} = \sigma^{+J}_{z'z'} = \langle S^2_{z'} \rangle = \frac{\mathcal{J}_+ \mathcal{J}_o}{\mathcal{J}_R} \tau$$

These results correspond to those derived in[6] and also in accordance with the analysis by Moretto.[11] We note that there is isotropy in the plane perpendicular to $\hat{R}$, where the spin variances are given by $\mathcal{J}_+\mathcal{J}_R/\mathcal{J}_o\ \tau$, while the variance in the $\hat{R}$-directon $\mathcal{J}_+\mathcal{J}_o/\mathcal{J}_R\ \tau$, i.e., larger by a fractor of $(\mathcal{J}_o/\mathcal{J}_R)^2 \approx 2$.

5.2b L -aligned coordinate system

The above analysis was carried out with reference to the I-aligned coordinate system x'y'z'. For the dynamical studies it is of greater interest to employ the fluctuating intrinsic coordinate system xyz which is aligned with $\vec{L}$: $\hat{z} = \hat{R}$, $\hat{y} = \hat{L}$, $\hat{x} = \hat{y} \times \hat{z}$ (see Chapter 2). The xyz results can be obtained from the above x'y'z' results by averaging over the small fluctuating rotation around the common z-axis which aligns one coordinate system with the other; this method is analogous to the transformation from the intrinsic xyz system to the external XYZ system discussed in Section 2.4. The associated fluctuating rotation angle ζ' is given by $\sin\zeta' = -L_{x'}/L_0$ where $L_0 = \langle L \rangle$ in x'y'z'. For the mean values we then find

$$\langle S_y^F \rangle = \langle -S_{x'}^F \sin\zeta' + S_{y'}^F \cos\zeta' \rangle$$

$$\approx \langle S_{y'}^F \rangle \left(1 - \frac{\sigma_{x'x'}^{LL}}{2L_0^2}\right) + \frac{\sigma_{x'x'}^{FL}}{L_0} \qquad (5.14)$$

and expressions for the covariances also follow.[12)]

An alternative method is to proceed in analogy with the treatment in 5.2a and bring the rotational hamiltonian on normal form with respect to the xyz system. For this purpose we need to introduce the auxillary spin variable

$$\vec{s} = \vec{S}^+ - \frac{J_+}{J_0} J_y \hat{y} \qquad (5.15)$$

and obtain

$$\mathcal{H}_{tot} = \frac{1}{2\mathcal{I}_A}\left(\frac{\mathcal{I}_A}{\mathcal{I}_+}\vec{S}^+ + \vec{S}^-\right)^2 + \frac{1}{2\mathcal{I}_B}\left(\frac{\mathcal{I}_B}{\mathcal{I}_+}\vec{S}^+ - \vec{S}^-\right) + \frac{(J_y - S_y^+)^2}{2\mathcal{I}_R}$$

$$= \frac{J^2}{2\mathcal{I}_0} + \frac{1}{2\mathcal{I}_+}\frac{\mathcal{I}_R}{\mathcal{I}_0}\left(S_z^2 + S_x^2\right) + \frac{1}{2\mathcal{I}_+}\frac{\mathcal{I}_0}{\mathcal{I}_R}S_y^2 + \frac{\vec{S}^{-2}}{2\mathcal{I}_-} \qquad (5.16)$$

This result is quite similar to (5.7) for the x'y'z' system with the notable exception of the x-component of the positive modes, s_x, the in-plane component of the wriggling mode. This mode is no longer degenerate with the normal component of the wriggling mode, s_y, but rather with the tilting mode s_z. Thus the previous isotropy in the plane perpendicular to the dinuclear axis $\hat{R}$ is replaced by isotropy in the plane perpendicular to the orbital angular momentum $\vec{L}$.

However, when proceeding to derive expressions for the moments of the equilibrium spin distribution it must be taken into account that the jacobian of the transformation (5.15) is not constant since $\hat{y}$ depends on $\vec{S}^+$ through the direction of $\vec{L}$. As a consequence, the mean value of s_y is not zero, as one might naively have expected from (5.16), but smaller than zero by an amount proportional to the temperature; this is of course a consequence of the fact that the y-axis is always aligned with $\vec{L}$.

Using either method, the following results can be obtained. The mean values are given by

$$\langle J_y \rangle = J - \frac{\mathcal{I}_+ \mathcal{I}_o}{\mathcal{I}_R} \frac{\tau}{J}$$

$$\langle L_y \rangle = \frac{\mathcal{I}_R}{\mathcal{I}_o} J \qquad (5.17)$$

$$\langle S_y^+ \rangle = \frac{\mathcal{I}_+}{\mathcal{I}_o} J - \frac{\mathcal{I}_+ \mathcal{I}_o}{\mathcal{I}_R} \frac{\tau}{J}$$

We note that $\langle L_y \rangle$ is greater than $\langle L_y' \rangle$ while $\langle J_y \rangle$ and $\langle S_y^+ \rangle$ are smaller than $\langle J_y' \rangle$ and $\langle S_y' \rangle$, respectively, as one would expect.

As expected from the normal form (5.16) we find for F,G = S^+, L, J

$$\sigma_{yy}^{FG} = \sigma_{y'y'}^{FG}$$

$$\sigma_{zz}^{FG} = \sigma_{z'z'}^{FG} \qquad (5.18)$$

For the z-components this also follows immediately from the fact that the fluctuating rotation leaves the z-components unaffected. Furthermore, σ_{xx}^{LF} vanishes since $L_x \equiv 0$, and, since then $J_x = S_x^+$,

$$\sigma_{xx}^{JJ} = \sigma_{xx}^{++} = \sigma_{xx}^{+J} = \frac{\mathcal{I}_+ \mathcal{I}_o}{\mathcal{I}_R} \tau \qquad (5.19)$$

Thus, the xx-variance is increased by the factor $(\mathcal{I}_o/\mathcal{I}_R)^2 \approx 2$, relative to the x'x'-variance.

5.2c Individual fragment spins

The preceding discussion has been made in terms of the normal rotational modes in the disphere, as is most instructive. It is, of course, ultimately of interest to calculate the distribution in terms of the individual fragment

spins $\vec{S}^F$, F = A, B. It easily follows that at thermal equilibrium the mean fragment spins are given by

$$\langle S^F_{y'} \rangle = \frac{\mathcal{I}_F}{\mathcal{I}_o} J - \frac{\mathcal{I}_F \mathcal{I}_+}{\mathcal{I}_R} \frac{\tau}{2J} \tag{5.20}$$

in the I-aligned system and

$$\langle S^F_{y} \rangle = \frac{\mathcal{I}_F}{\mathcal{I}_o} J - \frac{\mathcal{I}_F \mathcal{I}_o}{\mathcal{I}_R} \frac{\tau}{J} \tag{5.21}$$

in the L-aligned system. Furthermore, the various variances are

$$\begin{aligned}
\sigma^{FG}_{x'x'} &= \left(\frac{\mathcal{I}_R}{\mathcal{I}_o} \mathcal{I}_F \mathcal{I}_G + \epsilon_{FG} \mathcal{I}_A \mathcal{I}_B \right) \frac{\tau}{\mathcal{I}_A + \mathcal{I}_B} \\
\sigma^{FG}_{y'y'} &= \left(\frac{\mathcal{I}_R}{\mathcal{I}_o} \mathcal{I}_F \mathcal{I}_G + \epsilon_{FG} \mathcal{I}_A \mathcal{I}_B \right) \frac{\tau}{\mathcal{I}_A + \mathcal{I}_B} \\
\sigma^{FG}_{z'z'} &= \left(\frac{\mathcal{I}_o}{\mathcal{I}_R} \mathcal{I}_F \mathcal{I}_G + \epsilon_{FG} \mathcal{I}_A \mathcal{I}_B \right) \frac{\tau}{\mathcal{I}_A + \mathcal{I}_B}
\end{aligned} \tag{5.22}$$

in the I-aligned internal system and

$$\begin{aligned}
\sigma^{FG}_{xx} &= \left(\frac{\mathcal{I}_o}{\mathcal{I}_R} \mathcal{I}_F \mathcal{I}_G + \epsilon_{FG} \mathcal{I}_A \mathcal{I}_B \right) \frac{\tau}{\mathcal{I}_A + \mathcal{I}_B} \\
\sigma^{FG}_{yy} &= \left(\frac{\mathcal{I}_R}{\mathcal{I}_o} \mathcal{I}_F \mathcal{I}_G + \epsilon_{FG} \mathcal{I}_A \mathcal{I}_B \right) \frac{\tau}{\mathcal{I}_A + \mathcal{I}_B} \\
\sigma^{FG}_{zz} &= \left(\frac{\mathcal{I}_o}{\mathcal{I}_R} \mathcal{I}_F \mathcal{I}_G + \epsilon_{FG} \mathcal{I}_A \mathcal{I}_B \right) \frac{\tau}{\mathcal{I}_A + \mathcal{I}_B}
\end{aligned} \tag{5.23}$$

in the L-aligned internal system. (The symbol ϵ_{FG} is one if F = G and minus one otherwise.) We note that the L-aligned results (5.21) and (5.22) are identical to the stationary solution (5.4) of the dynamical equations (2.39). The second terms arise from the isotropic negative modes (bending and twisting) while the first terms arise from the

positive modes (wriggling and tilting). We note again that the in-plane variances of the postive modes interchange their sizes under the transformation between xyz and x'y'z'. A different normal form of the rotational hamiltonian (5.5) for an asymmetrical disphere has been introduced by Schmitt and Pacheco.[13] This leads to different definitions of the wriggling and bending modes, but the result expressed in the original variables, eq. (5.22), is of course the same.

5.3 Dynamical evolution of the spins along the reaction normal

In this section we consider the components of the fragment spins $\vec{S}^A$ and $\vec{S}^B$ in the direction perpendicular to the reaction plane, S_y^A and S_y^B, respectively. In order to bring out the essential features as simply as possible, we assume that the nuclear geometry is fixed, i.e., the form factor N as well as a,b,R,c_{ave}, $\mathcal{I}_A$, $\mathcal{I}_B$, $\mathcal{I}_R$ are all constant in time. It is convenient to introduce a two-dimensional vector notation, so that the mean components are given by $\underset{\rightarrow}{S} = (\langle S_y^A \rangle, \langle S_y^B \rangle)$ and the associated covariances are

$$\underset{\leftrightarrow}{\sigma} = \begin{pmatrix} \sigma_{yy}^{AA} & \sigma_{yy}^{AB} \\ \sigma_{yy}^{BA} & \sigma_{yy}^{BB} \end{pmatrix} \tag{5.24}$$

where $\sigma_{yy}^{AB} = \sigma_{yy}^{BA}$ so that $\underset{\leftrightarrow}{\sigma}$ is symmetric.

5.3a Dynamical equations

In present discussion we ignore the small correction terms proportional to $1/L_y$ in the dynamical equations for the mean values. The temporal evolution of the above quantities can then be written as

$$\dot{\underset{\rightarrow}{S}} = \underset{\rightarrow}{d} - \underset{\rightarrow}{S} \cdot \underset{\leftrightarrow}{K}$$

$$\dot{\underset{\leftrightarrow}{\sigma}} = 2\underset{\leftrightarrow}{D} - \underset{\leftrightarrow}{\sigma} \cdot \underset{\leftrightarrow}{K} - \underset{\leftrightarrow}{K}^{\dagger} \cdot \underset{\leftrightarrow}{\sigma} \tag{5.25}$$

where we have introduced

$$\underset{\rightarrow}{d} = mN \frac{R}{\mathcal{I}_R} J(a, b) \tag{5.26}$$

$$\underset{\leftrightarrow}{D} = mN\tau^* \begin{pmatrix} a^2 + c_{ave}^2 & ab - c_{ave}^2 \\ ab - c_{ave}^2 & b^2 + c_{ave}^2 \end{pmatrix} \tag{5.27}$$

$$\underset{\leftrightarrow}{K} = mN \begin{pmatrix} \frac{a^2 + c_{ave}^2}{\mathcal{I}_A} + \frac{aR}{\mathcal{I}_R} & \frac{ab - c_{ave}^2}{\mathcal{I}_A} + \frac{bR}{\mathcal{I}_R} \\ \frac{ab - c_{ave}^2}{\mathcal{I}_B} + \frac{aR}{\mathcal{I}_R} & \frac{b^2 + c_{ave}^2}{\mathcal{I}_B} + \frac{bR}{\mathcal{I}_R} \end{pmatrix} \tag{5.28}$$

We note that while the diffusion matrix $\underset{\leftrightarrow}{D}$ is symmetric, this is only so for $\underset{\leftrightarrow}{K}$ when A = B. We note that $\underset{\leftrightarrow}{K}$ has the determinant

$$K = |\underset{\leftrightarrow}{K}| = \frac{\mathcal{I}_0 R^2 c_{ave}^2}{\mathcal{I}_A \mathcal{I}_B \mathcal{I}_R} (mN)^2 \tag{5.29}$$

5.3b Equilibrium

As time grows, the solutions to the dynamical equations approach their equilibrium values, which are characterized by the stationary condition $\underset{\rightarrow}{S} = \underset{\rightarrow}{0}$ and $\underset{\leftrightarrow}{\sigma} = \underset{\leftrightarrow}{0}$. Thus the equilibrium values are determined by the equations

$$\underset{\rightarrow}{S} \circ \underset{\leftrightarrow}{K} = \underset{\rightarrow}{d}$$

$$\underset{\leftrightarrow}{\sigma} \circ \underset{\leftrightarrow}{K} + \underset{\leftrightarrow}{K}^{+} \circ \underset{\leftrightarrow}{\sigma} = 2\,\underset{\leftrightarrow}{D} \tag{5.30}$$

It can readily be verified that the corresponding solutions are

$$\underset{\rightarrow}{S}(\infty) = \left(\frac{\gamma_A}{\gamma_0} J\,,\ \frac{\gamma_B}{\gamma_0} J \right)$$

$$\underset{\leftrightarrow}{\sigma}(\infty) = \frac{\gamma_A \gamma_B}{\gamma_0} \tau \begin{pmatrix} \frac{\gamma_B}{\gamma_A} + 1 & -1 \\ -1 & \frac{\gamma_B}{\gamma_B} + 1 \end{pmatrix} \tag{5.31}$$

in accordance with our previous discussion of thermal equilibrium in section 5.1.

5.3c Evolution of the mean values

The dynamical equation (5.25) for $\underset{\rightarrow}{S}$ has the general solution

$$\underset{\rightarrow}{S}(t) = \underset{\rightarrow}{S}_1 \left(1 - e^{-\kappa_1 t}\right) + \underset{\rightarrow}{S}_2 \left(1 - e^{-\kappa_2 t}\right) \tag{5.32}$$

where κ_1 and κ_2 are the eigenvalues of $\underset{\leftrightarrow}{K}$ determined by $|\underset{\leftrightarrow}{K} - \kappa \underset{\leftrightarrow}{I}| = 0$.

In order to determine $\underset{\rightarrow}{S}_1$ and $\underset{\rightarrow}{S}_2$ we exploit the facts that at long times we have

$$\underset{\rightarrow}{S}_1 + \underset{\rightarrow}{S}_2 = \underset{\rightarrow}{S}(\infty) = \underset{\rightarrow}{d} \circ \underset{\leftrightarrow}{K}^{-1} \qquad (t \to \infty) \tag{5.33}$$

and at short times we have

$$\underset{\sim}{S}_1 \kappa_1 t + \underset{\sim}{S}_2 \kappa_2 t = \underset{\sim}{d}\, t \qquad (t \to 0) \tag{5.34}$$

These two linear equations can easily be solved to give

$$\begin{aligned} \underset{\sim}{S}_1 &= \frac{1}{\kappa_1 - \kappa_2} \left[\underset{\sim}{d} - \kappa_2 \underset{\sim}{S}(\infty) \right] \\ \underset{\sim}{S}_2 &= \frac{1}{\kappa_1 - \kappa_2} \left[\kappa_1 \underset{\sim}{S}(\infty) - \underset{\sim}{d} \right] = \underset{\sim}{S}(\infty) - \underset{\sim}{S}_1 \end{aligned} \tag{5.35}$$

The two eigenvalues κ_i are determined by

$$\begin{aligned} 0 &= | \underset{\leftrightarrow}{K} - \kappa \underset{\leftrightarrow}{I} | \\ &= (K^{AA} - \kappa)(K^{BB} - \kappa) - K^{AB} K^{BA} \\ &= K - (K^{AA} + K^{BB})\kappa + \kappa^2 \end{aligned} \tag{5.36}$$

Therefore,

$$\begin{aligned} 2\kappa_\pm &= K^{AA} + K^{BB} \pm \left[(K^{AA} + K^{BB})^2 - 4K \right]^{1/2} \\ &= \left(\frac{1}{\bar{\mu}} + \frac{c_{am}^2}{\bar{J}} \pm \left[\left(\frac{1}{\bar{\mu}} + \frac{c_{am}^2}{\bar{J}} \right)^2 - 4 \cdot \frac{J_0 R^2 c_{am}^2}{J_A J_B J_R} \right]^{1/2} \right) mN \end{aligned} \tag{5.37}$$

where

$$\begin{aligned} \frac{1}{\bar{\mu}} &= \frac{a^2}{J_A} + \frac{b^2}{J_B} + \frac{R^2}{J_R} \\ \frac{1}{\bar{J}} &= \frac{1}{J_A} + \frac{1}{J_B} = \frac{1}{J_-} \end{aligned} \tag{5.38}$$

In the limit where $c_{ave}^2 << R^2$ we thus find

$$\kappa_1 \equiv \kappa_+ \approx \left(\frac{1}{\tilde{\mu}} + \frac{c_{ave}^2}{\bar{J}} - \frac{J_0 \tilde{\mu} R^2 c_{ave}^2}{J_A J_B J_R}\right) mN \approx \frac{mN}{\tilde{\mu}} \equiv \tilde{\kappa}_1$$

$$\kappa_2 \equiv \kappa_- \approx \frac{J_0 \tilde{\mu} R^2 c_{ave}^2}{J_A J_B J_R} mN \equiv \tilde{\kappa}_2 << \tilde{\kappa}_1 \qquad (5.39)$$

i.e., there is a short relaxation time, $t_1 = 1/\kappa_1$, associated with the temporary establishment of a rolling motion, and a long relaxation time, $t_2 = 1/\kappa_2$, associated with the ultimate approach to the thermal limit. It is useful to introduce the rolling spin $\underset{\rightarrow}{S}_{roll} \equiv \frac{\tilde{\mu} R}{J_R} J(a,b)$. It then follows that

$$\underset{\rightarrow}{S}_1 = \underset{\rightarrow}{d}\, t_1 + \sigma\left(\frac{c_{ave}^2}{R^2}\right) \approx \underset{\rightarrow}{S}_{roll} \qquad (5.40)$$

so that we have approximately the simple result

$$\underset{\rightarrow}{S}(t) \approx \underset{\rightarrow}{S}_{roll}\left(1 - e^{-\tilde{\kappa}_1 t}\right) + \left(\underset{\rightarrow}{S}(\infty) - \underset{\rightarrow}{S}_{roll}\right)\left(1 - e^{-\tilde{\kappa}_2 t}\right) \qquad (5.41)$$

5.3d Evolution of the covariances

In the special case of a symmetric dinucleus, A = B, the matrix $\underset{\leftrightarrow}{K}$ is symmetric and the same transformation diagonalizes $\underset{\leftrightarrow}{K}$ and $\underset{\leftrightarrow}{K}^\dagger$ simultaneously. Hence, in that simple case the spin covariances can be treated within the same two-dimensional formalism. However, in general $A \neq B$ and it is necessary to employ a three-dimensional formulation. Thus, the spin covariances are represented by the quantity

$$\underset{\Rightarrow}{\sigma} = (\sigma_{yy}^{AA}, \sigma_{yy}^{AB}, \sigma_{yy}^{BB}) \tag{5.42}$$

Furthermore, we need the diffusion coefficients

$$\begin{aligned}\underset{\Rightarrow}{D} &= (D_{yy}^{AA}, D_{yy}^{AB}, D_{yy}^{BB}) \\ &= mN\tau^*(a^2 + c_{ave}^2, ab - c_{ave}^2, b^2 + c_{ave}^2)\end{aligned} \tag{5.43}$$

and the coupling matrix

$$\underset{\Leftrightarrow}{K} = \begin{pmatrix} 2K^{AA} & K^{AB} & 0 \\ 2K^{BA} & K^{AA}+K^{BB} & 2K^{AB} \\ 0 & K^{BA} & 2K^{BB} \end{pmatrix} \tag{5.44}$$

where the elements are those of the 2 x 2 matrix $\underset{\leftrightarrow}{K}$ introduced in the treatment of the mean values, eq. (5.28).

With these notational tools, the equation of motion for the covariances can be written

$$\dot{\underset{\Rightarrow}{\sigma}} = 2\underset{\Rightarrow}{D} - \underset{\Rightarrow}{\sigma} * \underset{\Leftrightarrow}{K} \tag{5.45}$$

Furthermore, the equilibrium solution is given by

$$\underset{\Rightarrow}{\sigma}(\infty) = 2\underset{\Rightarrow}{D} * \underset{\Leftrightarrow}{K}^{-1} = \frac{\gamma_A\gamma_B}{\gamma_0}\tau\left(\frac{\gamma_B}{\gamma_B}+1, -1, \frac{\gamma_B}{\gamma_A}+1\right) \tag{5.46}$$

in accordance with our previous result.

The general dynamical solution has the form

$$\underset{\Rightarrow}{\sigma}(t) = \sum_{i=1}^{3} \underset{\Rightarrow}{\sigma}_i \left(1 - e^{-k_i t}\right)$$

where k_i are the eigenvalues of $\underset{\Leftrightarrow}{K}$ determined by $|\underset{\Leftrightarrow}{K} - k \underset{\Leftrightarrow}{I}| = 0$. In order to determine $\underset{\Rightarrow}{\sigma}_i$ we proceed in analogy with the treatment of the mean values and exploit the relationship

$$\sum_{i=1}^{3} k_i^n \underset{\Rightarrow}{\sigma}_i = 2\underset{\Rightarrow}{D} * \underset{\Leftrightarrow}{K}^{n-1} \tag{5.47}$$

for $n = 0,1,2$. [For $n = 0$ the relation follows when $t \to \infty$, and for $n > 0$ it follows by expansion in powers of t for $t \to 0$.] We thus have the three equations

$$\begin{aligned}
&\underset{\Rightarrow}{\sigma}_1 + \underset{\Rightarrow}{\sigma}_2 + \underset{\Rightarrow}{\sigma}_3 = 2\underset{\Rightarrow}{D} * \underset{\Leftrightarrow}{K}^{-1} = \underset{\Rightarrow}{\sigma}(\infty) \\
&k_1 \underset{\Rightarrow}{\sigma}_1 + k_2 \underset{\Rightarrow}{\sigma}_2 + k_3 \underset{\Rightarrow}{\sigma}_3 = 2\underset{\Rightarrow}{D} \\
&k_1^2 \underset{\Rightarrow}{\sigma}_1 + k_2^2 \underset{\Rightarrow}{\sigma}_2 + k_3^2 \underset{\Rightarrow}{\sigma}_3 = 2\underset{\Rightarrow}{D} * \underset{\Leftrightarrow}{K}
\end{aligned} \tag{5.48}$$

They have the following solution

$$\begin{aligned}
\underset{\Rightarrow}{\sigma}_1 &= \left[2\underset{\Rightarrow}{D} * \underset{\Leftrightarrow}{K} - 2(k_2 + k_3)\underset{\Rightarrow}{D} + k_2 k_3 \underset{\Rightarrow}{\sigma}(\infty)\right] / k_{12} k_{13} \\
\underset{\Rightarrow}{\sigma}_2 &= \left[-2\underset{\Rightarrow}{D} * \underset{\Leftrightarrow}{K} + 2(k_1 + k_3)\underset{\Rightarrow}{D} - k_1 k_3 \underset{\Rightarrow}{\sigma}(\infty)\right] / k_{12} k_{23} \\
\underset{\Rightarrow}{\sigma}_3 &= \left[2\underset{\Rightarrow}{D} * \underset{\Leftrightarrow}{K} - 2(k_1 + k_2)\underset{\Rightarrow}{D} + k_1 k_2 \underset{\Rightarrow}{\sigma}(\infty)\right] / k_{13} k_{23}
\end{aligned} \tag{5.49}$$

where $k_{ij} \equiv k_i - k_j$. The three eigenvalues k_i are determined by

$$0 = |\underset{\Leftrightarrow}{K} - k\underset{\Leftrightarrow}{I}| = [(2K^{AA}-k)(2K^{BB}-k) - 4K^{AB}K^{BA}][K^{AA}+K^{BB}-k] \tag{5.50}$$

so that

$$k_1 = 2\kappa_1 \qquad k_2 = \kappa_1 + \kappa_2 \qquad k_3 = 2\kappa_2 \tag{5.51}$$

where κ_i are the eigenvalues of $\underset{\leftrightarrow}{K}$ pertaining to the mean values. It then follows that

$$\underset{\Rightarrow}{\sigma}_1 = \underset{\Rightarrow}{D}\, t_1 + o\left(\frac{c_{ave}^2}{R^2}\right) \approx \underset{\Rightarrow}{\sigma}_{roll}$$

$$\underset{\Rightarrow}{\sigma}_2 = o\left(\frac{c_{ave}^2}{R^2}\right) o\left(\frac{b-a}{R}\right) << \underset{\Rightarrow}{\sigma}_1, \underset{\Rightarrow}{\sigma}_3 \tag{5.52}$$

$$\underset{\Rightarrow}{\sigma}_3 = \underset{\Rightarrow}{\sigma}(\infty) - \underset{\Rightarrow}{\sigma}_1 + o\left(\frac{c_{ave}^2}{R^2}\right)$$

where $\underset{\Rightarrow}{\sigma}_{roll} \equiv \bar{\mu}\tau^*(a^2, ab, b^2)$. Consequently, we have approximately the simple form

$$\underset{\Rightarrow}{\sigma}(t) \approx \underset{\Rightarrow}{\sigma}_{roll}(1 - e^{-2\tilde{\kappa}_1 t}) + (\underset{\Rightarrow}{\sigma}(\infty) - \underset{\Rightarrow}{\sigma}_{roll})(1 - e^{-2\tilde{\kappa}_2 t}) \tag{5.53}$$

Thus, the evolution of the covariances also exhibits a quick relaxation towards a rolling situation followed by a slower relaxation towards the true equilibrium. The intermediate relaxation associated with the eigenvalue $k_2 \approx \frac{1}{2} k_1 \approx {}^{\kappa}1$ plays no essential role because of the relative smallness of the corresponding eigenvector $\underset{\Rightarrow}{\sigma}_2$; in the symmetric case $\underset{\Rightarrow}{\sigma}_2$ vanishes entirely. We note that σ^{AB}_{roll} is positive while $\sigma^{AB}(\infty)$ is negative, so that σ^{AB}_{yy} first increases relatively quickly and then, more slowly, decreases towards the negative asymptotic value.

5.4 Evolution in a symmetric disphere

In Section 5.1 we introduced the spins $\vec{S}^{+}$ and $\vec{S}^{-}$; they are particularly convenient variables when the two spheres are equal. In the symmetric case, where $a = b$ and $\mathcal{I}_A = \mathcal{I}_B$, the mixed mobility tensor M^{+-} (5.2) vanishes so that the dynamical equations for $\vec{S}^{-}$ decouple from the rest; furthermore, the mobility tensor $\overleftrightarrow{M}^{--}$ is then isotropic. For the remaining system it is advantageous to employ the total angular momentum $\vec{J}$ as a variable rather than $\vec{S}^{+}$ since the mobility tensors involving $\vec{J}$ all vanish due to the absolute conservation of $\vec{J}$.

The equations of motion for the symmetric disphere are then as follows. First, for the mean values,

$$\begin{aligned}
\dot{J}_y &= M^{LL}\left(-\tau^* \frac{J_y}{L_y^2} + \frac{1}{L_y}\frac{\sigma^{JJ}_{xx}}{\mathcal{J}_+}\right) \\
\dot{L}_y &= M^{LL}\left(\frac{J_y}{\mathcal{J}_+} - \frac{\mathcal{J}_0}{\mathcal{J}_R}\frac{L_y}{\mathcal{J}_+} + \frac{\tau^*}{L_y}\right) \\
\dot{S}^-_y &= -\left(\frac{M^{--}}{\mathcal{J}_-} + \frac{\tau^*}{L_y^2}\right) S^-_y
\end{aligned} \tag{5.54}$$

Furthermore, the normal variances decouple from the rest of the equations,

$$\begin{aligned}
\dot{\sigma}^{JJ}_{yy} &= \sigma(\tau^{*2}) \\
\dot{\sigma}^{JL}_{yy} &= \frac{M^{LL}}{\mathcal{J}_+}\sigma^{JJ}_{yy} - \frac{M^{LL}}{\mathcal{J}_+}\frac{\mathcal{J}_0}{\mathcal{J}_R}\sigma^{JL}_{yy} \\
\dot{\sigma}^{LL}_{yy} &= 2\tau^* M^{LL} - 2\frac{M^{LL}}{\mathcal{J}_+}\frac{\mathcal{J}_0}{\mathcal{J}_R}\sigma^{LL}_{yy} + 2\frac{M^{LL}}{\mathcal{J}_+}\sigma^{JL}_{yy} \\
\dot{\sigma}^{--}_{yy} &= 2\tau^* M^{--} - 2\frac{M^{--}}{\mathcal{J}_-}\sigma^{--}_{yy}
\end{aligned} \tag{5.55}$$

Here the last equation is decoupled entirely. The evolution of the in-plane covariances is governed by

$$\begin{aligned}
\dot{\sigma}^{JJ}_{xx} &= 2\tau^* M^{LL}\frac{J_y^2}{L_y^2} - 2\frac{M^{LL}}{\mathcal{J}_+}\frac{J_y}{L_y}\sigma^{JJ}_{xx} - 2\omega_R\sigma^{JJ}_{xz} \\
\dot{\sigma}^{JJ}_{xz} &= \omega_R\left(\sigma^{JJ}_{xx} - \sigma^{JJ}_{zz}\right) - \frac{M^{LL}}{\mathcal{J}_+}\frac{J_y}{L_y}\sigma^{JJ}_{xz} \\
\dot{\sigma}^{JJ}_{zz} &= 2\omega_R\sigma^{JJ}_{xz}
\end{aligned} \tag{5.56}$$

for the positive modes and by the decoupled system

$$\dot{\sigma}^{--}_{xx} = 2\tau^* M^{--} + 2\tau^* M^{LL} \frac{S_y^{-2}}{L_y^2} - 2\frac{M^{--}}{J_-}\sigma^{--}_{xx} - 2\omega_R \sigma^{--}_{xz}$$

$$\dot{\sigma}^{--}_{xz} = -2\frac{M^{--}}{J_-}\sigma^{--}_{xz} + \omega_R(\sigma^{--}_{xx} - \sigma^{--}_{zz}) \qquad (5.57)$$

$$\dot{\sigma}^{--}_{zz} = 2\tau^* M^{--} - 2\frac{M^{--}}{J_-}\sigma^{--}_{zz} + 2\omega_R \sigma^{--}_{xz}$$

for the negative modes. The results can be expressed in terms of $\vec{S}^+$ by use of the relations

$$S^+_y = J_y - L_y$$

$$\sigma^{++}_{ij} = \sigma^{JJ}_{ij}, \quad i,j = x,z \qquad (5.58)$$

$$\sigma^{++}_{yy} = \sigma^{JJ}_{yy} - 2\sigma^{JL}_{yy} + \sigma^{LL}_{yy} = \sigma^{LL}_{yy} + \sigma(\tau^{*2})$$

We now investigate the above equations in the same idealized case of fixed coefficients as was considered in Section 5.3 (except that now we need also explicitly assume that the rotational frequency ω_R remains constant). The initial condition is that $J_y = L_y = J$ with all the covariances being equal to zero.

Typical time scales for the approach to equilibrium can be obtained by dividing the asymptotic values by the respective initial time derivatives. This yields for the transversal spin components σ^{++}_{xx} and σ^{++}_{yy} the time scales $\frac{J_0}{J_R} t_{++}$ and $\frac{J_R}{J_0} t_{++}$, respectively, where

$$t_{++} = \frac{\tau^* J_+}{2\tau^* M^{LL}} = \frac{J_+}{2mNR^2} \qquad (5.59)$$

while for the components of $\overleftrightarrow{\sigma}^{--}$ we find

$$t_{--} = \frac{\tau^* \mathcal{I}_-}{2\tau^* M^{--}} = \frac{\mathcal{I}_-}{2mNc_{ave}^2} \tag{5.60}$$

Thus, $t_{++}/t_{--} = \sigma(c_{ave}^2/R^2) \ll 1$, as we also found in Section 5.3. We note that $t_{++} = \frac{\mathcal{I}_0}{\mathcal{I}_R} \frac{1}{2\tilde{\kappa}_+}$ and $t_{--} = \frac{1}{2\tilde{\kappa}_-}$ where $\tilde{\kappa}_\pm$ are the quantities introduced in (5.36). For two equal touching spheres the ratio $\mathcal{I}_0/\mathcal{I}_R$ equals 5/7 so this factor is not of qualitative importance.

The normal variance $\sigma_{zz}^{++} = \sigma_{zz}^{JJ}$ does not receive contributions directly through the transfer process but only indirectly by the orbital rotation of σ_{xx}^{JJ} via σ_{xz}^{JJ}. The time development at early times is

$$\sigma_{zz}^{++} \approx \frac{2}{3} \tau^* M^{LL} \omega_R^2 t^3 \tag{5.61}$$

which indicates that the time scale for the relaxation of the tilting mode is inversely proportional to the square of the orbital frequency ω_R. It should be added in this connection, that although the above expansion only remains valid during relatively early times the time scale for the equalibration still contains the factor $1/\omega_R^2$.

After these introductory considerations, we proceed to investigate the dynamical solution to the equations. Neglecting terms of the order $\mathcal{I}_+ \tau^*$ relative to terms of the order L_y^2, we obtain the following leading-order solution for the mean values,

$$J_y = J = \text{constant}$$

$$L_y = \frac{J_R}{J_0} J \left[1 + \frac{J_+}{J_R} e^{-\frac{J_0}{J_R}\frac{t}{2t_{++}}} \right] \tag{5.62}$$

$$S_y^+ = J_y - L_y = \frac{J_+}{J_0} J \left[1 - e^{-\frac{J_0}{J_R}\frac{t}{2t_{++}}} \right]$$

$$S_y^- = 0$$

where t_{++} is the relaxation time given in (5.59).

For the covariances in the y-direction we find

$$\sigma_{yy}^{++} = \sigma_{yy}^{LL} = \frac{J_+ J_R}{J_0} \tau^* \left[1 - e^{-\frac{J_0}{J_R}\frac{t}{t_{++}}} \right] \tag{5.63}$$

$$\sigma_{yy}^{JL} = o(\tau^{*2}), \quad \sigma_{yy}^{JJ} = o(\tau^{*2})$$

These results also follow from the analysis in Section 5.3 by considering the special case of symmetry, A = B. In this case the rolling spin $\underset{\rightarrow}{S}_{roll}$ is equal to the sticking spin $\underset{\rightarrow}{S}(\infty)$ so that the second eigenvector $\underset{\rightarrow}{S}(\infty) - \underset{\rightarrow}{S}_{roll}$ vanishes and the mean values exhibit a pure relaxation with the short time scale t_1. For the covariances, the intermediate eigenvector vanishes due to the symmetry and the simple form (5.53) for the evolution of the covariances is exact. Furthermore, $\underset{\Rightarrow}{\sigma}^{++}_{roll}$ is equal to $\underset{\Rightarrow}{\sigma}^{++}(\infty)$ so that the $\underset{\Rightarrow}{\sigma}^{++}$ exhibits a pure relaxation with the short time scale $\frac{1}{2}t_1$ and the above result follows. Furthermore, $\underset{\Rightarrow}{\sigma}^{--}_{roll}$ vanishes so that $\underset{\Rightarrow}{\sigma}^{--}$ exhibits a pure relaxation with the long time scale $\frac{1}{2}t_2$ and the result (5.67) follows.

The equations (5.56) for σ_{xx}^{JJ}, σ_{xz}^{JJ}, σ_{zz}^{JJ} contain the time- dependent quantity L_y, both implicitely through the orbital frequency ω_R and explicitely. Therefore, the exact solution is rather intransparent. Fortunately, it is a fairly good approximation to first treat L_y as a time-independent parameter while solving the equations and then subsequently substitute the time-dependent L_y given above in (5.62). We then need to solve three coupled linear equations with constant coefficients; this can be done by the same method as employed in Section 5.3.

The appropriate relaxation times are given by the inverse of the eigenvalues of the coefficient matrix which are found to be

$$\begin{aligned} k_1 &= k_2 + [\, k_2^2 - 4\omega_R^2 \,]^{1/2} \approx 2k_2 \\ k_2 &= \tfrac{1}{2} \frac{J_y}{L_y} \frac{1}{t_{++}} \\ k_3 &= k_2 - [\, k_2^2 - 4\omega_R^2 \,]^{1/2} \approx 4\omega_R^2 \frac{L_y}{J_y} t_{++} = \frac{\epsilon^2}{2} k_2 \end{aligned} \tag{5.64}$$

The approximate expressions for k_1 and k_3 hold provided the dimensionless quantity $\epsilon \equiv 4\omega_R t_{++} L_y / J_y$ is small compared to unity, as is the case when the orbital rotation, which is characterized by the time scale ω_R^{-1}, is slow in comparison with the short relaxation time t_{++} in (5.59). We note that asymptotically, when $L_y/J_y = \mathcal{J}_R/\mathcal{J}_0$, the large eigenvalue k_1 is equal to the one derived in 5.3 for the y-components, see Eqs. (5.51 and 5.39).

The dynamical solution for the in-plane variances is given by

$$\begin{pmatrix} \sigma_{xx}^{++} \\ \sigma_{xz}^{++} \\ \sigma_{zz}^{++} \end{pmatrix} = \frac{\mathcal{J}_+ \tau^*}{1-\epsilon^2} \begin{pmatrix} k_1 t_{++} \bar{e}_1 - \epsilon^2 \bar{e}_2 + k_2 t_{++} \bar{e}_3 \\ 2\omega_R t_{++} (-\bar{e}_1 + 2\bar{e}_2 - \bar{e}_3) \\ k_2 t_{++} \bar{e}_1 - \epsilon^2 \bar{e}_2 + k_1 t_{++} \bar{e}_3 \end{pmatrix} \tag{5.65}$$

where we have used the short-hand notation $\bar{e}_i = 1 - \exp(-k_i t)$ for $i = 1,2,3$. The time scale for the relaxation of σ_{xx}^{++} is $\approx t_{++}$ (to within the factor $\mathcal{J}_R/\mathcal{J}_0$). When this time is short compared to the orbital rotation, i.e., when $\epsilon << 1$, the main part of σ_{zz} relaxes on the time scale

$$t_{+z} = \frac{1}{k_2} \approx (4\omega_R^2 \frac{L_y}{\mathcal{J}_y} t_{++})^{-1} \approx \frac{4}{\epsilon^2} t_{++} \tag{5.66}$$

We note that this time scale is proportional to the square of the orbital frequency ω_R and hence usually fairly long.

Finally, let us consider the negative modes. The equations for the covariances of $\vec{S}^-$ are very simple due to the isotropy of the associated mobility tensor. Since the initial distribution is isotropic (namely $\sim\delta(\vec{S}^-)$) the dynamical solution remains isotropic at all times and we readily find (for example by considering the equation for σ_{yy}^{--})

$$\overleftrightarrow{\sigma}^{--} = \mathcal{J}_- \tau^* [\, 1 - e^{-t/t_{--}} \,] \overleftrightarrow{I} \tag{5.67}$$

where t_{--} is the relaxation time (5.60) for the covariances of the negative spin modes.

6. Illustrative applications

In the proceding section we have discussed the characteristic features of the spin evolution with an emphasis on the qualitative aspects. We now wish to illustrate the theory quantitatively by making applications to some cases of actual experimental interest. The ultimate comparison with the data is postponed to the subsequent paper II since the sequential decay process need to be discussed first.

6.1 Time evolution of the geometry

The mobility tensors, and hence the transport coefficients, for the angular momenta depend on the dinuclear geometry through the center separation R and the neck radius c. It is therefore instructive to start by considering the time evolution of these two quantities. In Fig. 2 they are shown as functions of time for a number of specified angular momenta J in the reaction 1400 MeV ^{165}Ho + ^{165}Ho. The two nuclei approach each other on a Coulomb trajectory and R decreases steadily. When the two surfaces are about 1.7 fm apart the neck degree of freedom is activated and the neck radius grows rapidly. The maximum neck opening is achieved around the time of closest approach and is maintained for a while as the two nuclei recede. Towards the end of the reaction phase the neck shrinks rapidly and finally vanishes rather abruptly. After this time the two nuclei separate on another Coulomb trajectory.

A pictorial impression of the evolution of the dinuclear geometry can be gained from Fig. 3 which displays the overall dinuclear shape at three different points in time (shortly after the neck has opened, at the time of turning, and right before the neck collapses), for three selected angular

momenta in the same Ho + Ho reaction. The dots indicate previous and future locations of the nuclear centers at equidistant points in time separated by 10^{-22} sec. (The dashed contours indicate the spin distributions and are discussed in Section 6.2).

The present model contains essentially only one shape degree of freedom, namely the neck radius c, and the shapes in Fig. 3 look rather crude relative to shapes obtained with models including more shape variables. Therefore, it is of interest to compare the calculated evolution of R and c with the evolution obtained with models of damped reactions which leave more freedom for the nuclear shapes. Fig. 4 shows the time evolution of R and c for a head-on collision in the reaction 1535 MeV ^{208}Pb + ^{208}Pb. Comparison is made with the Time-Dependent Hartree-Fock model and the Coherent Surface Excitation model.[14] Closest correspondence is obtained between our model and TDHF, both as regards the neck radius and the reaction time as the overall evolution of the center separation. The CSE model yields a somewhat smaller neck opening and a somewhat shorter reaction time.

The information in Fig. 4 can be represented in a different manner by plotting the dynamical trajectory of the system in the Rc-plane, as shown in Fig. 5. The early time evolution is seen to be very similar in our model and TDHF. During most of the recession, our neck radius exceeds that of TDHF, for the same value of R, while that of the CSE is considerably smaller. Towards the end of the reaction our neck radius collapses at a $\approx 10\%$ smaller R-value than the other two, which are rather similar to one another at this stage. The fact that more elongated shapes can be achieved in TDHF and CSE is due to the incorporation of more shape degrees of freedom in these models. Some idea

of how a more detailed treatment of the nuclear shape degrees of freedom would affect the transfer-induced angular-momentum transfer can be gained by considering the expressions for the asymptotic values and relaxation times given in Section 5. A smaller neck radius, as obtained with the CSE, would lead to longer relaxation times, especially for the negative spin modes for which the relaxation time would exceed the reaction time by about a factor of four. Furthermore, more elongated shapes, as obtained with both TDHF and CSE, would lead to smaller values of the final mean spin in the fragments. Of importance is also the fact that both the CSE and the TDHF models contain degrees of freedom associated with the shape of the nuclear surfaces. These may carry angular momentum and thus have a substantial effect on the dynamics and the final values of the fragment spins. Finally, we note that the static deformation of nuclei such as Ho may also affect the angular-momentum dynamics. In the present model we include only the minimum number of angular-momentum degrees of freedom, namely those associated with the total spins of the the two final fragments.

6.2 Dynamical evolution of the angular momenta

We now consider in some detail the calculated dynamical evolution of the angular momenta during the reaction phase.

6.2a The reaction 1400 MeV ^{165}Ho + ^{165}Ho

In order to illustrate the transport of angular momentum in realistic cases, we first consider the symmetric reaction Ho + Ho at 1400 MeV bombarding energy. This reaction has been studied experimentally.[15)]

As an introducton, we consider the various relaxation times introduced in Section 5. They are shown in Fig. 6 as functions of time, for a number of different values of the total angular momentum J. We note that throughout the reaction phase the relaxation times t_{++} associated with the two wriggling modes are considerably shorter than t_{--} associated with the negative modes, as already expected since $c^2 << R^2$. The relaxatin time for the tilting mode is fairly long but has an opposite behavior, both as a function of time and in its dependence on J. By comparing the relaxation times with the reaction times it is possible to obtain an expectation for how far the various modes will evolve towards equilibrium. Thus, for not too large impact parameter, we expect the wriggling modes to achieve nearly complete relaxation, contrary to the negative modes for which this is at most expected for the smallest impact parameters. The tilting mode is generally expected to gain little excitation.

The calculated dynamical evolution of the mean fragment spin projection is shown in Fig. 7, for three selected J-values. For the highest value, J = 400 $\hbar$, the reaction is over before the equilibrium mean value can be reached. For the intermediate value, J = 320 $\hbar$, the equilibrium value is nearly achieved around the time of closest approach. This equilibrium mean spin decreases as the two fragment recede and the relative moment of inertia grows. Therefore, the mean spin exhibits a maximum as a function of time. The same is true at the most central reaction, J = 100 $\hbar$, but here the equilibrium values are of course smaller.

The calculated spin covariances are displayed in Fig. 8 as functions of time. The figure has three parts. The first shows the dynamical evolution

during the reaction phase. It is clearly seen how σ_{xx}^{FG} and σ_{yy}^{FG} increase rapidly at early times; this is a reflection of the fast wriggling relaxation time (see Fig. 6). The local bumps in σ_{xx}^{FG} and σ_{yy}^{FG} around the time of closest approach ($t \approx 3 \cdot 10^{-22}$ sec.) are caused by a minimum in the effective temperature τ^*. [The effective temperature is initially nearly proportional to the relative nuclear velocity and hence at first it decreases. Later on, when the relative motion has subsided, τ^* is close to the intrinsic temperature τ which increases in time. Thus τ^* exhibits a minimum which occurs approximately at the turning point of the relative motion.] The evolution of σ_{zz}^{FG} is considerably slower, as expected from Fig. 6. Most of σ_{zz}^{FG} is associated with the negative twisting mode as evidenced by the fact that the covariance σ_{zz}^{AB} is negative, but, as the difference between σ_{zz}^{AA} and σ_{zz}^{AB} indicates, there is also a fair amount of tilting. The second part of the figure shows, on a condensed time scale, the rotation of the covariances along the exit Coulomb trajectory. Finally, the third part shows the result of transforming to the external coordinate system XYZ. This transformation is seen to have a substantial effect on the x-components; in fact σ_{XX}^{AB} becomes negative.

The equiprobability contours of the fragment spin distribution are ellipsoids whose common shape and orientation are determined by the appropriate covariances. In order to given a visual impression of the spin evolution we have included in Fig. 3 contours of the spin distribution projected onto the xz-plane. The contours are drawn at a distance of one standard derivation from the mean (which is zero in the xz-plane). One notes how the fairly peripheral collision ($J = 440\hbar$) inhibits the build-up of negative spin modes so

the distribution is very elongated. Furthermore, the smallness of the form factor prevents the distribution from aligning itself relative to the dinuclear axis. For J = 320 $\hbar$ the window grows wider and the isotropic negative modes are more readily excited; the distribution also follows better the turning dinuclear axis. These features are even more apparent for J = 100 $\hbar$.

6.2b The reaction 610 MeV ^{86}Kr + ^{209}Bi

In order to illustrate the dynamical spin evolution in an asymmetric case we consider the reaction 610 MeV ^{86}Kr + ^{209}Bi which has been studied experimentally.[16] The practically similar reaction has also been studied.[17]

Fig. 9 is analogous to Fig. 7 and shows the time evolution of the mean spin projections for three selected values of J. The qualitative features of the evolution are the same as in the symmetric case (Fig. 7). We note that at early times the two spins are more similar than at later times. This is because the rolling spins towards which the values tend at first, scale as the nuclear radii while the sticking spins, towards which the values tend ultimately, scale as the fifth power of the radii.

In Fig. 10 the time evolution of the spin covariances are displayed, in analogy to Fig. 8 for Ho + Ho. The features are similar to those of Fig. 8 and we note that at early times the variances grow in proportion to the rolling value (5.52).

6.3 Energy-conditioned cross sections

We now wish to illustrate the dependence of the final spin distribution on the kinetic-energy loss TKEL, as obtained by integrating of all J-values and exploiting the calculated covariance between the relative energy and the spins.

First, in Fig. 11, we show the normal component of the fragment spin, $S_Y^A = S_Y^B$, for the Ho + Ho reaction. The figure displays the distribution in the TKEL-S_Y^A plane calculated for specified values of the total angular momentum J. The distribution of S_Y^A for a specified value of TKEL is obtained by adding up the contributions from all the J-values, properly weighted, and then cutting along the devised value of TKEL. This procedure leads to the conditional mean values shown in Fig. 12. One notes how the mean spin first rises with TKEL, then drops off as the contributing impact parameters grow smaller.

The associated spin covariance tensors $\overleftrightarrow{\sigma}^{FG}$ are also readily calculated using the methods discussed in Section 3. Each of the three tensors $\overleftrightarrow{\sigma}^{AA}$, $\overleftrightarrow{\sigma}^{AB}$, $\overleftrightarrow{\sigma}^{BB}$ can be characterized by the orientation of the corresponding principal coordinate system, $X_oY_oZ_o$, in which it is diagonal, and its three principal variances $\sigma^{FG}_{X_oX_o}$, $\sigma^{FG}_{Y_oY_o}$, $\sigma^{FG}_{Z_oZ_o}$.

Due to the up-down symmetry of the scattering problem the principal systems are aligned with the reaction normal so their orientation can be specified by a single angle, e.g., the angle θ_o between the beam axis and the axis of the largest in-plane variance. For a symmetric system, all three covariance tensors have the same principal orientation. The same simple feature remains true in asymmetric cases as well to within a few degrees. The principal angle θ_o for the Ho + Ho case is shown in Fig. 13 as a function of TKEL. Also shown on this figure is the scattering angle θ_{CM} together with the calculated variances in θ_{CM} and TKEL for selected values of J.

It is an important simplifying feature that the angle θ_o is approximately equal to $\theta_{CM}/2$. This is to be expected since most of the exchange occurs

around the turning point where the dinuclear axis is perpendicular to $\Theta_{CM}/2$. For small TKEL Θ_o is slightly larger than $\Theta_{CM}/2$. This is because the transformation from the internal to the external reference frame reduces the spin variance perpendicular to the emission direction and thus effects a slight rotation of the principal system towards the ejection direction. For larger TKEL this effect is counteracted and ultimately dominated by a shift of Θ_o away from the ejection direction due to the asymmetry of the relative trajectory around the turning point: the system spends longer time together after the turning than before and, furthermore, since better contact is established the relaxation times are shorter and the principal frame will be oriented more forwards.

For our discussion of the in-plane spin covariances it is convenient to adopt the major principal direction as the X-axis. (We drop the subscript o for notatinal convenience.) It follows from the above discussion that the Z-axis is then approximately aligned with that direction the dinuclear axis had at the time of closest approach. Furthermore, the relaxation time relevant for the positive modes along the X-direction is the wriggling time t_{++} while the relevant time scale for the positive modes along the Z-axis is well approximated by the tilting time t_{+z}. These times were shown in Fig. 6.

The corresponding principal covariances are shown in Fig. 14. The principal variances σ_{ii}^{AA} all increase steadily with TKEL, except for a slight decrease in σ_{YY}^{AA} at the largest TKEL. [This latter feature may be an artifact of the upper bound imposed in TKEL by our limited shape parametrization.] Due to the strong correlation between S_Y^A and TKEL at small TKEL, the conditional value of σ_{YY}^{AA} for fixed TKEL becomes smaller

than σ_{YY}^{AA} calculated for the corresponding value of J, and σ_{YY}^{AA} builds up less rapidly than σ_{XX}^{AA} for small TKEL. Of special importance are the covariances σ_{ii}^{AB}. The covariance along the normal direction, σ_{YY}^{AB}, is always positive, due to the dominance of the positive wriggling mode for small TKEL, and due to the contributions from quite a wide range of angular momenta J at large TKEL. The dependence of the relaxation times on J, as shown in Fig. 6, is reflected in the dependence of the in-plane covariances σ_{XX}^{AB} and σ_{ZZ}^{AB} on TKEL. The larger in-plane component, σ_{XX}^{AB} first increases to substantial positive values for small TKEL, due to the very short relaxation time for the wriggling mode, and for large TKEL, σ_{XX}^{AB} decreases and finally becomes rather small due to the increasing excitation of the negative in-plane bending mode. For large J, the tilting relaxation time, t_{+z} is smaller than the twisting relaxation time t_{--}, and the smaller in-plane component of the covariance, σ_{ZZ}^{AB}, attains small positive values for small TKEL. With decreasing J the twisting relaxation time becomes smaller and the tilting time longer. Consequently, with increasing TKEL, σ_{ZZ}^{AB} changes sign and finally, for large TKEL, attains substantial negative values.

6.5 Comparison to a statistical model

We wish to compare our dynamical results from Figure 15 for the covariances with the results of a statistical model, in which the relaxation times are so short that the equilibrium values (5.23) for the covariances are reached towards the end of the collision for all impact parameters.

As input information to the statistical model one needs to know, as a function of TKEL, the effective temperature τ^* and the moments of inertia $\mathfrak{I}_A$, $\mathfrak{I}_B$, $\mathfrak{I}_R$ at the time when the distribution freezes, as the two nuclei loose contact. To carry through the transformations (2.47-54) to the external frame, the scattering angle should be known, too. A special problem is the assignment of the average spin and total angular momentum, also entering the transformation.

Our objective here is not to formulate and apply a statistical model to the Ho + Ho collision, but to compare the covariances of the statistical and dynamical models under similar circumstances. Therefore, we adopt for the statistical model the calculated total angular momenta and scattering angles as given in Figure 13. To calculate the relative moment of inertia $\mathfrak{I}_R$ at the time when the two nuclei loose contact, we use an average value of R = 18 fm, as can be inferred from Figure 2. For the mean values of the spins, we adopt two alternative prescriptions: (i) the equilibrium value, as given by equations (5.21), once J and $\mathfrak{I}_R$ are specified. This is what we expect to be the most reasonable prescription when the relaxation times for mean values and covariances are related to each other. For the purpose of illustrations we also apply another presentation: (ii) the mean values from Figure 11, as calculated dynamically. As the effective temperature is concerned, we do not include the effect of the relative motion, but insert the temperature τ associated with the heat content in the two nuclei at the time of separation as calculated dynamically. This temperature is to a good approximation proportional to the square root of the total kinetic energy loss.

In equilibrium, the in-plane covariances are isotropic in the intrinsic frame, and the transformation to the external frame introduces an anisotropy. Inserting into the expression (2.47-54) we find that the angle ψ from the final direction of motion after the collision to the major principal axis of the in-plane covariance matrix is given by:

$$\Psi = \tfrac{1}{2}\arctan\left(\frac{-2\sigma_{xz}^{++}}{\sigma_{zz}^{++} - \sigma_{xx}^{++}}\right) = \tfrac{1}{2}\arctan\left(\frac{\cos\Theta_{cm}}{\sin\Theta_{cm} - \frac{S_y^+}{J\sin\Theta_{cm}}}\right) \qquad (6.1)$$

where Θ_{CM} is the center-of-mass scattering angle. For the angle between the beam direction and the principal axis, we find, expanding the arctan and keeping terms to first order in S_y^+/J:

$$\theta_o = \Theta_{cm} - \Psi \approx \frac{\pi}{4} + \frac{\Theta_{cm}}{2} + \frac{S_y^+}{4J}\cot\Theta_{cm} \qquad (6.2)$$

Thus, the X-axis of the principal system forms this angle with the beam axis, and we obtain for the principal variances of the positive modes, to second order in S_y^+/J:

$$\sigma_{xx}^{++} \approx \tau J_+ \frac{J_o}{J_R}\left[1 + \frac{S_y^+}{J\sin^2\Theta_{cm}}(1-\sin\Theta_{cm})\left(\sin\Theta_{cm} + \frac{S_y^+}{2J}\right)\right]$$
$$\sigma_{zz}^{++} \approx \tau J_+ \frac{J_o}{J_R}\left[1 - \frac{S_y^+}{J\sin^2\Theta_{cm}}(1+\sin\Theta_{cm})\left(\sin\Theta_{cm} - \frac{S_y^+}{2J}\right)\right] \qquad (6.3)$$

Figure 15 shows the angle θ_0 and Figure 16 shows the spin covariances in the principal system obtained with the statistical model. For the figures, an exact diagonalization was carried out, but the approximate expressions (6.2) and (6.3) are accurate to within less than one percent for all the quantitites shown, except for the largest TKEL, where the scattering angle approaches 180° and all expressions diverge.

As expected for a statistical model, the dispersions grow roughly as the fourth root of the total kinetic energy loss. This is espceially true for the dispersion in the normal direction, σ_{YY}^{FG} which is unaffected by the transformation to the external frame. For all variances in one nucleus σ_{II}^{AA}, only a rather small anisotropy is introduced by the transformation to the external frame, whereas the covariances are affected in the most dramatic way. The covariances σ_{II}^{AB} are, however, small compared to the variances within one nucleus σ_{II}^{AA}.

From the expression (6.3), it is evident that the smallest in-plane covariance, σ_{ZZ}^{FG}, is most sensitive to the actual value of S_y^+/J, and in Fig. 16 the dashed curves shown σ_{ZZ}^{FG} when the dynamical value is used for S_y^+/J. Generally, the result is not very sensitive to which value is used. For large J, and hence small average TKEL, the smallness of the values obtained for S_y^+/J with the dynamical results from Figure 11, implies that hardly any change is introduced by the transformation from the intrinsic frame to the external frame. For J smaller than 420$\hbar$ (average TKEL larger than 140 MeV), S_y^+ becomes practically equilibrated at the time of closest approach and overshoots the value corresponding to rigid rotation at

the separation distance. So the dashed and full curves on Fig. 16 cross each other at a TKEL of 140 MeV.

By inserting the equilibrium value of S_y^+/J into the expression (6.3) for σ_{ZZ}^{++}, we obtain approximately:

$$\sigma_{zz}^{++} \approx \tau \mathcal{J}_+ \frac{\mathcal{J}_o}{\mathcal{J}_R} \left[1 - 2 \frac{\mathcal{J}_+}{\mathcal{J}_o} \right] \approx \tau \mathcal{J}_+ \frac{\mathcal{J}_R}{\mathcal{J}_o} = \sigma_{YY}^{++} \qquad (6.4)$$

Thus, these variances look much like the variances in the internal I-aligned coordinate system, c.f. equation (5.22), namely with one of the in-plane variance being large and the two other variances being small and equal. The essential difference between the I-aligned and the external system is the orientation of the principal system. In the I-aligned system, the direction of the largest variance is given by the axis connecting the nuclei at separation. In the external system, which is the one relevant for experiments, the direction of the largest spin variance is given by the expression (6.1), or, to within approximately $\pm 5^\circ$, it is at an angle $\Theta_{CM}/2 + 45^\circ$ to the beam direction. This is a characteristic feature of the statistical model, both for a symmetric collision, such as the Ho + Ho collision, and for asymmetric collisions as well.

Comparing the dynamical and statistical results, several differences are apparent. First of all, the direction of the principal system for the statistical model is shifted by 45° relative to the dynamical results. Secondly, the dynamical results display a much larger in-plane anisotropy of the

covariances. For the normal covariances, σ_{YY}^{FG}, on the other hand, we do not attach so much significance to the difference since part of the result in the dynamical case comes from the integration over impact parameter at fixed TKEL. A similar integration in the statistical model would diminish the difference between the two results.

7. Discussion

We conclude this paper by discussing various other models addressing angular momentum in damped nuclear reactions. We do not wish to give a full discussion of those models but concentrate on the aspects relevant to the topic of the present work.

7.1 Other transport models

Although several other transport models have been developed for damped nuclear reactions (e.g., refs. [18-20]), none of those include a sufficient number of spin variables to specify completely the final angular momenta of the two reaction products. The most detailed model so far is the one discussed below.

7.1a Transport model of Wolschin et al.

Wolschin et al.[21] have studied the aligned components of the fragment spins within a transport model which has its origin in the quantum-statistical treatment of dissipation processes formulated by Nörenberg et al.[22,23]. The form factors for angular momentum transport are estimated on the basis of a gaussian parameterization of the dependence on single particle energy and angular momentum of the interaction matrix elements for exciting and transferring nucleons during a reaction[18]. In actual calculations, the form factors are taken to be constant during a phenomenologically determined effective interaction time. Applied to mass transfer, this formalism gave the first quantitative account of the mass diffusion[24].

In treating the time evolution of the individual spins in ref.[21], the diffusion coefficients for the two normal spin components, D_{yy}^{AA} and

D_{yy}^{BB} in our notation, are taken in accordance with the measured mean γ-multiplicities for the Kr and Sm case considered, while the mixed diffusion coefficient, D_{yy}^{AB}, is assumed to be negligible. Actually, this latter ansatz appears to be in conflict with the underlying scheme for calculating the form factors[18] with nucleon transfer between the two nuclides being responsible for a specific part of the diffusion coefficient. Indeed, the mixed diffusion coefficient D_{yy}^{AB} is generally expected to be of a size comparable to D_{yy}^{AA} and D_{yy}^{BB}. In our model, as we have seen in the preceding, the mixed coefficient is responsible for the build-up of strong positive spin correlations at early times (the rolling situation, cf. Section 5). Only later on, on a longer time scale, does the spin covariance approach its slightly negative equilibrium value. In contrast to this characteristic evolution, the calculations by Wolschin et al. yield a monotonic decrease of the spin covariance from the initial value of zero towards the final equilibrium value; due to the absence of the mixed diffusion coefficient there is no intermediae excursion of the covariance into the positive regime. There is thus an essential qualitative difference between the results by Wolschin et al. and ours.

7.2 Time-dependent Hartree-Fock model

The TDHF model[25] is self-consistent, microscopic and quantal. It gives a parameter-free description at the time evolution of the one-body density matrix. In particular, the model provides a good impression of the evolution of the nuclear density distribution, and the mean field, during a damped reaction and may thus offer valuable guidance for identifying the proper macroscopic variables.

Due to its inherently one-body nature, the TDHF model cannot address fluctuations and correlations in a realistic manner and it is thus most useful in dynamical situations where fluctuations are expected to be of only minor importance.

Since it is relatively costly to perform TDHF calculations, certain simplifications are usually imposed. Thus, the spin-orbit force is neglected and often no distinction is made between neutrons and protons, so that each orbital has a four-fold spin-isospin degeneracy. This of course reduces the number of degrees of freedom in the system. Furthermore, the wave functions have often been restricted to have axial symmetry (possibly in a rotating frame). It is clear that fully three-dimensional calculations are of largest interest for studies of the angular-momentum dynamics. However, even this most general TDHF treatment can only calculate the aligned angular momentum components while no reliable information can be obtained about depolarization, misalignment, etc.

7.3 Models with nuclear deformations

7.3a Coherent Surface Excitation model

The Coherent Surface Excitation model[14] describes the reaction system as two deformable nuclei. The deformation degrees of freedom are those associated with the standard coherent surface excitations of various multipolarities; for each particular mode the strength function is idealized as an essentially undamped low-frequency mode plus a high-frequency mode with a substantial width. The multipole-multipole interaction due to the mutual Coulomb and nuclear forces provide the coupling mechanism which exchanges

energy between the relative motion and the intrinsic vibrations. In addition, a proximity friction is added (but the associated fluctuating force has not been included so far). The ensuing coupled classical equations of motion are solved for an ensemble of initial conditions representing the classical approximation to the zero-point motion of the vibrational modes; in this way finite dispersions are produced even for a single impact parameter.

This model was employed in ref.[26] to investigate the angular-momentum transfer in the Kr + Pb reaction at 610 MeV. The fragment spin distribution was calculated as a function of either impact parameter or energy loss and subsequently the angular distribution of fission fragments from the target-like reaction product was derived.

The simultaneous inclusion of surface vibrations coupling via the nuclear proximity force and the stochastic transfer of nucleons is not straightforward and in their attempt to accomplish this the authors have made several approximations. Perhaps most severe in the present context is the complete neglect of the fluctuating component of the dissipative force produced by the nucleon transfers. As the present study demonstrates, this force gives rise to substantial dispersions in the angular momenta, in fact being of sizes similar to those obtained in ref.[26] resulting exclusively from the zero-point vibrations.

For the same reaction, the present nucleon-exchange generated angular momentum dispersions are typically 50% larger than those obtained in ref.[27], except for the normal direction in which the zero-point motion generates large fluctuations. It is not obvious how the simultaneous inclusion of both sources of fluctuation would affect the results. For those modes which have short relaxation times with respect to the nucleon-exchange

process, the effect of the zero-point fluctuations would probably quickly be forgotten by the system. On the other hand, the large normal spin dispersions caused by the zero-point fluctuations might well survive the inclusion of the exchange-induced fluctuations. If so, even rather large impact parameters would still contribute to a wide range of energy losses.

The coherent surface excitation model, with or without some form of nucleon transfer, is readily capable of yielding predictions about the correlations between the two fragment spins. This would seem a worthwhile task in view of the several specific qualitative predictions made by the present nucleon-exchange model.

7.3b Collision of deformed nuclei

In all preceding models the nuclei are initially assumed to have a spherical equilibrium shape. To study the effect on angular momentum transfer of static deformations a model has been developed by Min et al.[27] In that model two spheroids, capable of undergoing damped vibrations, collide under the action of conservative Coulomb and nuclear forces as well as a proximity friction force.

In the case of Ho + Ho, their prime case, they obtain appreciable spin transfers and misalignments, of sufficient magnitude to account for the data. They take this as an indication that this agency is the dominant source for the spin transfer in damped reactions.

We wish to express some reservation about this conjecture. If the initial static deformations were the main source of spin transfer and misalignment one should observe drastic differences between reactions involving deformed and spherical nuclei. This appears not to be the case. Furthermore, static deformations are a consequence of shell effects and are thus expected

to disappear at the high excitations usually achieved in a damped reaction. Thus, towards the end of the reaction phase there is no particular stabilization around a deformed shape and the employed equations of motion are inadequate. However, there is little doubt that at the early reaction stage the presence of initial deformations are of importance and it would be interesting to pursue this question theoretically as well as experimentally.

7.4 Statistical models

The preceeding models discussed are all dynamical in that no a priori assumption is made about the relaxation times for the considered angular-momentum variables: their final value is a result of a calculated dynamical evolution during the reaction phase. It is instructive to contrast these dynamical results with those obtained in a purely statistical treatment. At any time during the reaction phase, a well-defined equilibirum distribution exists, associated to the instantaneous geometrical configuration of the dinucleus. The instantaneous equilibrium distribution can be obtained from the dynamical equation by artifically increasing the form factors for the angular-momentum transport, so that the relaxation times become infinitesimal. The angular momenta will then instantly adjust to the ever changing dinuclear configuration and one obtains a time-dependent equilibrium distribution as an instructive reference. In such a statistical model the observed distribution then arises from the instantaneous equilibrium at the time of neck collapse when the form factors go abruptly to zero and the two reaction partners loose contact.

The above described model appears to be the conceptually clearest statistical model. The statistical spin distribution has a general validity

beyond the specific mechanisms which are responsible for the angular momentum dynamics during a reaction, and therefore the statistical model offers a valuable reference distribution when discussing dynamical models. It is worth noticing, though, that the statistical model is not self-contained since it requires the specification of the separation between the two nuclei at the time when the spin distribution is determined.

For the mean spin vectors the statistical model yields the rigid rotation values (subject to small corrections). In actual reactions it is clear that rigid rotation is not achieved for the smallest energy losses. Therefore, in discussing the statistical model, separate recipies have been employed for the mean spin vectors and the attention has focussed on the equilibration of the variances.

In the literature various statistical models have been formulated and we discuss them in turn below.

7.4a Moretto's treatment

The formulation of a statistical model for damped reactions was first made by Moretto et al.[11]. In actual comparisons with data[15,28] the mean spin vector dominates most of the measured observables. The average γ-multiplicity has therefore been used to estimate the mean spin vector (as a function of energy loss) under the assumption of fully equilibrated spin variances, and the out-of-plane correlation of sequential decay has subsequently been invoked to provide a consistency check.

As we have discussed and displayed in figures 13-16, the rather long relaxation times obtained for some of the modes with the present transfer induced transport theory imply significant differences between our results and the results of the statistical model. One such difference is obtained for the

direction of the major in-plane variance. The analysis by Moretto et al. is carried out in the body-fixed I-aligned coordinate system. In the I-aligned frame the major axis is along the line connecting the centers of the nuclei when the spin distribution is determined and thus a discussion of the reaction dynamics is required. In contrast to this, we transform to the external frame, as is necessary in order to make contact with observed quantities. In the L-aligned frame the statistical in-plane variances are isotropic while the transformation to the external frames introduces an anisotropy whose major direction is determined kinematically rather than dynamically, being a simple function of the scattering angle.

On the other hand the transformation to the external frame leaves the spin magnitude invariant and the alignment practically unchanged, so the analysis of the γ-multiplicity and the out-of-plane angular correlations is not affected.

It is also worthwhile noticing that Moretto's statistical model focusses on a certain limited aspect of the data only and many basic observables, such as angular distributions and cross sections, can not be addressed.

Within the framework of the transfer-induced transport theory, it is not possible to justify the underlying assumption of quick relaxation for all the dinuclear spin modes. According to our analysis of relaxation times (Section 5), only the two wriggling modes are generally expected to have relaxation times sufficiently short in comparison with the reaction time to permit equilibrium to be established.

7.4b Friedman's treatment

Friedman has presented[29], a statistical treatment of angular momenta in damped reactions which has a starting point conceptually close to ours but which deviates essentially with respect to a key result. The object of study is a disphere with given energy

$$E_i = \frac{J^2}{2\mathcal{J}_R} + T_R + V_R = \frac{L^2}{2\mathcal{J}_R} + V_R + \frac{S^{A\,2}}{2\mathcal{J}_A} + \frac{S^{B\,2}}{2\mathcal{J}_B} + Q \qquad (7.1)$$

$$= E_{rot} + V_R + Q = \frac{J^2}{2\mathcal{J}_o} + E_{rot}^{intr} + V_R + Q$$

Here the relative radial energy consists of a fixed barrier energy V_R and a kinetic energy T_R which is totally dissipated. For a specified value of the total angular momentum J, the statistical distribution of the spin variables is

$$P_{\vec{J}}(\vec{S}^A, \vec{S}^B, \vec{L}) \sim \rho(Q) \qquad (7.2)$$

where ρ is the level density and $Q = E_i - J^2/2\mathcal{J}_0 - V_{12} - E_{rot}^{intr}$ is the generated internal excitation (the heat). It is then clear that $P_{\vec{J}}$ has a maximum when Q is maximal, i.e. when E_{rot}^{intr}, the energy carried by the six normal modes of intrinisic dinuclear rotation, is minimal. This of course, occurs for $E_{rot}^{intr} = 0$, i.e., for a rigid rotation of the system. Therefore, the most probable value of the spin $\vec{S}^F$ is

$$\langle \vec{S}^F \rangle_{\vec{J}} = \frac{\mathcal{J}_F}{\mathcal{J}_o} \vec{J} + \sigma(\tau) \qquad (7.3)$$

Furthermore, the most likely energy loss is

$$\Delta \tilde{E}_J = E_i - V_R - \frac{\mathcal{J}_R}{\mathcal{J}_0} \frac{J^2}{2\mathcal{J}_0} + \sigma(\tau) \tag{7.4}$$

These results are in accordance with the treatment by Friedman.

The above analysis pertains to a specified value of $\vec{J}$. The observable probability distribution is a sum of such contributions.

$$P(\vec{S}^A, \vec{S}^B, \vec{L}) = \int d\vec{J}\, P_{\vec{J}}(\vec{S}^A, \vec{S}^B, \vec{L}) \tag{7.5}$$

Here the specific measure on $\vec{J}$ is dictated by the conditions associated with a collision experiment, but the following considerations remain valid also if the measure is distorted not too violently.

It is of experimental interest to gate on the energy loss TKEL. For a specified value TKEL, the dominantly contributing J-value, J_{TKEL}, is approximately determined by

$$TKEL = E_i - V_R - \frac{\tilde{J}_{TKEL}^2}{2\mathcal{J}_0} \frac{\mathcal{J}_R}{\mathcal{J}_0} \tag{7.6}$$

so that

$$\tilde{J}_{TKEL} = \left\{ 2\mathcal{J}_0 \frac{\mathcal{J}_0}{\mathcal{J}_R} \left[(TKEL)_{max} - TKEL \right] \right\}^{1/2} \tag{7.7}$$

Consequently, the corresponding conditional mean values of the spins will be close to the dominant spins associated with $J = \tilde{J}$,

$$\langle S^F \rangle_{TKEL} \approx \frac{\mathcal{J}_F}{\mathcal{J}_0} \tilde{J}_{TKEL} \tag{7.8}$$

$$= \left\{ 2\mathcal{J}_F \frac{\mathcal{J}_F}{\mathcal{J}_R} \left[(TKEL)_{max} - TKEL \right] \right\}^{1/2}$$

This approximate treatment is valid as long as the spin distribution is not fluctuation dominated, i.e., as long as the mean spins are larger than the fluctuations; this covers most of the energy-loss range.

The result obtained by Friedman is in striking contrast to the above result. In his attempt to obtain a conditional distribution he replaces the specification of J with a specification of TKEL. This procedure amounts effectively to abandoning the conservation of angular momentum in each thermal ensemble (or, equivalently, permitting exchange of angular momentum with the thermal reservoir). Not surprisingly he finds that the mean spins are proportional to the square root of the temperature, as is typical of a thermal distribution in the absence of an overall conserved angular momentum. It seems clear to us that the employed procedure is not justified for the physical situation encountered in a reaction process.

Acknowledgment

During part of this work, one of us (TD) was supported by a Niels Bohr Fellowship granted by the Royal Danish Academy of Science.

References

1. W. V. Schröder and J. R. Huizenga, Ann. Rev. Nucl. Sci. 27 (1977) 465
2. C. F. Tsang, Phys. Scripta 10A (1974) 90
3. W. Nörenberg, Phys. Lett. 53B (1974) 289
4. H. Hofmann and P. J. Siemens, Nucl. Phys. A257 (1976) 165
5. J. Randrup, Nucl. Phys. A327 (1979) 490
6. J. Randrup, Nucl. Phys. A383 (1983) 468
7. W. V. Schröder, J. R. Birkelund, J. R. Huizenga, W. W. Wilcke and J. Randrup, Phys. Rev. Lett. 44 (1980) 308
8. W. V. Schröder, J. R. Huizenga and J. Randrup, Phys. Lett. 98B (1981) 355
9. H. C. Britt, H. Erkkila, A. Gavron, Y. Patin, R. H. Stokes, M. P. Webb, P. R. Christensen, O. Hansen, S. Pontoppidan, F. Videbæk, R. L. Ferguson, F. Plasil, G. R. Young and J. Randrup, Phys. Rev. 26C (1982) 1999
10. J. Randrup, Phys. Lett. 110B (1981) 25
11. L. G. Moretto and R. P. Schmitt, Phys. Rev. C21 (1980) 204
12. J. Randrup, Proceeding of the Nordic Winter School on Nuclear Physics, Hemsdel, Norway, 10-20 April 1983; World Scientific, Singapore (in press)
13. R. P. Schmitt and A. J. Pacheco, Nucl. Phys. A379 (1982) 313
14. R. A. Broglia, C. H. Dasso and A. Winther, Proc. Int. School of Physics, "Enrico Fermi," Varenna, Italy, July 1979 (North Holland, Amsterdam, 1982), p. 327
15. R. J. McDonald, A. J. Pacheco, G. J. Wozniak, H. H. Bolotin, L. G. Moretto, C. Schuck, S. Shih, R. M. Diamond and F. S. Stephens, Nucl. Phys. A373 (1982) 54
16. P. Dyer, R. J. Puigh, R. Vandenbosch, T. O. Thomas, M. S. Zisman and L. Nunnelly, Nucl. Phys. A322 (1979) 205

17. D. von Harrach, P. Glässer, Y. Cigelekoglu, R. Männer and H. J. Specht, Phys. Rev. Lett. 42 (1979) 1728

18. S. Ayik, G. Wolschin, W. Nörenberg, Z. Phys. A286 (1978) 271
W. Nörenberg, Lectures presented at the Predeal International School in Physics, Predeal, Romania, 1978.

19. H. A. Weidenmüller, Prog. Part. Nucl. Phys. 4 (1980) 273

20. H. Hofmann and P. J. Siemens, Nucl. Phys. A275 (1977) 464;
M. Berlanger, P. Grange, H. Hofmann, C. Ngo, J. Richert, Z. Phys. A286 (1978) 207

21. J. Q. Li, and G. Wolschin, Phys. Rev. C27 (1983) 590

22. W. Nörenberg, Z. Phys. Z274 (1975) 241, Erratum A276 (1976) 84

23. S. Ayik, B. Schurmann and W. Norenberg, Z. Phys. A277 (1976) 299

24. W. Nörenberg, Phys. Lett. 52B (1974) 289

25. K. T. R. Davies, K. R. S. Devi, S. E. Koonin, M. R. Strayer, to appear in Heavy Ion Science (editor D. A. Bromley) Plenum Press

26. R. A. Broglia, G. Pollarolo, C. H. Dasso and T. Døssing, Phys. Rev. Lett. 43 (1979) 1649

27. D. P. Min, Y. S. Koh, C. Gregoire, preprint (1982)

28. D. J. Morrissey, G. J. Wozniak, L. G. Sobotka, A. J. Pacheco, R. J. McDonald, C. C. Hsu and L. G. Moretto, Nucl. Phys. A389 (1982) 120

29. W. A. Friedman, Phys. Lett. 98B (21)

Fig. 1 The spherical triangle spanned by the directions $\hat{L} = \hat{y}$, $\hat{J}$, $\hat{Y} \sim \hat{R}$ $\hat{t}$, where $\hat{t}$ is the beam direction. The angle at $\hat{Y}$ is equal to the scattering angle Θ, which is the angle between $\hat{R}$ and $\hat{t}$, since $\hat{R}\cdot\hat{L} = 0$ and $\hat{J}\cdot\hat{t} = 0$. The direction of $\hat{J}$ relative to $\hat{L}$ is given by the polar coordinates (ϑ,φ). When ϑ and ξ are small we may employ planar trigonometry and obtain $\xi \approx \vartheta \sin(\varphi+\Theta)/\sin\Theta = \vartheta\cos\varphi + \vartheta\sin\varphi\cot\Theta \approx \hat{J}_x + \hat{J}_z \cot\Theta$, since $\hat{J}_x = \sin\vartheta\cos\varphi \approx \vartheta\cos\varphi$ and $\hat{J}_z = \sin\vartheta\sin\varphi \approx \vartheta\sin\varphi$.

Fig. 2. The time evolution of the dinuclear separation R and the radius of the small cylindrical neck c joining the two spheres, for various values of the total angular momentum J in the reaction 1400 MeV ^{165}Ho + ^{165}Ho.

Fig. 3. For three different values of the total angular momentum J, the dinuclear complex produced in the reaction 1400 MeV ^{165}Ho + ^{165}Ho is shown at three different points in time: shortly after the neck has opened, at the time of closest approach, and right before the neck collapses. (The actual times indicated are measured from the time of the nuclei approach to a surface separation of s = 4 fm.) The dots indicate past and future locations of the nuclear centers at intervals of 10^{-22} sec. The dashed ellipses indicate the one-sigma contours of the in-plane distribution of the nuclear angular momenta $\vec{S}^A$ and $\vec{S}^B$ scaled so that one fm corresponds to two $\hbar$ (the nucleides have a radius of 6.3 fm).

Fig. 4. The time evolution of the dinuclear center separation R and the neck radius c as obtained in three different calculations of the head-on reaction 1535 MeV ^{208}Pb and + ^{208}Pb. TDHF: The Time-Dependent Hartree-Fock model[13], CSE: The Coherent Surface Excitation model[14] and NET: the present Nucleon Exchange Transport model.

Fig. 5. The information from Fig. 4 combined to a dynamical trajectories in the R-c plane.

Fig. 6. Calculated local relaxation times for the reaction 1400 MeV ^{165}Ho + ^{165}Ho for various values of the total angular momentum J. The relaxation times for the two positive perpendicular modes (wriggling) are denoted t_{++}, while the one of the positive longitudinal mode (tilting) is denoted t_{+z}. The relaxation time for the three negative modes (bending and twisting) is denoted t_{--}.

Fig. 7. Calculated time evolution of the mean fragment spin $\langle S_y \rangle$ in the reaction 1400 MeV angular momentum J. The neck snapping, after which the spins remain constant, is indicated by a small vertical bar.

Fig. 8. Calculated time evolution of the various spin covariances σ_{ij}^{FG} in the reaction 1400 MeV ^{165}Ho + ^{165}Ho, for a total angular momentum of J = 320 $\hbar$. At the time of neck snapping (t = 12.6 10^{-22}) the time scale is changed by a factor of ten. After the asymptotic values have been reached, the effect of transforming to the external reference frame XYZ is shown on the right.

Fig. 9. The time evolution of the mean fragment spins $\langle S_y^F \rangle$ in the reaction 610 MeV ^{86}Kr + ^{209}Bi, for three values of the angular momentum J.

Fig. 10. The time evolution of the spin covariances σ_{ij}^{FG} in the reaction 610 MeV ^{86}Kr + ^{209}Bi, for J = 160 . Analogous to Fig. 8.

Fig. 11. The distributions in the TKEL-S_y^A plane in the reacion 1400 MeV ^{105}Ho + ^{105}Ho, calculated for specified values of the total angular momentum J; TKEL is the total kinetic energy loss and S_y^A is the component of the final fragment spin along the reaction normal.

Fig. 12. The mean normal spin $\langle S_y^A \rangle$ as a function of the incurred energy loss TKEL, as calculated by integrating over all J-values. The reaction 1400 MeV ^{105}Ho + ^{105}Ho.

Fig. 13. For the reaction 1400 MeV ^{165}Ho + ^{165}Ho, various angles of interest are shown as functions of the total kinetic energy loss TKEL: The CM scattering angle θ_{CM} (together with the dispersions in TKEL and θ_{CM} for the corresponding dominant J-value), half this quantity, $\theta_{CM}/2$, and the angle θ_o (dashed curve) required to align the major in-plane principal axis with the beam.

Fig. 14. The spin dispersions along the principal directions as functions of the incurred energy loss TKEL, as calcuated for the reaction 1400 MeV ^{165}Ho + ^{165}Ho by integrating over all J-values.

Fig. 15. As a function of kinetic energy loss TKEL in the reaction 1400 MeV $^{165}Ho + {}^{165}Ho$ the following angles are shown: 1) The calculated CM scattering angle θ_{CM}, 2) the principal angle θ_0 for the spin covariance tensor in the statistical model (θ_0 is the angle between the beam and the largest principal axis), 3) the approximation $\pi/4 + \theta_{CM}/2$ to θ_0.

Fig. 16. The principal spin dispersions calculated in the statistical model, as functions of kinetic energy loss TKEL in the reaction 1400 MeV $^{165}Ho + {}^{165}Ho$. The values of θ_{CM}, R, S_y^+ and J are as dynamically calculated. The dashed curves show the results for σ_{zz}^{AA} and σ_{zz}^{AB} when the statistical values are used for S_y^+.

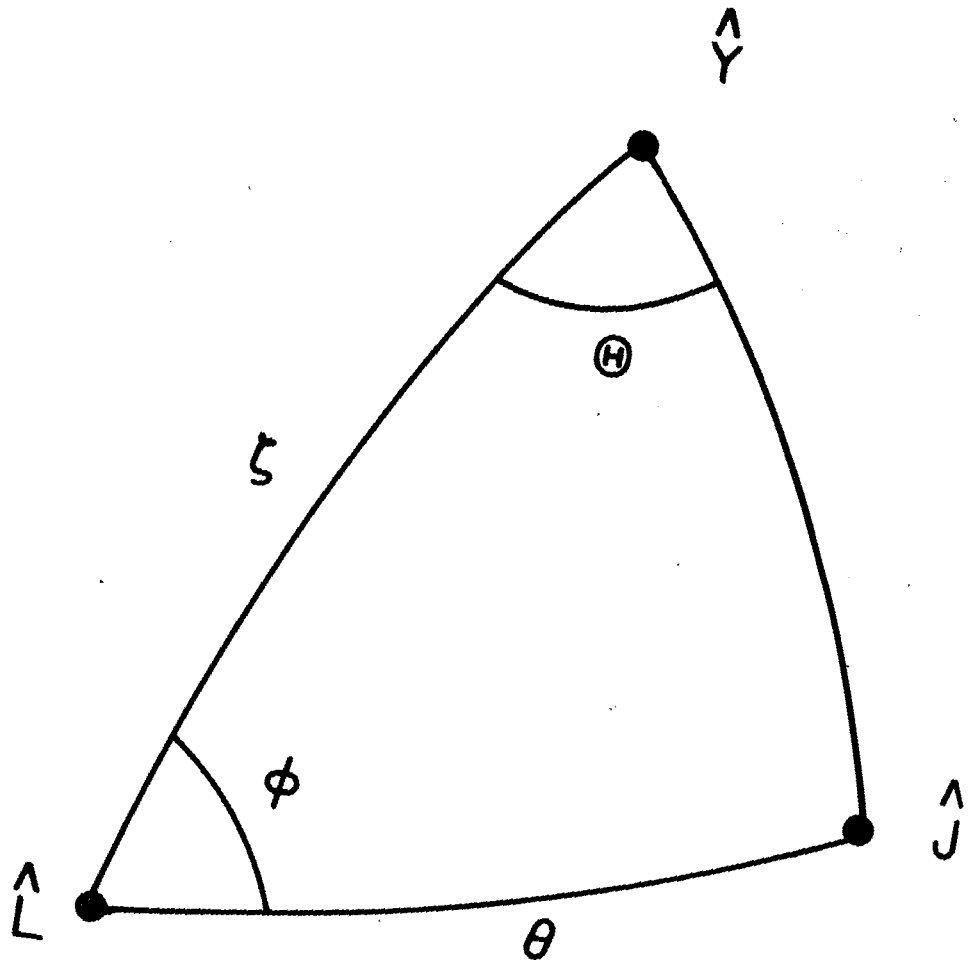

XBL 837-423

Fig. 1

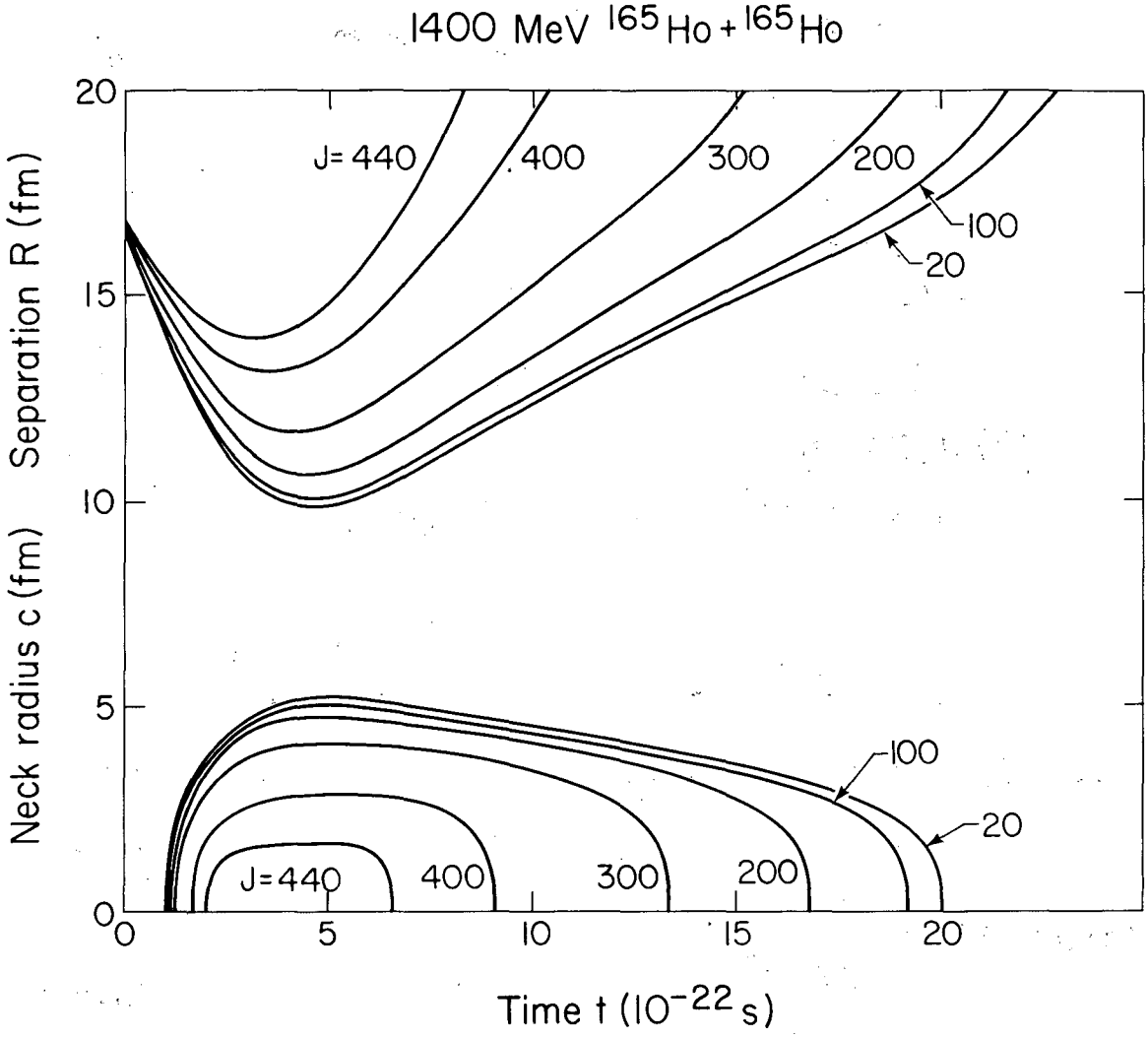

XBL 841-22

Fig. 2

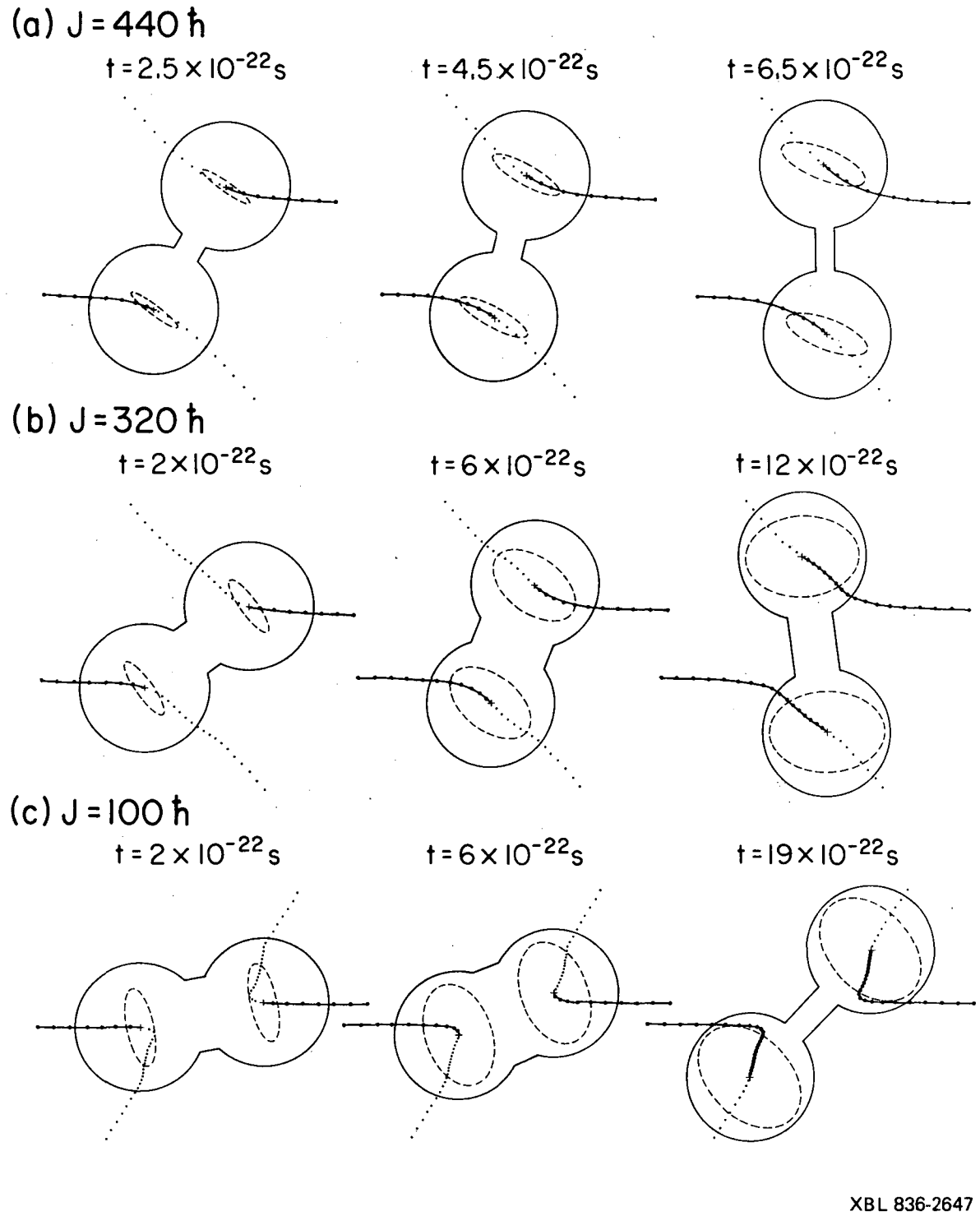
(a) J = 440 ħ
t = 2.5 × 10^-22 s
t = 4.5 × 10^-22 s
t = 6.5 × 10^-22 s
(b) J = 320 ħ
t = 2 × 10^-22 s
t = 6 × 10^-22 s
t = 12 × 10^-22 s
(c) J = 100 ħ
t = 2 × 10^-22 s
t = 6 × 10^-22 s
t = 19 × 10^-22 s
XBL 836-2647

Fig. 3

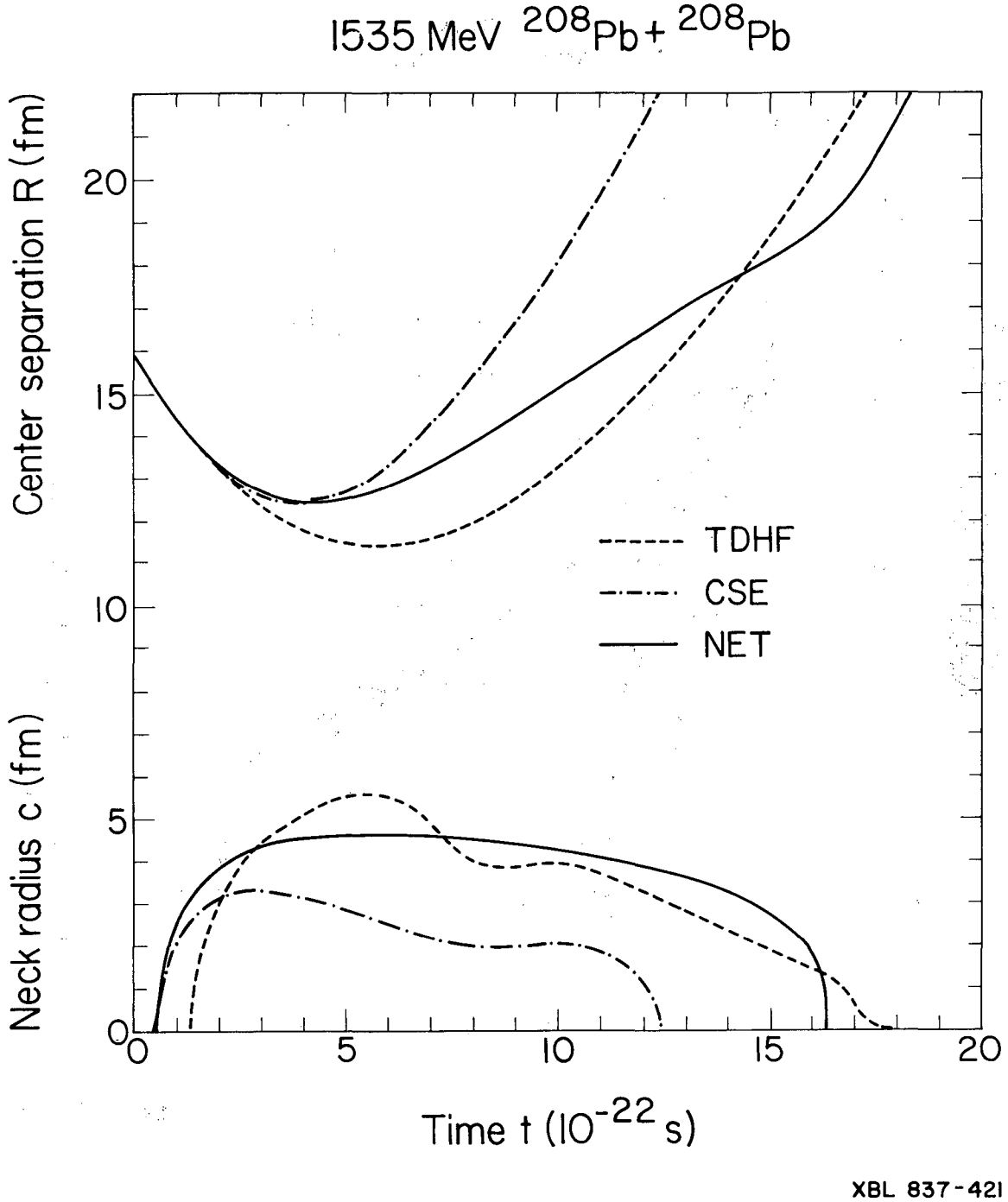
1535 MeV ^{208}Pb + ^{208}Pb
Center separation R (fm)
Neck radius c (fm)
Time t (10^{-22} s)
TDHF
CSE
NET
0
5
10
15
20
XBL 837-421

Fig. 4

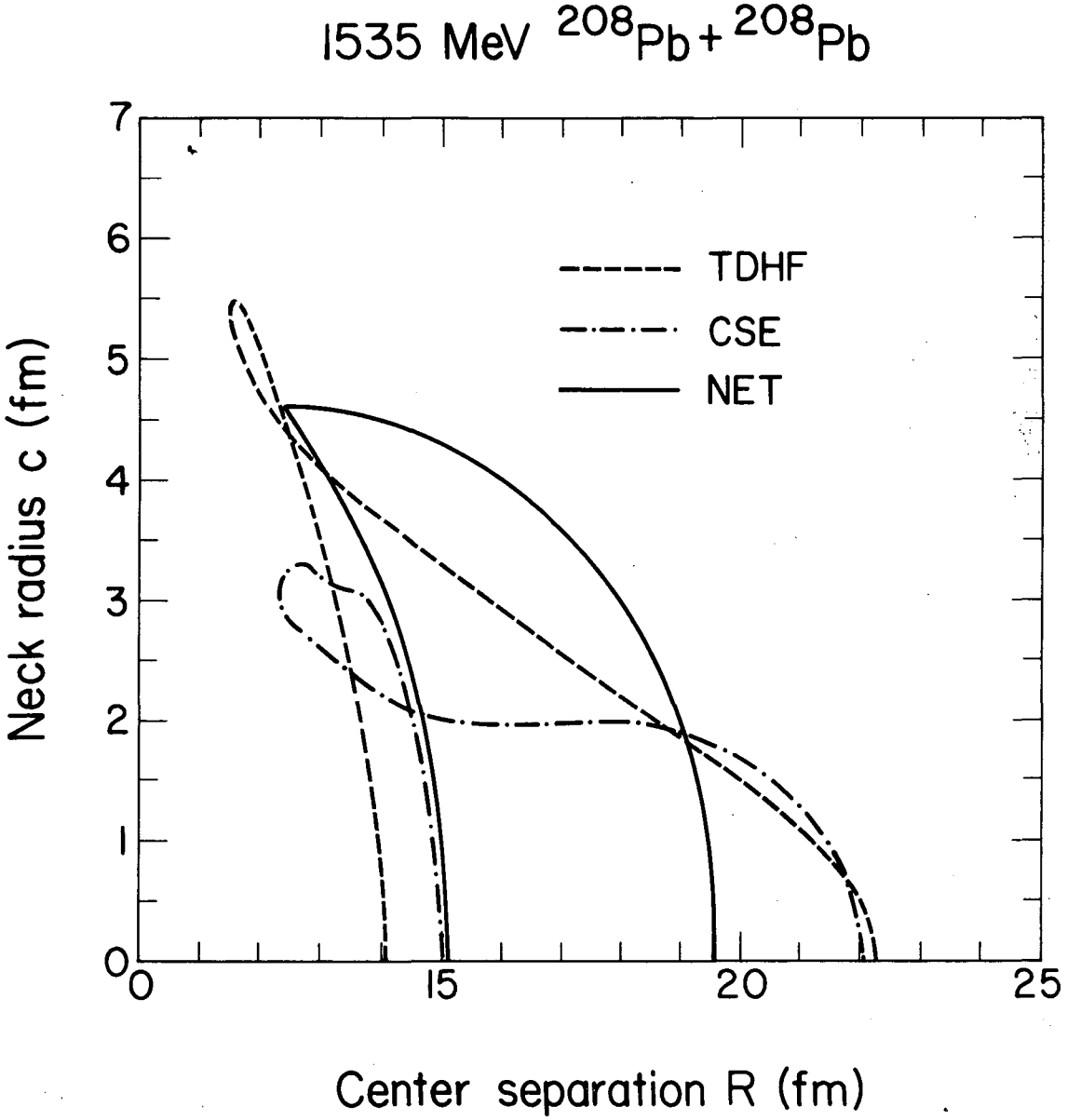

XBL 837-424

Fig. 5

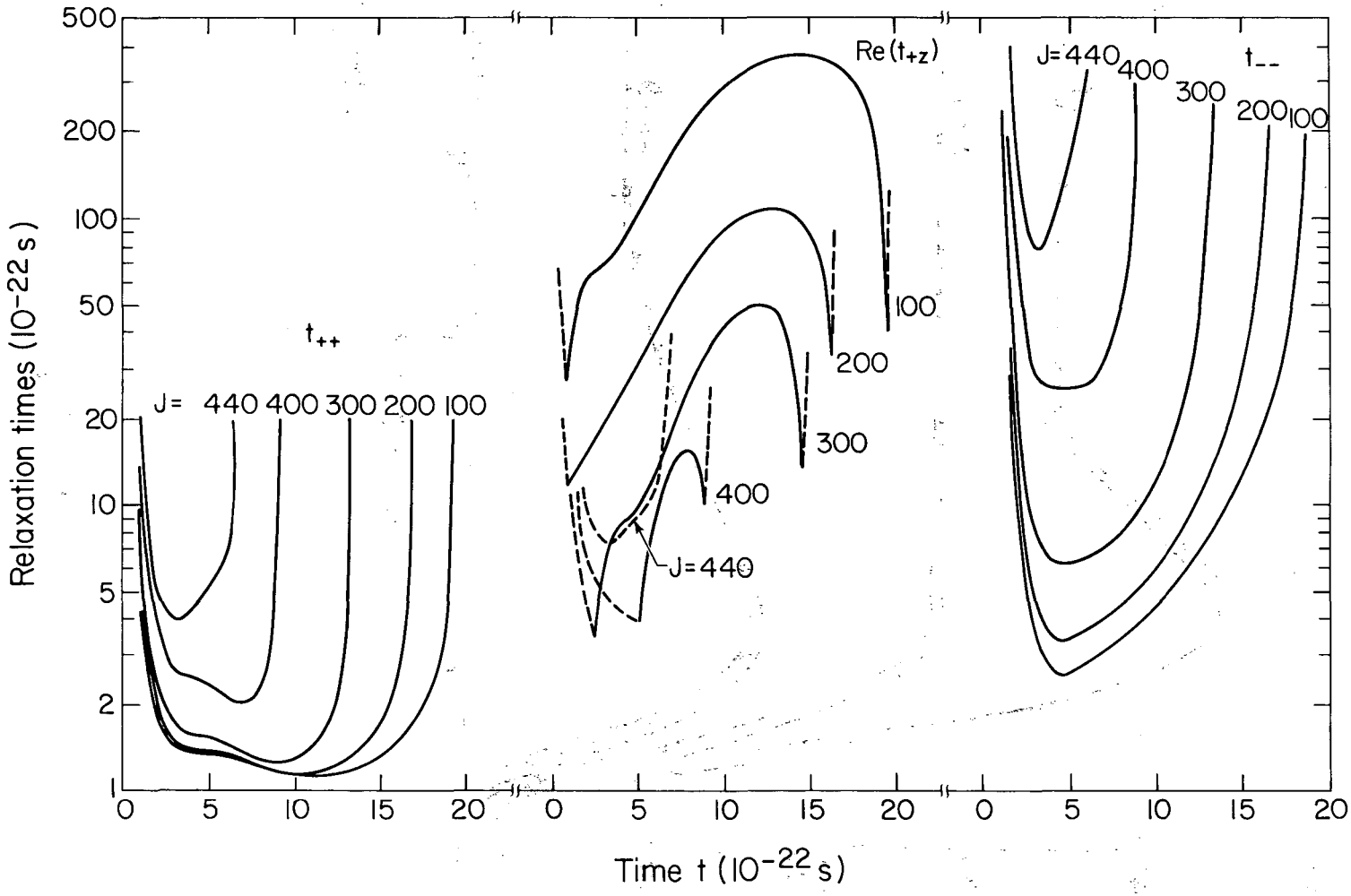

XBL 841-23

Fig. 6

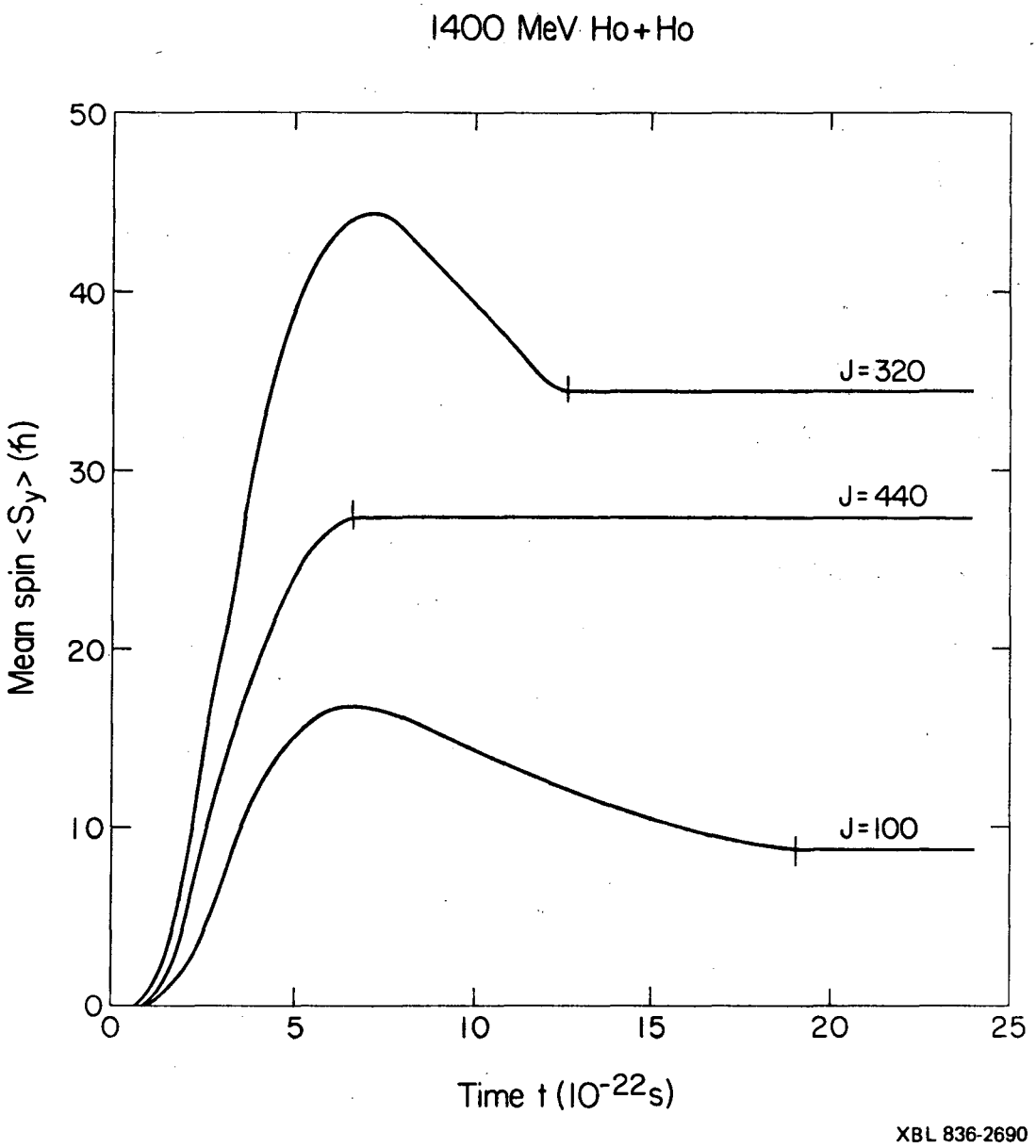
1400 MeV Ho+Ho
Mean spin <Sy> (ħ)
Time t (10^-22 s)
J=320
J=440
J=100
0
10
20
30
40
50
0
5
10
15
20
25
XBL 836-2690

Fig. 7

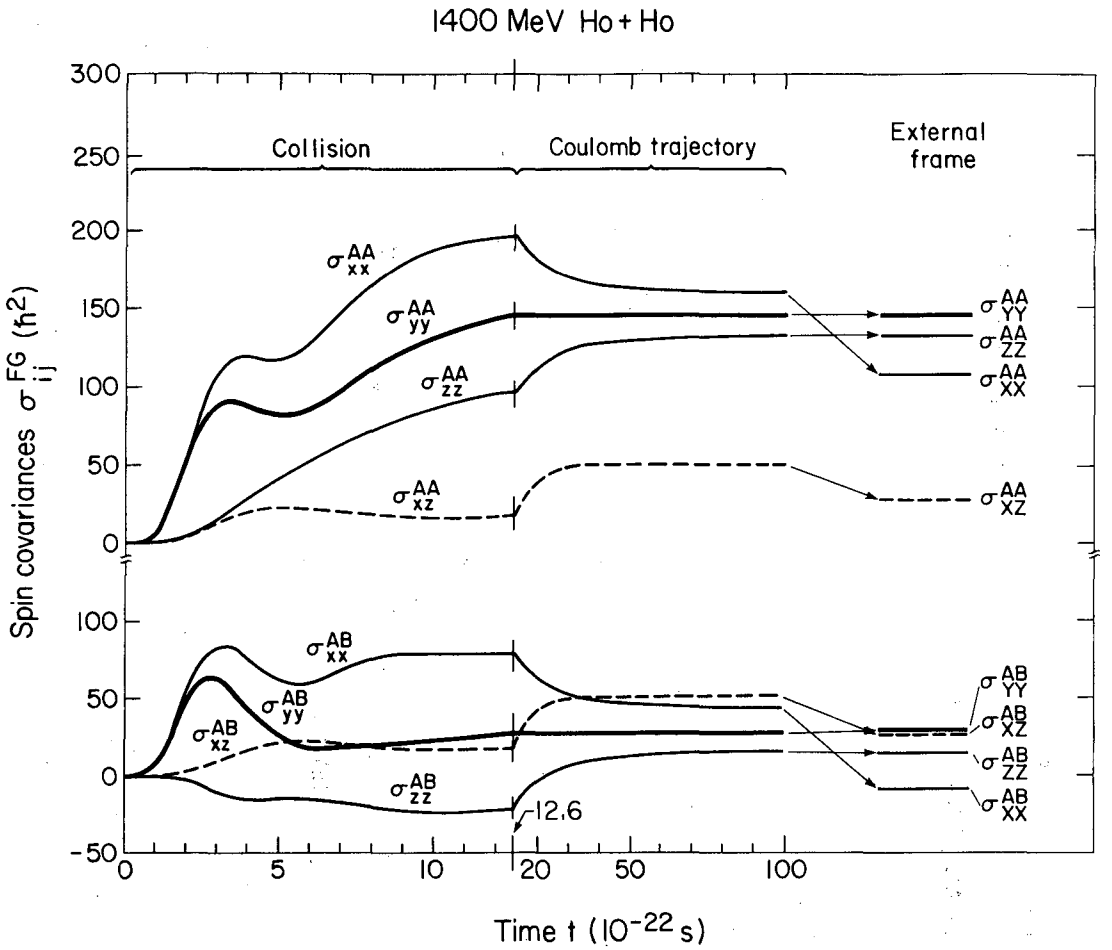
1400 MeV Ho + Ho
Collision
Coulomb trajectory
External frame
Spin covariances σ_{ij}^{FG} ($\hbar^2$)
σ_{xx}^{AA}
σ_{yy}^{AA}
σ_{zz}^{AA}
σ_{xz}^{AA}
σ_{YY}^{AA}
σ_{ZZ}^{AA}
σ_{XX}^{AA}
σ_{XZ}^{AA}
σ_{xx}^{AB}
σ_{yy}^{AB}
σ_{xz}^{AB}
σ_{zz}^{AB}
σ_{YY}^{AB}
σ_{XZ}^{AB}
σ_{ZZ}^{AB}
σ_{XX}^{AB}
12,6
Time t (10^{-22} s)
XBL 836-2693

Fig. 8

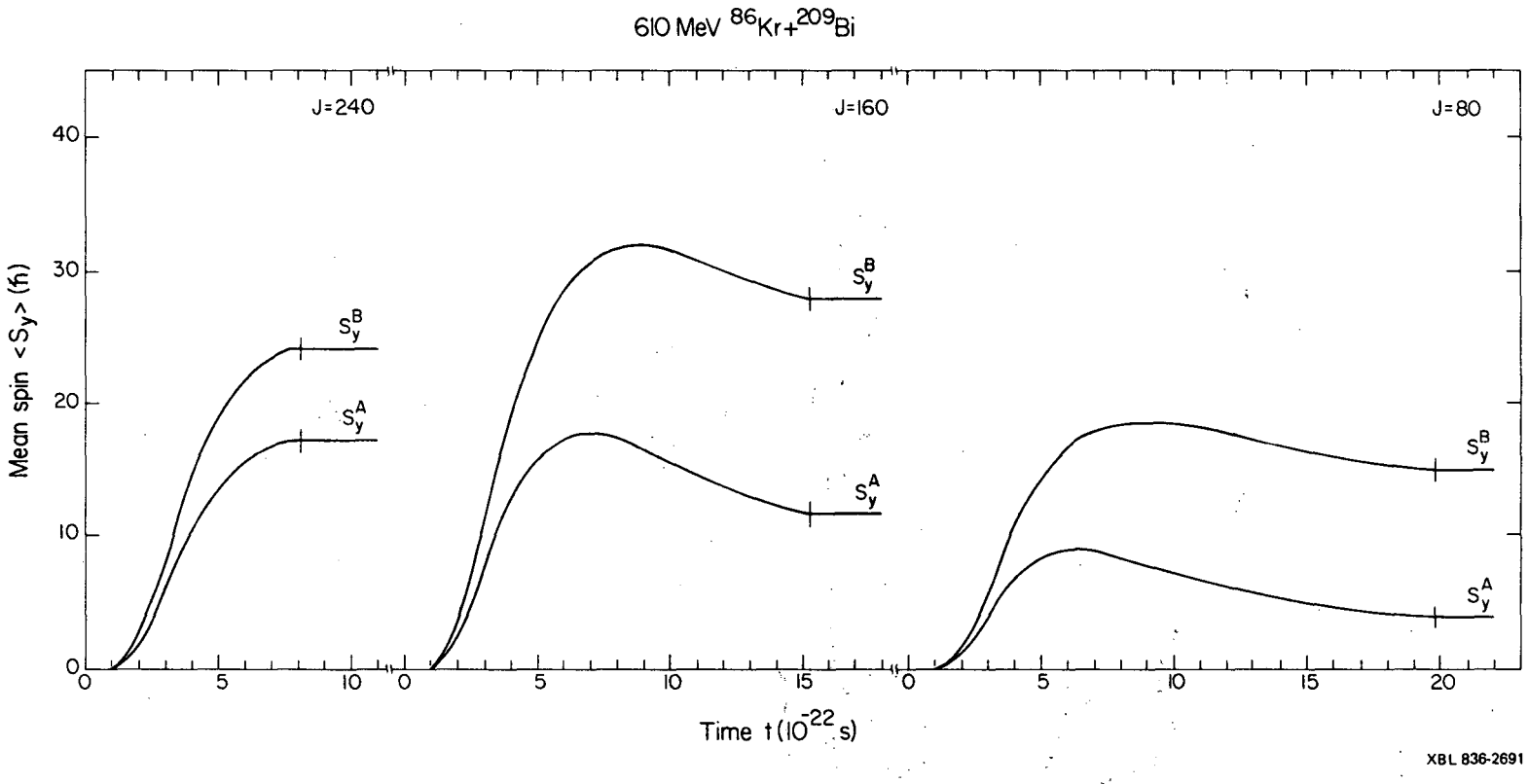
610 MeV $^{86}Kr+^{209}Bi$
J=240
J=160
J=80
Mean spin $<S_y>$ (ħ)
S_y^B
S_y^A
Time t (10^{-22} s)
XBL 836-2691

Fig. 9

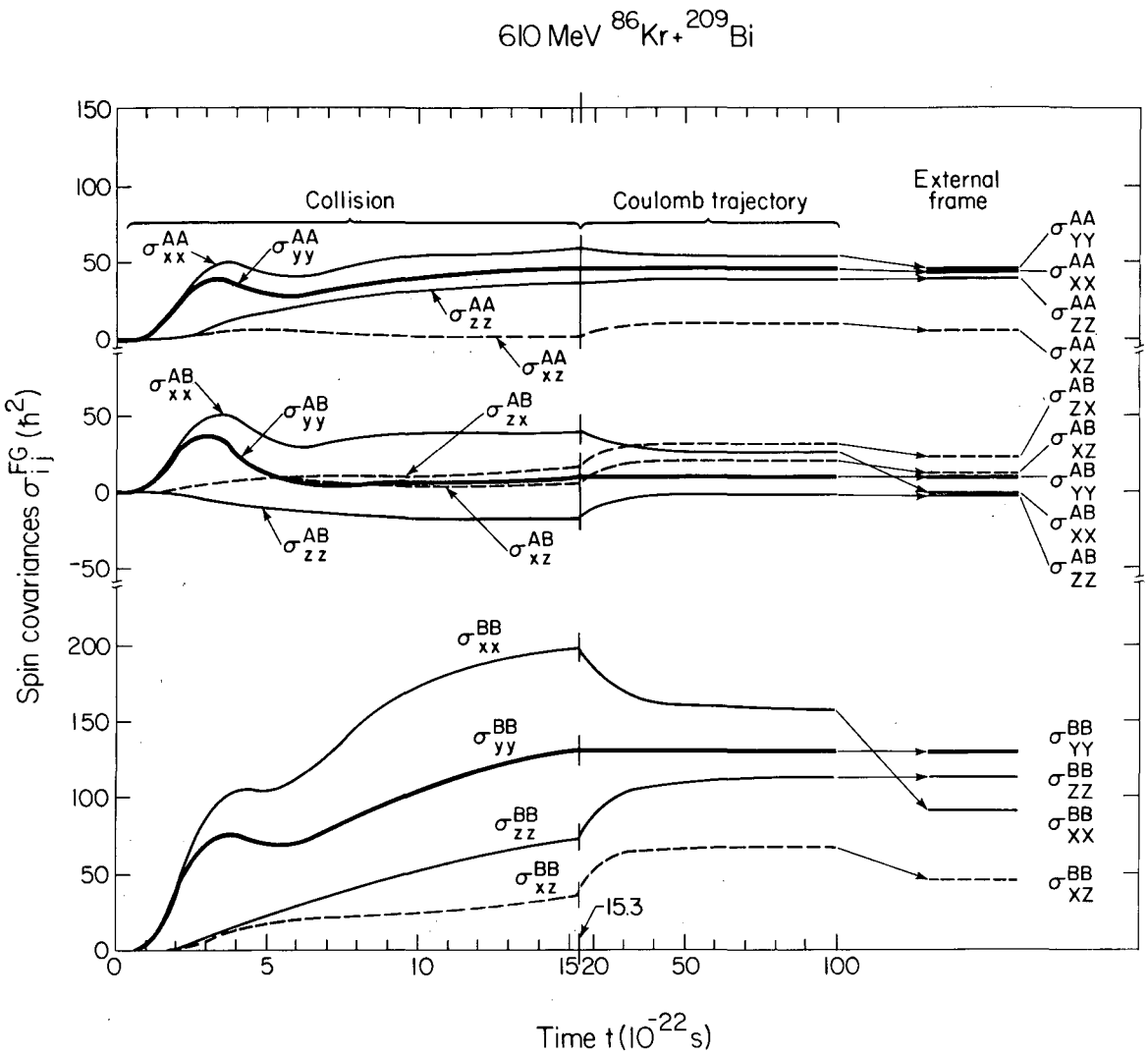
610 MeV $^{86}Kr + ^{209}Bi$
Collision
Coulomb trajectory
External frame
Spin covariances σ^{FG}_{ij} ($\hbar^2$)
Time t (10^{-22} s)
15.3
XBL 836-2692

Fig. 10

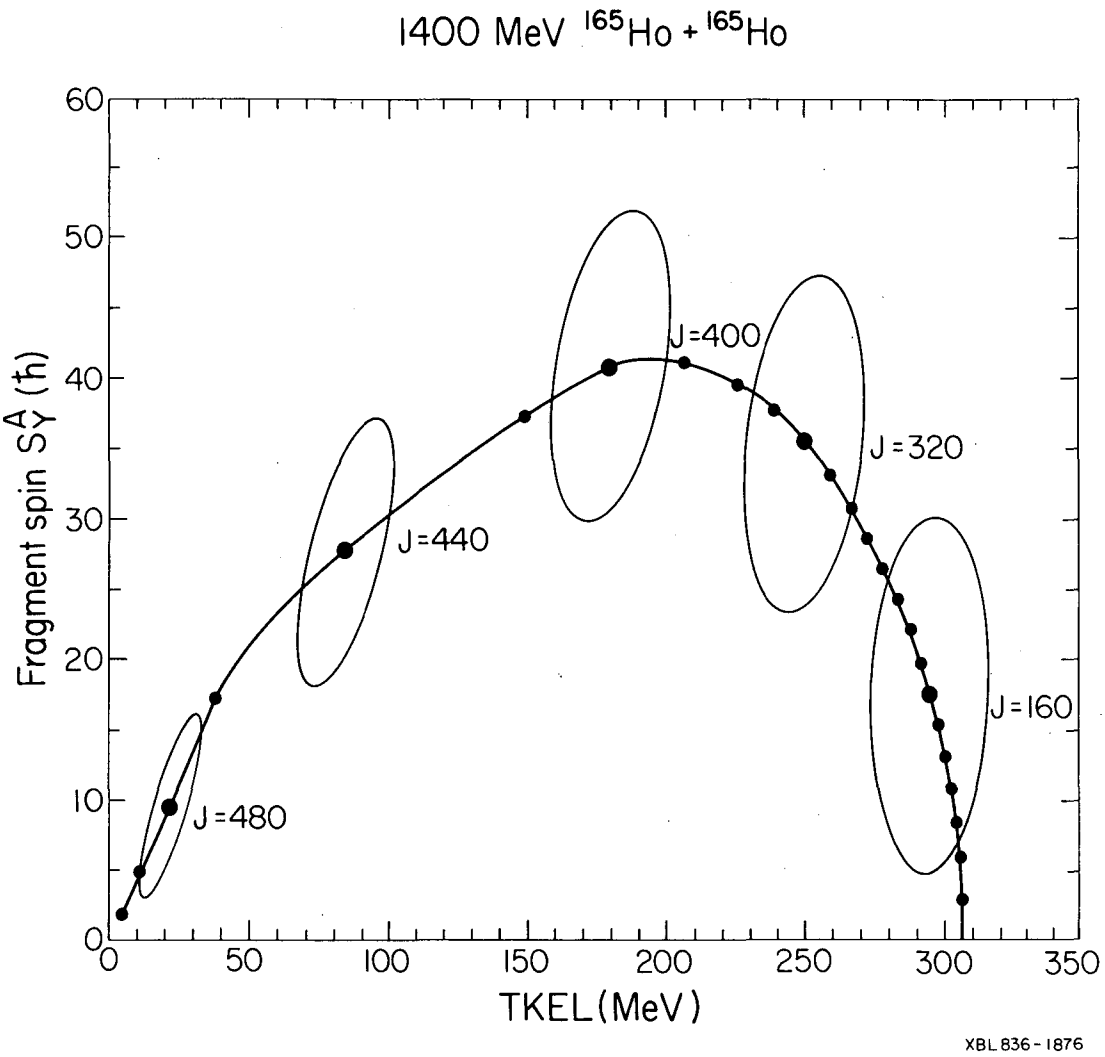
1400 MeV ^{165}Ho + ^{165}Ho
Fragment spin S_Y^A (ħ)
TKEL(MeV)
J=480
J=440
J=400
J=320
J=160
0
10
20
30
40
50
60
0
50
100
150
200
250
300
350
XBL 836-1876

Fig. 11

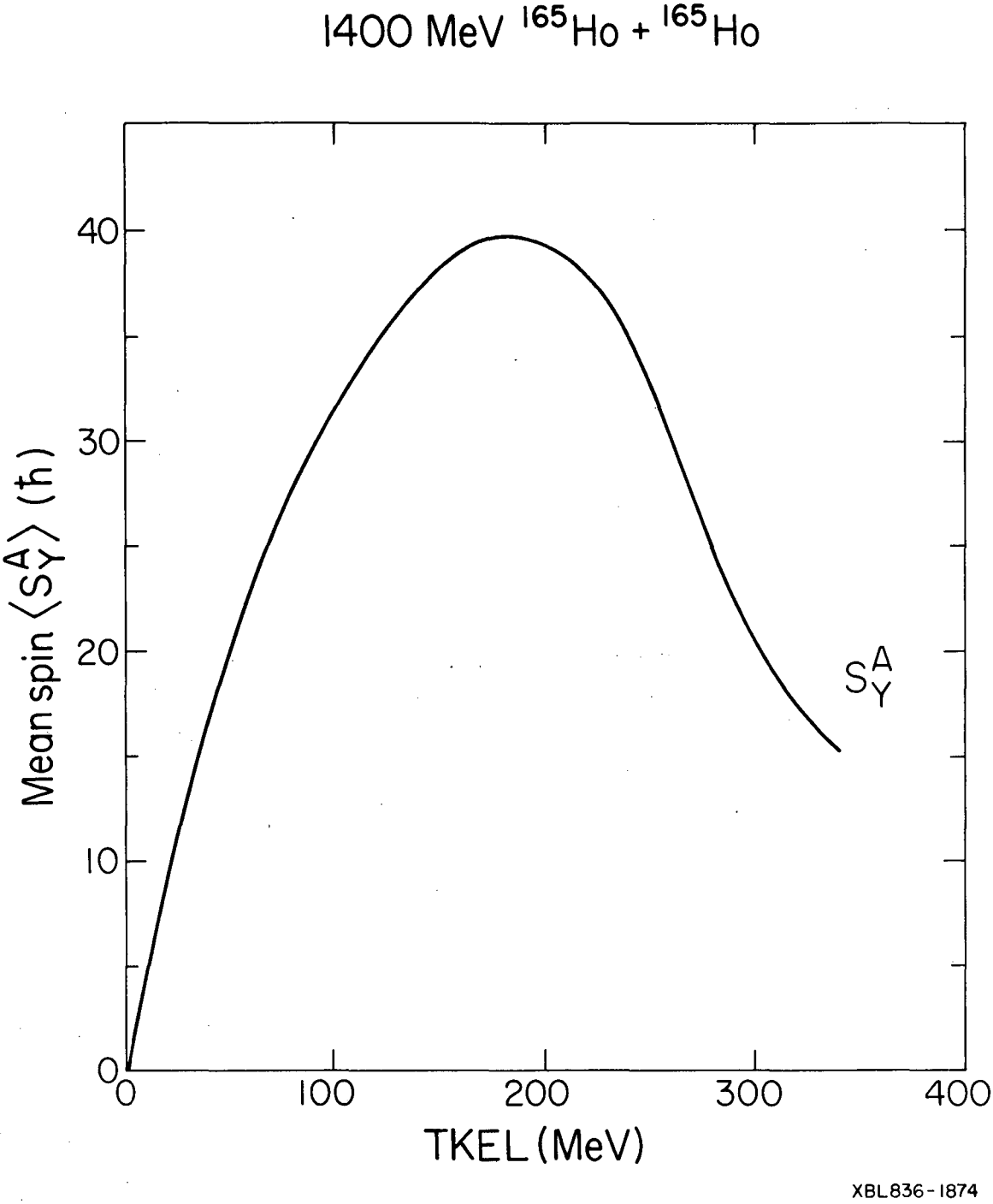
1400 MeV ^{165}Ho + ^{165}Ho
Mean spin $\langle S_Y^A \rangle$ (ħ)
0
10
20
30
40
0
100
200
300
400
TKEL (MeV)
S_Y^A
XBL836-1874

Fig. 12

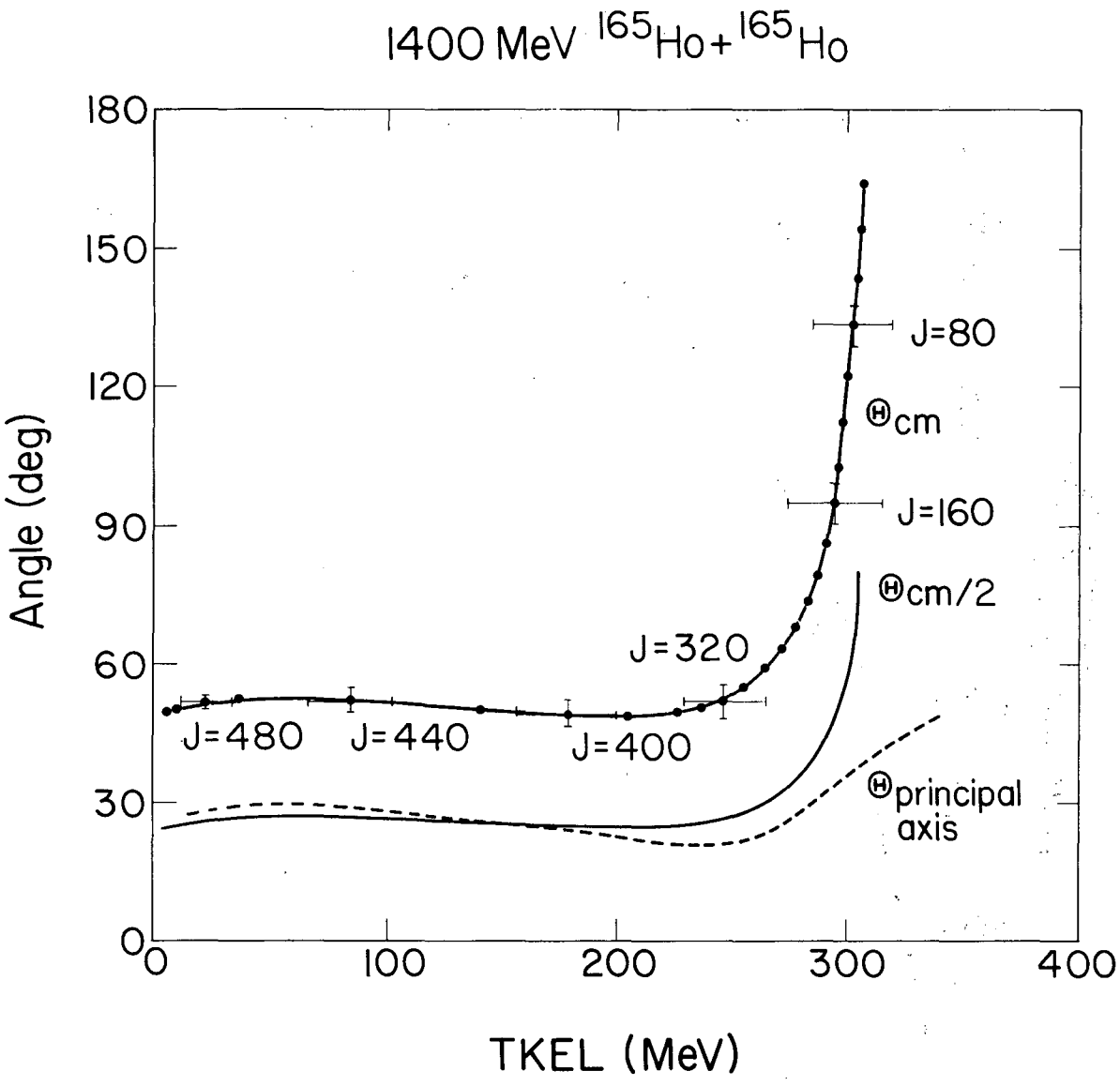
1400 MeV 165Ho+165Ho
180
150
120
90
60
30
0
Angle (deg)
0
100
200
300
400
TKEL (MeV)
J=80
Θcm
J=160
Θcm/2
J=320
J=480
J=440
J=400
Θprincipal axis
XBL 837-422

Fig. 13

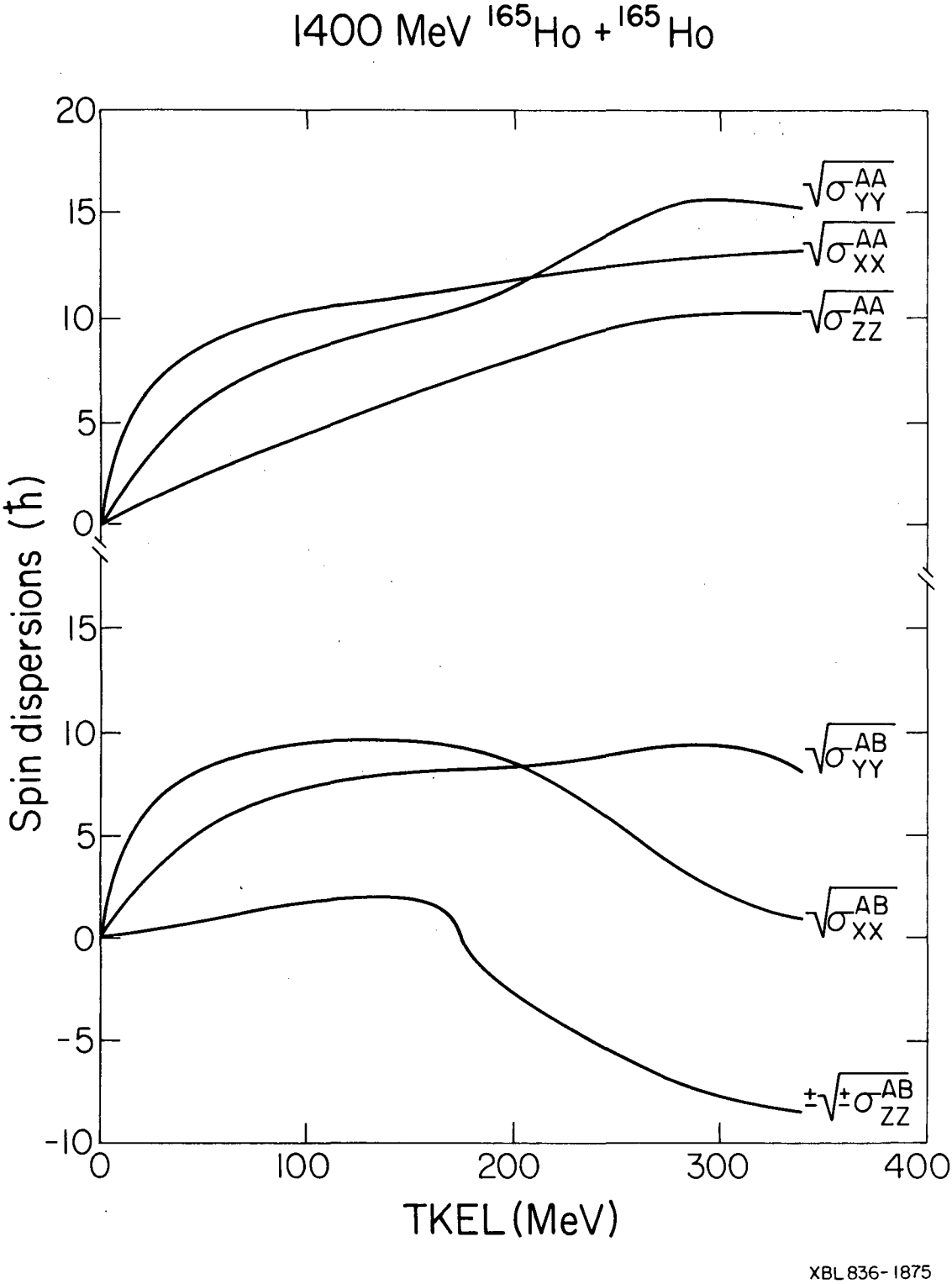
1400 MeV ^{165}Ho + ^{165}Ho
Spin dispersions (ħ)
TKEL (MeV)
$\sqrt{\sigma^{AA}_{YY}}$
$\sqrt{\sigma^{AA}_{XX}}$
$\sqrt{\sigma^{AA}_{ZZ}}$
$\sqrt{\sigma^{AB}_{YY}}$
$\sqrt{\sigma^{AB}_{XX}}$
$\pm\sqrt{\pm\sigma^{AB}_{ZZ}}$
20
15
10
5
0
15
10
5
0
-5
-10
0
100
200
300
400
XBL 836-1875

Fig. 14

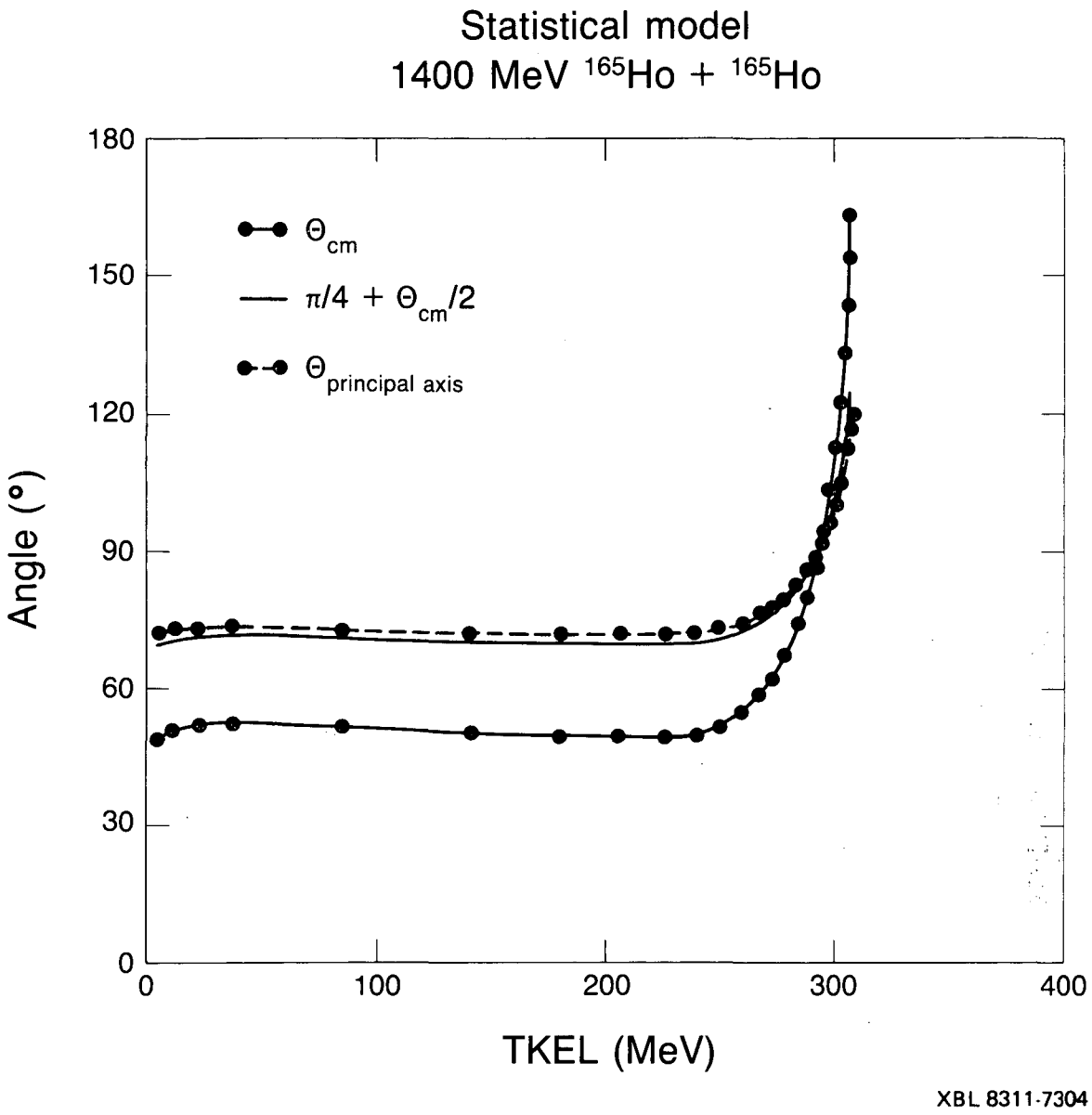
Statistical model
1400 MeV 165Ho + 165Ho
Θcm
π/4 + Θcm/2
Θprincipal axis
Angle (°)
180
150
120
90
60
30
0
0
100
200
300
400
TKEL (MeV)
XBL 8311-7304

Fig. 15

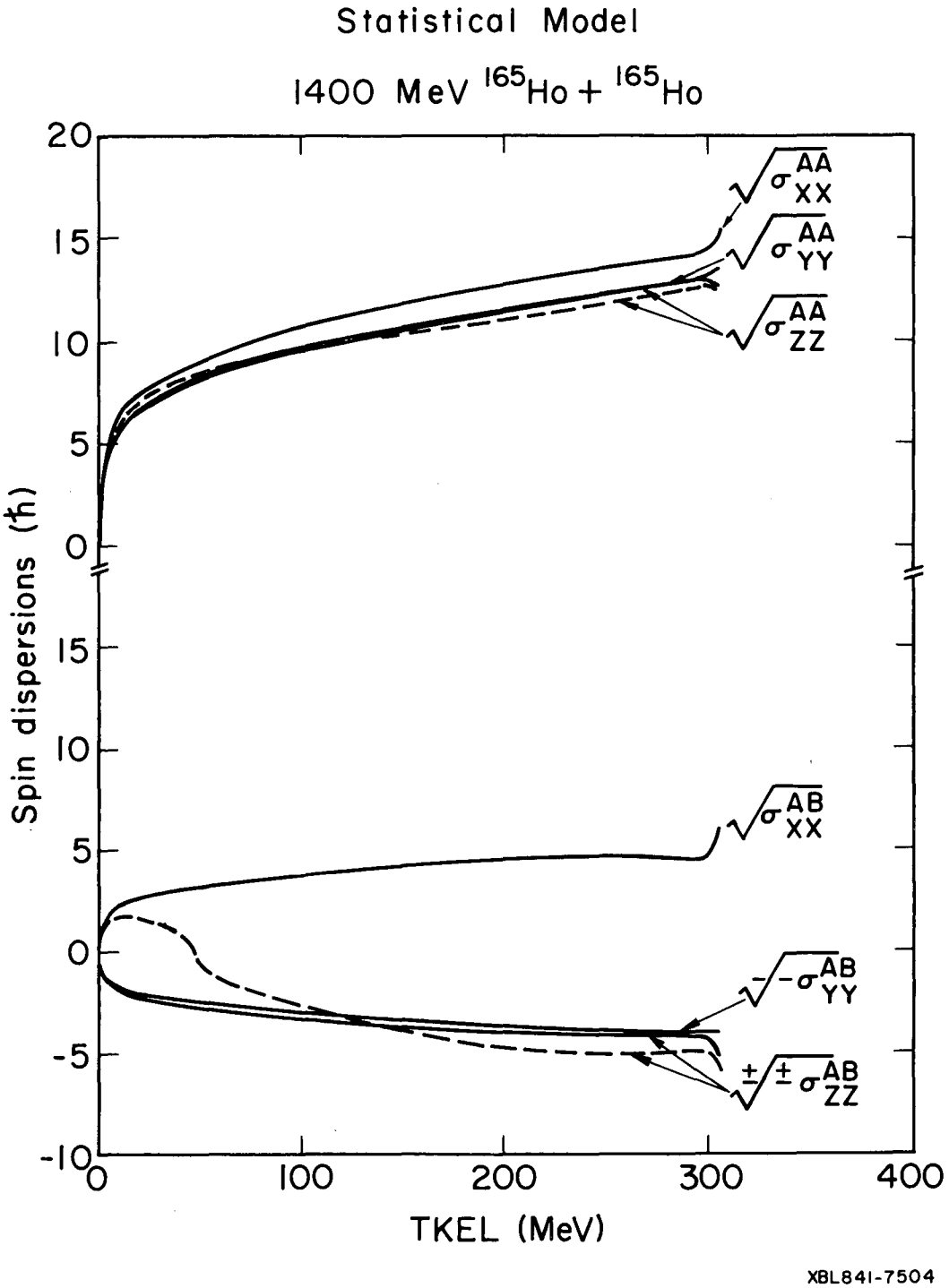
Statistical Model
1400 MeV ^{165}Ho + ^{165}Ho
Spin dispersions (ħ)
TKEL (MeV)
$\sqrt{\sigma^{AA}_{XX}}$
$\sqrt{\sigma^{AA}_{YY}}$
$\sqrt{\sigma^{AA}_{ZZ}}$
$\sqrt{\sigma^{AB}_{XX}}$
$\sqrt{-\sigma^{AB}_{YY}}$
$\pm\sqrt{\pm\sigma^{AB}_{ZZ}}$
20
15
10
5
0
15
10
5
0
-5
-10
0
100
200
300
400
XBL841-7504

Fig. 16

TECHNICAL INFORMATION DEPARTMENT
LAWRENCE BERKELEY LABORATORY
UNIVERSITY OF CALIFORNIA
BERKELEY, CALIFORNIA 94720